

# **Low-voltage-activated $\text{Ca}^{2+}$ channels: From burst generators to $\text{Ca}^{2+}$ sources in thalamic oscillatory activity**

**Inauguraldissertation**

zur

Erlangung der Würde eines Doktors der Philosophie  
vorgelegt der  
Philosophisch-Naturwissenschaftlichen Fakultät  
der Universität Basel

von

Lucius D. Cueni

aus Dittingen Basel-Land

Basel 2007

Genehmigt von der Philosophisch-Naturwissenschaftlichen Fakultät  
auf Antrag von

Prof. Dr. Markus A. Rüegg  
Dr. Anita Lüthi  
Prof. Dr. Kaspar Vogt  
Prof. Dr. Heinrich Reichert

Basel, den 13. Dezember 2007

Prof. Dr. Hans-Peter Hauri  
Dekan der Philosophisch-  
Naturwissenschaftlichen Fakultät

# Danksagung

Meinen ersten und auch ganz besonderen Dank möchte ich Anita Lüthi widmen. Anita Lüthi gab mir die Möglichkeit, in ihrem Labor diese Arbeit zu schreiben und hat mit ihren anregenden, wissenschaftlichen Diskussionen und Hilfestellungen bei wissenschaftlichen und technischen Problemen massgeblich zum Erfolg dieser Dissertation beigetragen. Hervorheben möchte ich auch die Förderung auf vielen Ebenen, die ich durch Anita Lüthi in der Zeit in ihrem Labor erfahren habe.

Kaspar Vogt möchte ich für die Übernahme des Koreferates und für die kritischen und konstruktiven Inputs zu meiner Publikation danken. Markus Rüegg gilt der Dank als Fakultätsverantwortlichen.

Des Weiteren möchte ich meinen ehemaligen und derzeitigen Arbeitskollegen Samuel Frère, Lazar Sumanovski, Caroline Kopp, Mira Kuisle, Fabio Longordo und Nicolas Wanaverbecq für die angenehme Atmosphäre im Labor danken. Nicolas Wanaverbecq gilt dabei ein spezieller Dank, da er immer ein offenes Ohr für meine Fragen hatte.

Renato Zedi und seinen Mitarbeitern von der Tierzuchtstation, der Bibliothekarin Frau Karin Flügel, sowie Remo Strittmatter und dessen Mitarbeiter von der mechanischen Werkstatt möchte ich herzlich für ihre Unterstützung und prompte Arbeit danken.

Meine Dissertation wurde vom Schweizerischen Nationalfonds zur Förderung der wissenschaftlichen Forschung finanziert. Der Reisefonds der Universität Basel und der Schweizer Gesellschaft für Physiologie ermöglichten mir die Teilnahme an den internationalen Konferenzen in Washington und Atlanta.

Der letzte Dank gilt allen mir nahestehenden Personen, die mich auf meinem Weg zum Ziel unterstützt haben.

# Table of contents

<b>Table of contents.....</b>	<b>1</b>
<b>1 Summary .....</b>	<b>3</b>
<b>2 Zusammenfassung.....</b>	<b>5</b>
<b>3 Introduction .....</b>	<b>7</b>
<b>The universality and versatility of Ca<sup>2+</sup> signalling: Ca<sup>2+</sup> sinks and Ca<sup>2+</sup> sources in neurons and exemplary cases .....</b>	<b>8</b>
3.1 Evolutionary aspects .....	10
3.2 Ca <sup>2+</sup> sources and Ca <sup>2+</sup> sinks in neuronal cells .....	10
3.2.1 Ca <sup>2+</sup> sources.....	11
3.2.1.1 Voltage-gated Ca <sup>2+</sup> -permeable channels .....	11
3.2.1.2 Ligand-gated Ca <sup>2+</sup> conducting channels.....	15
3.2.1.2.1 Plasmamembrane-bound ligand-gated Ca <sup>2+</sup> conducting channels .....	15
3.2.1.2.2 Intracellular Ca <sup>2+</sup> release channels .....	20
3.2.2 Ca <sup>2+</sup> sinks .....	23
3.2.2.1 The extrusion mechanisms .....	23
3.2.2.2 The sequestration mechanisms .....	27
<b>4 Aims of the thesis.....</b>	<b>30</b>
<b>5 Results .....</b>	<b>31</b>
5.1 Introduction to the paper .....	31
5.1.1 Mice lacking the gene encoding the Ca <sub>v</sub> 3.1 channel exhibit severe sleep disturbance .....	31
5.1.2 The role of Ca <sub>v</sub> 3 channels in the generation of NREMS related rhythms.....	32
5.1.3 Does Ca <sup>2+</sup> provided by Ca <sub>v</sub> 3 have a signalling role in nRt neurons? .....	35
5.2 Publication 1.....	37
5.3 Publication 2.....	89
<b>6 General discussion.....</b>	<b>108</b>
6.1 The role of Ca <sub>v</sub> 3 channels during nRt oscillations .....	108
6.2 SK channel gating during nRt oscillations .....	110
6.3 The role of SERCA during nRt oscillations.....	114
<b>7 Conclusions and outlook.....</b>	<b>117</b>
7.1 Gating of SK2 channels by Ca <sup>2+</sup> in nRt .....	118

7.2	Modulation of SK2 channel function in nRt .....	119
7.3	Consequences of SK2-lack on nRt function .....	120
7.4	SK2 channel function in sleep.....	121
<b>8</b>	<b>References .....</b>	<b>124</b>
<b>9</b>	<b>List of abbreviations.....</b>	<b>133</b>
<b>10</b>	<b>Curriculum vitae .....</b>	<b>136</b>

# 1 Summary

$\text{Ca}^{2+}$  ions play key signalling roles in all fundamental neurophysiological processes. The diversity of these roles is accomplished with astounding specificity, velocity and flexibility. Voltage-gated  $\text{Ca}^{2+}$  channels represent an important  $\text{Ca}^{2+}$  source in neurons, as they allow for  $\text{Ca}^{2+}$  influx upon excitatory electrical stimulation. My thesis has addressed the signalling roles of the third of the three major classes of VGCCs, the  $\text{Ca}_v3$   $\text{Ca}^{2+}$  channel family. These channels give rise to the low-voltage activated  $\text{Ca}^{2+}$  currents, also called T-type  $\text{Ca}^{2+}$  currents, and are predominantly found in neurons capable of generating rhythmic burst discharges. For example, in thalamic neurons,  $\text{Ca}^{2+}$  influx through these channels is well known to be critical for the generation of rhythmic burst discharges during neuronal oscillations typical during sleep. However, whether  $I_T$ -mediated  $\text{Ca}^{2+}$  entry adopts signalling roles in thalamic neurons has not been addressed. I hypothesized that identifying  $\text{Ca}^{2+}$ -dependent targets of  $\text{Ca}_v3$  channels in the thalamus would help to elucidate  $\text{Ca}^{2+}$ -dependent signalling processes related to sleep, and, thus, ultimately help to assess the roles of sleep in neuronal function. I have identified a dual signalling role for  $\text{Ca}^{2+}$  entry through  $\text{Ca}_v3$  channels using electrophysiological, imaging, genetic, and computational techniques. I also demonstrate that this  $\text{Ca}^{2+}$  signalling process occurs in a compartmentalized structure and is highly organized. In the nRt, which is well-known for its vigorous bursting activity during sleep-related large-scale oscillations, we found that  $I_T$ -mediated  $\text{Ca}^{2+}$  signalling is the dominant  $\text{Ca}^{2+}$  source in nRt dendrites, raising  $\text{Ca}^{2+}$  to a high level of  $\sim 0.7 \mu\text{M}/\text{burst}$ . In these dendrites, the  $\text{Ca}^{2+}$ -dependent SK2-type  $\text{K}^+$  channels are selective targets of T-type  $\text{Ca}^{2+}$ . These SK2 channels are located exclusively in nRt dendrites and are gated rapidly by  $I_T$ . However, this rapid coupling between T-type  $\text{Ca}^{2+}$  and SK channels is not static. Instead, we identified SERCA pumps as modulators of the functional complex of  $\text{Ca}_v3$  and SK2 channels. This modulation occurs in a competitive manner, since SERCA pumps sequester  $\text{Ca}^{2+}$  from the same pool of  $\text{Ca}^{2+}$  ions that gates SK2 channels, while  $\text{Ca}^{2+}$  entering through other sources is not taken up. The interplay of  $\text{Ca}_v3$  channels, SK2 channels and SERCA pumps suggests that nRt dendrites are specialized in handling T-type  $\text{Ca}^{2+}$  to regulate oscillatory dynamics. Moreover, my work suggests that these cells have developed unique strategies to handle large, repetitive  $\text{Ca}^{2+}$  oscillations, and to sequester them specifically, thereby potentially using them to control

endoplasmic reticulum-dependent neuronal functions, such as  $\text{Ca}^{2+}$ -induced  $\text{Ca}^{2+}$  release or even protein synthesis.

In collaborative efforts, we addressed the physiological relevance of our findings *in vivo* by studying the sleep behaviour and physiology of SK2 KO mice. Knocking out SK2, the selective target for T-type  $\text{Ca}^{2+}$ , revealed a strong attenuation of low-frequency rhythmic activity in the EEG during NREMS and a destabilization of sleep behaviour that is manifested by an enhancement of NREMS fragmentation. These data indicate that SK2 channels strongly control sleep, and the selective weakening of frequency bands related to nRt function indicates that the signalling complex identified in my work could act as an amplifier of the synaptic and cellular events leading to large-scale thalamocortical oscillations typical for normal sleep.

Altogether, my thesis presents a fully reconstructed link, from a single gene encoding a  $\text{Ca}^{2+}$ -gated  $\text{K}^+$  channel, to the mechanism of its gating via T-type  $\text{Ca}^{2+}$ , to its role in cellular activity, to one of the most dramatic disturbances of a healthy sleep EEG. I demonstrate that sleep is accompanied by large, unique  $\text{Ca}^{2+}$  signalling events in thalamic neurons that might contribute to steer the electroencephalographic manifestation and behavioural stabilization of sleep. I propose that the identification of the molecular basis of these processes will help identify targets to improve sleep quality in disease.

## 2 Zusammenfassung

$\text{Ca}^{2+}$ -Ionen spielen eine Schlüsselrolle in allen fundamentalen neurophysiologischen Prozessen. Die Vielfältigkeit dieser Rollen wird durch eine erstaunliche Spezifität, Geschwindigkeit und Flexibilität garantiert. Spannungsabhängige  $\text{Ca}^{2+}$ -Kanäle sind wichtige  $\text{Ca}^{2+}$ -Quellen in Neuronen, da sie als Antwort auf exzitatorische elektrische Stimuli einen  $\text{Ca}^{2+}$ -Einstrom erlauben. Spannungsabhängige  $\text{Ca}^{2+}$ -Kanäle werden in drei Hauptklassen unterteilt,  $\text{Ca}_v1$ ,  $\text{Ca}_v2$  und  $\text{Ca}_v3$ . In meiner Dissertation befasste ich mich mit der Frage, welche Rolle die spannungsabhängigen  $\text{Ca}^{2+}$ -Kanäle der  $\text{Ca}_v3$ - $\text{Ca}^{2+}$ -Kanalfamilie in der neuronalen Signalfunktion von  $\text{Ca}^{2+}$  spielen.  $\text{Ca}_v3$ -Kanäle findet man vorwiegend in Neuronen, die zu gebündelten rhythmischen Entladungen fähig sind.  $\text{Ca}_v3$ -Kanäle liegen der Generation von  $\text{Ca}^{2+}$ -Strömen zugrunde, die ihre Aktivierungsschwelle bei relativ hyperpolarisiertem Membranpotential haben, den sogenannten T-Strömen. In thalamischen Neuronen zum Beispiel sind T-Ströme entscheidend für die Generation von heftigen, rhythmischen Entladungen während schlaftypischen neuronalen Oszillationen. Ob jedoch  $\text{Ca}_v3$ -vermitteltes (T-typ)  $\text{Ca}^{2+}$  neben der elektrogenen Funktion auch eine Signalfunktion in thalamischen Neuronen innehat, wurde bisher nicht untersucht. Ich stellte die Hypothese auf, dass das Finden von Interaktionszielen des T-typ- $\text{Ca}^{2+}$  im Thalamus hilft, für Schlaf potenziell wichtige  $\text{Ca}^{2+}$ -abhängige Signalprozesse zu verstehen. Dies kann letztendlich helfen, die Rolle von Schlaf auf neuronaler Ebene zu verstehen. In meiner Dissertation habe ich mit elektrophysiologischen, bildgebenden, molekularbiologischen und computergestützten Techniken eine duale Signalfunktion von T-typ- $\text{Ca}^{2+}$  identifiziert. Des Weiteren zeige ich, dass diese  $\text{Ca}^{2+}$ -Signalprozesse räumlich abgegrenzt und in hohem Grad organisiert sind. In Neuronen des nRt, die für seine lebhaften, gebündelten Entladungsaktivitäten während schlafspezifischen Oszillationen bekannt sind, haben wir gezeigt, dass T-typ- $\text{Ca}^{2+}$  die intradendritale  $\text{Ca}^{2+}$ -Konzentration auf den hohen Wert von  $0.7 \mu\text{M}$  pro gebündelte Entladung rasch ansteigen lässt, und die dominante  $\text{Ca}^{2+}$ -Quelle in den Dendriten der Neuronen des nRt darstellt. Die im nRt ausschliesslich in den Dendriten exprimierten  $\text{Ca}^{2+}$ -abhängigen Kaliumkanäle des Typs SK2 sind ein selektives Ziel. Die schnelle funktionale Kopplung dieser beiden Kanäle ist nicht statisch. Wir haben gezeigt, dass die SERCA-Pumpen die Stärke dieser Kopplung modulieren. Die Modulation der Stärke der Kopplung des Signalkomplexes aus  $\text{Ca}_v3$ - und SK2-Kanälen basiert auf einer Konkurrenz zwischen SK2-



Kanälen und SERCA-Pumpen selektiv um T-typ- $\text{Ca}^{2+}$ . Das Zusammenspiel von  $\text{Ca}_v3$ -Kanälen, SK2-Kanälen und SERCA-Pumpen lässt vermuten, dass Dendriten des nRt im Umgang mit T-typ-  $\text{Ca}^{2+}$  spezialisiert sind, um die Dynamik von Oszillationen zu regulieren. Die Resultate meiner Arbeit lassen sogar vermuten, dass diese Zellen eine einzigartige Strategie im Umgang mit grossen, repetitiven Konzentrationsschwankungen von dendritischem  $\text{Ca}^{2+}$  entwickelt haben, und mit dessen spezifischen Aufnahme möglicherweise ihre ER-abhängigen Funktionen, wie CICR oder Proteinsynthese, kontrollieren. Die Kollaboration mit einer anderen Forschungsgruppe ermöglichte es uns, Fragen über die physiologische und verhaltensbiologische Bedeutung unserer Resultate *in vivo* nachzugehen, indem wir das Schlafverhalten und die Schlafphysiologie von SK2 KO Mäusen untersuchten. SK2 KO Mäuse zeigen im EEG während des NREMS eine ausgeprägte Verminderung von niederfrequenten Rhythmen und eine Destabilisierung des Schlafverhaltens, das sich in einer Zunahme der Schlafunterbrüche äussert. Diese Resultate deuten darauf hin, dass SK2 den Schlaf stark kontrolliert. Weiter deutet die selektive Verminderung von Frequenzbändern, welche mit der Aktivität des nRt in Zusammenhang stehen, darauf hin, dass der dreiteilige, funktionelle Komplex als Verstärker von synaptischen oder zellulären Funktionen agieren könnte, die im gesunden Organismus zu schlaftypischen thalamocorticalen Oszillationen führen.

Zusammenfassend beschrieb ich in meiner Dissertation einen komplett rekonstruierten Zusammenhang zwischen einem einzigen Gen, welches einen  $\text{Ca}^{2+}$ -abhängigen Kaliumkanal codiert, über dessen selektiven Öffnung durch T-typ- $\text{Ca}^{2+}$ , deren physiologischen Bedeutung auf zellulärer Ebene, und einer der dramatischsten Störungen eines Schlaf EEGs. Ich zeige, dass Schlaf von grossen  $\text{Ca}^{2+}$ -Signalen in thalamischen Neuronen begleitet ist, welche beitragen die elektroenzephalographische Manifestation und die Stabilisierung des Schlafverhaltens zu lenken. Ich denke, dass die Identifikation der molekularen Basis dieses Prozesses helfen wird, pharmakologische Ansätze zur Verbesserung der Schlafqualität im kranken Organismus zu finden.

# **3 Introduction**

# **The universality and versatility of $\text{Ca}^{2+}$ signalling: $\text{Ca}^{2+}$ sinks and $\text{Ca}^{2+}$ sources in neurons and exemplary cases**

Otto Loewi, the Nobel laureate in physiology or medicine from 1936, once said: “Ja, Kalzium das ist alles...”. Indeed,  $\text{Ca}^{2+}$  ions are a most ubiquitous and versatile cellular messenger that couple electrical excitation to the activation of intracellular enzymes and signal transduction cascades.  $\text{Ca}^{2+}$  ions control a seemingly endless number of physiological processes, ranging from classical examples such as rapid muscle contraction and neurotransmitter release, to dendritic integration and synaptic plasticity, to long-term changes in gene transcription, cell proliferation and death, and thus ultimately to brain development, sensory motor control, learning and memory, and cognitive processing (Petersen et al., 2005). Thanks to the universality and diversity of  $\text{Ca}^{2+}$  signalling, the brain is uniquely able to adapt and modify its function for the long-term in response to brief, salient stimuli. In fact, a fully  $\text{Ca}^{2+}$ -independent cellular process has been documented in only a few cases (see e.g. (Akiba and Sato, 2004; Doherty and Walsh, 1991)).

The universality and versatility of  $\text{Ca}^{2+}$  functions is enabled through the diversification of its signalling mechanisms at multiple levels, from the initial  $\text{Ca}^{2+}$  entry to the ultimate signalling tasks.

First, the  $\text{Ca}^{2+}$  signalling network is composed of a relatively limited number of  $\text{Ca}^{2+}$  sinks and sources, each of which, however, is found in multiple isoforms with different biophysical properties and subcellular locations.

Second,  $\text{Ca}^{2+}$  signals vary in terms of their spatio-temporal patterning.  $\text{Ca}^{2+}$  signals may take place within spatial domains ranging from nanometres to meters (Berridge, 1997) and time windows ranging from fractions of seconds to days. This gives rise to a highly irregular distribution of intracellular  $\text{Ca}^{2+}$  levels within the cytosol at any given moment in time. For example,  $\text{Ca}^{2+}$  ions control fast and highly localized processes such as the fusion of neurotransmitter-containing synaptic vesicles (Schneggenburger and Neher, 2000), which occur at the synaptic terminals within nanometer domains. On the other hand,  $\text{Ca}^{2+}$  ions link dendritic electrical activity to slowly occurring changes in gene expression, triggered in the nucleus that is tens of micrometers distant (Finkbeiner and Greenberg, 1998).

Third, thousands of  $\text{Ca}^{2+}$ -sensitive proteins with different affinities, and subcellular locations act as  $\text{Ca}^{2+}$  sensors. Some of these proteins, such as calbindin or parvalbumin, merely act as buffers for  $\text{Ca}^{2+}$ , some others, such as PKC and phospholipase A, use  $\text{Ca}^{2+}$  as a trigger for enzymatic activities, or, like CaM, act as a mediator without any intrinsic enzymatic activity as  $\text{Ca}^{2+}$  sensors or signal transducers for other proteins (Heizmann and Hunziker, 1991).

Fourth, some  $\text{Ca}^{2+}$  signalling components are regulated or modulated by other signalling compounds and pathways, including  $\text{Ca}^{2+}$  itself (Catterall, 2000). The rate, for example, of  $\text{Ca}^{2+}$  sequestration by SERCA pumps is dependent on the  $[\text{Ca}^{2+}]_L$  (Solovyova et al., 2002).

Fifth, in addition to the role of  $\text{Ca}^{2+}$  as a second messenger and a direct gating molecule,  $\text{Ca}^{2+}$  acts, like all cations, as a positive charge carrier in neurons. Electrochemically driven  $\text{Ca}^{2+}$  entry into the cytoplasm gives rise to an electrical signal. The electrogenic function further adds to the diversity of  $\text{Ca}^{2+}$  signalling because  $\text{Ca}^{2+}$  entry results in membrane depolarization. For example, in thalamic neurons, the influx of  $\text{Ca}^{2+}$ -carried positive charge through low voltage-activated  $\text{Ca}^{2+}$  channels triggers the generation of rhythmic burst discharges, as typically occurs during slow-wave sleep (Pape et al., 2004).

In summary,  $\text{Ca}^{2+}$  plays a trimodal signalling role by acting as a second messenger, a direct gating molecule and an electrogenic signal carrier.

The aim of this introductory chapter is to introduce the reader to the diversity of the neuronal  $\text{Ca}^{2+}$  sinks and sources. Based on review articles, this chapter is intended to highlight that  $\text{Ca}^{2+}$  has evolved into a selective signalling ion in spite of its ubiquity and universality. Furthermore, we wish to stress that the diversity of the basic elements of  $\text{Ca}^{2+}$  signalling in terms of molecular composition, kinetics, and spatial distribution underlies the specificity of  $\text{Ca}^{2+}$  signalling. For each of the  $\text{Ca}^{2+}$  sources and sinks mentioned, we will describe their basic biophysical properties relevant for their function, and we will focus in particular on highlighting some of the best known physiological processes in which these sources and sinks are well characterized and functionally interesting. The introductory chapter will not introduce the reader to the numerous down-stream  $\text{Ca}^{2+}$ -sensitive proteins and modulators of  $\text{Ca}^{2+}$  sinks and  $\text{Ca}^{2+}$  sources.

### 3.1 Evolutionary aspects

About 3.3 billion years ago, when the first living cells started to develop,  $\text{Ca}^{2+}$  was abundant in the igneous rocks of the hot earth's crust. However,  $\text{Ca}^{2+}$  was bound as  $\text{CaO}$  and therefore not available for use. Heavy rainfalls dissolved the  $\text{Ca}^{2+}$  and cooled the earth, leading to various chemical and biological reactions and eventually to further dissolution of free  $\text{Ca}^{2+}$ . This sudden rise of extracellular free  $\text{Ca}^{2+}$  caused serious problems for early life, since a high  $\text{Ca}^{2+}$  concentration leads to organellar damage, causes the aggregation of proteins and nucleic acids, and leads to precipitation of phosphates (Jaiswal, 2001). It is believed that this evolutionary pressure led to the evolution of the  $\text{Ca}^{2+}$  handling mechanisms aimed at keeping a low  $[\text{Ca}^{2+}]_i$ .

Several arguments offer an explanation to why  $\text{Ca}^{2+}$  was preferred as an intracellular signalling molecule over other ions such as  $\text{Na}^+$ ,  $\text{K}^+$  or  $\text{Mg}^{2+}$ , which are also abundant in biological systems. First, the uniquely large  $\text{Ca}^{2+}$  gradient (1000-fold, compare to  $\text{Na}^+$ : 10-fold) that exists across the plasma membrane allowed for a robust  $\text{Ca}^{2+}$  influx that could be used as an external signal. Secondly,  $\text{Ca}^{2+}$  has, compared to the other ions, a favourable chemical nature (Jaiswal, 2001).  $\text{Ca}^{2+}$  ions exhibit, for example, a high affinity to the oxygen in carboxylate groups found frequently in amino acids (Jaiswal, 2001). Another parameter allowing  $\text{Ca}^{2+}$  to evolve into the favourite signalling molecule is its rapid binding kinetics.  $\text{Ca}^{2+}$  binds to and dissociates from a protein more quickly by a factor of up to  $\sim 100$  compared to  $\text{Mg}^{2+}$  (Jaiswal, 2001). Furthermore,  $\text{Ca}^{2+}$  exhibits, due to its ionic radius, high coordination numbers and often irregular coordination geometry, which puts  $\text{Ca}^{2+}$  at an advantage in acting as a cross-linker in biology (Jaiswal, 2001). Finally,  $\text{Ca}^{2+}$  is able to bind in a unique manner to components of biological membranes like long-chain alkyl carboxylates and phosphatidylserine, a phospholipid, and affect the orientation, fluidity and fusion of the membranes (Jaiswal, 2001).

### 3.2 $\text{Ca}^{2+}$ sources and $\text{Ca}^{2+}$ sinks in neuronal cells

The extracellular free  $\text{Ca}^{2+}$  concentration ( $\sim 1\text{-}2$  mM) is about 10,000 times higher than the resting free  $[\text{Ca}^{2+}]_i$  ( $\sim 50\text{-}100$  nM) and is therefore abundantly available to cells. However,

it is not usable for intracellular  $\text{Ca}^{2+}$  signalling unless it is capable of crossing the plasmamembrane barrier and entering the cytosol. At this moment,  $\text{Ca}^{2+}$  levels increase dramatically, and have been estimated to go up to 0.1 mM in localized signalling events such as neurotransmission, thus leading to a 1000-fold decrease in the  $\text{Ca}^{2+}$  gradient across the membrane. To handle these extreme fluctuations in intracellular levels of  $\text{Ca}^{2+}$ , specialized  $\text{Ca}^{2+}$  entry pathways must exist to allow the exchange of  $\text{Ca}^{2+}$  between the extracellular and intracellular compartments. Moreover, due to the toxicity of free intracellular  $\text{Ca}^{2+}$ ,  $[\text{Ca}^{2+}]_i$  must be returned to basal levels as soon as possible, though without compromising its signalling function. This task is achieved by high-affinity cytosolic  $\text{Ca}^{2+}$  buffers and efficient extrusion and sequestration systems.

The goal of this chapter is to highlight the biophysical diversity of the restricted number of basic  $\text{Ca}^{2+}$  signalling network components, which guarantee  $\text{Ca}^{2+}$  entry into the cytosol and its sequestration or extrusion.

### **3.2.1 $\text{Ca}^{2+}$ sources**

#### ***3.2.1.1 Voltage-gated $\text{Ca}^{2+}$ -permeable channels***

Voltage-gated channels that act as a  $\text{Ca}^{2+}$  source can be divided into the classical VGCCs and voltage-gated cation channels. These  $\text{Ca}^{2+}$ -permeable ion channels sense the membrane potential and react to its depolarization by opening a gate that allows  $\text{Ca}^{2+}$  to enter the cell. Voltage-gated  $\text{Ca}^{2+}$  channels mediate a rapid, selective  $\text{Ca}^{2+}$  influx in response to membrane depolarization, whereas cation channels are permeable to several cations. Notably, most, if not all, neuronal cells express more than one type of VGCCs (Hille, 1992), highlighting the need for a diversity of  $\text{Ca}^{2+}$  entry according to the extracellular signals to be conveyed. Indeed, the pharmacological blockade of single classes of VGCCs typically abolishes the transduction of membrane depolarization into distinct cellular responses, despite the presence of multiple  $\text{Ca}^{2+}$  channels in the same cells (Goldberg and Wilson, 2005). Thus, it is not the increase in  $\text{Ca}^{2+}$  per se, but indeed the specific portal through which it enters the cytosol, which determines the cellular response.

The diversity of  $\text{Ca}^{2+}$  channels is evident when considering their molecular constitution. The VGCCs are composed of four or five distinct subunits ( $\alpha_1$ -,  $\beta$ -,  $\alpha_2$ -,  $\delta$ - and  $\gamma$ -subunit). The pore-forming  $\alpha_1$ -subunit, which is organised in four homologous domains (I-IV), comprises

the voltage sensor and gating apparatus, and most of the known sites of channel modulation by G-protein, phosphorylation,  $\text{Ca}^{2+}$ /CaM, drugs, and toxins (Catterall, 2000). The intracellular  $\beta$ - and extracellular  $\alpha_2$ -subunit, and the  $\delta$ -subunit have an auxiliary function and further modulating properties, such as phosphorylation (Catterall, 2000). Ten different types of VGCCs  $\alpha_1$ -subunits have been cloned, which are pooled into 3 subfamilies, the  $\text{Ca}_v1$  subfamily with 4 members,  $\text{Ca}_v1.1$  to  $\text{Ca}_v1.4$ , the  $\text{Ca}_v2$  and the  $\text{Ca}_v3$  subfamilies with 3 members each.

This diversity in the molecular composition gives rise to an assortment of  $\text{Ca}^{2+}$  currents with distinct voltage dependence and kinetic properties, two characteristics that essentially determine the amplitude and time course of intracellular  $\text{Ca}^{2+}$  signals. Traditionally, these were divided into two major classes. The LVA currents, which exhibit a low activation threshold of activation of about  $\sim -70$  mV, and the HVA currents, which are activated at membrane potentials positive to approximately  $-30$  mV (Hille, 1992). LVA currents typically activate around resting membrane potentials after a hyperpolarizing input, decay comparatively rapidly, with a decay time of  $\tau \sim 20$ -50 ms and show a low single-channel conductance (4-11 pS). Because of their transient activation characteristics, they were named T-type  $\text{Ca}^{2+}$  currents (T for transient) (Hille, 1992). Four different currents were distinguished within the family of HVA currents. The L-type currents exhibit a very large single-channel conductance ( $\sim 25$  pS) and a slow decay time of  $\tau > 1$  s. This current has been named L-type  $\text{Ca}^{2+}$  current due to its long-lasting kinetics (L for long) (Catterall, 2000). The N-type  $\text{Ca}^{2+}$  current (N for new) differs from the L- and the T-type  $\text{Ca}^{2+}$  currents in terms of its intermediate voltage dependence and its different inactivation kinetics (more negative and faster than L-type, but more positive and slower than T-type). Last, the P/Q and the R-currents, exhibiting properties comparable to those of the N-type  $\text{Ca}^{2+}$  current, were distinguished by their pharmacological properties and their strong expression in cerebellar cells (P for Purkinje, R for Resistant) (Catterall, 2000). These basic biophysical differences suggest that, by virtue of their intrinsic characteristics, the VGCC family is structured so that it may represent a  $\text{Ca}^{2+}$  source for different physiological needs. Indeed, it turns out that the long-lasting L-type  $\text{Ca}^{2+}$  currents are typically involved in activity-dependent gene expression, in synaptic plasticity, and cell survival (Lipscombe et al., 2004), whereas N-, R- and P/Q-type  $\text{Ca}^{2+}$  currents are well-known for their role in neurotransmitter release (Catterall, 2000) and  $\text{I}_T$  mediate neuronal rebound bursts (Perez-Reyes, 2003). Additionally,  $\text{Ca}^{2+}$  currents play distinct roles in shaping neuronal excitability. One of the most prominent roles has been described in recent years and involves the generation of dendritic  $\text{Ca}^{2+}$

transients in response to a critical frequency of back-propagating APs, of coincident synaptic input, and of AP discharge (Larkum et al., 2003).

It is now clear that the original classification of  $\text{Ca}^{2+}$  currents in terms of their gating properties has a molecular correlate in the three major types of  $\alpha_1$ -subunit cloned so far. Indeed, heterologous expression of these in mammalian cell lines or *Xenopus* oocytes largely reproduces some of the essential current properties, including activation range, kinetics and pharmacology. Channels, which belong to the  $\text{Ca}_v1$  subfamily, have been found to mediate L-type currents, whereas channels belong to the  $\text{Ca}_v2$  subfamily mediate P/Q- ( $\text{Ca}_v2.1$ ), N- ( $\text{Ca}_v2.2$ ) and R-type  $\text{Ca}^{2+}$  currents ( $\text{Ca}_v2.3$ ). The channels, which belong to the  $\text{Ca}_v3$  subfamily mediate the  $I_T$ . Further diversification in detailed properties, such as voltage dependence, current density, drug sensitivity and binding properties to intracellular synaptic proteins, like CASK, SNAP-25, syntaxin and Mint-1, arises from splice variants of the  $\alpha_1$  pore-forming subunit and from auxiliary subunit isoforms that are expressed in the recorded cells (Catterall et al., 2005).

In addition to the differences conferred by their molecular properties, other aspects of  $\text{Ca}^{2+}$  channels contribute to the diversity of their function as a  $\text{Ca}^{2+}$  source. Among the most important aspects are their selective coupling to downstream effectors, modulation by G-proteins, and phosphorylation (Catterall, 2000). For example the selective coupling of  $\text{Ca}_v2.1$  or  $\text{Ca}_v2.2$  to syntaxin, a component of the SNARE protein complex critical for the fusion of synaptic vesicles with the presynaptic membrane, shifts the voltage dependence of steady-state inactivation during long depolarizing prepulses towards more negative membrane potentials, which results in the inhibition of the channel activity (Catterall, 2000). G-protein-mediated modulation of channel properties has been predominantly reported from the  $\text{Ca}_v2$  subfamily. Multiple G-protein coupled pathways interact with  $\text{Ca}_v2$  channels, further increasing the diversity of the channel. In rat sympathetic ganglion neurons, for example,  $\text{Ca}_v2.2$  channels are regulated by five different G-protein coupled pathways (Dolphin, 2003). The activation of the  $G_i$ - or  $G_s$ -protein coupled receptors, such as  $\text{GABA}_B$  receptors,  $\alpha_2$ -adrenergic receptors, A1 adenosine receptors and the opioid receptors  $\mu$  and  $\delta$ , decelerate the current activation kinetics of  $\text{Ca}_v2.1$  and  $\text{Ca}_v2.2$  channels and shift their activation threshold towards more positive membrane potentials via direct binding of the  $G_{\beta\gamma}$  subunit with the consequence of channel inhibition (Dolphin, 2003). This  $G_i$ - or  $G_s$ -protein coupled receptor-mediated channel inhibition is reversed by direct phosphorylation of the channels via PKC, which indicates a crosstalk between different G-protein coupled pathways in modulating VGCC activity (Catterall, 2000).



Hyperpolarization-activated HCN channels are voltage gated ion channels, traditionally known to be permeable to  $\text{Na}^+$  and  $\text{K}^+$  cations. However, it has been recently demonstrated that they are slightly permeable to  $\text{Ca}^{2+}$ , rendering them members of voltage-gated channels that act as a  $\text{Ca}^{2+}$  source (Yu et al., 2004; Zhong et al., 2004). HCN channel-mediated current is typically activated by a hyperpolarized membrane potential below approximately -60 mV, gates with an activation time constant ranging between hundreds of milliseconds and seconds, and shows no inactivation (Frère et al., 2004). HCN channels are best known as pacemakers for rhythmic discharges in cardiac sinoatrial cells and some central neurons, but whether  $\text{Ca}^{2+}$  entry through HCN channels plays a role in this function, and other functions attributed to this channel (Frère et al., 2004), is not yet clear. So far, this  $\text{Ca}^{2+}$  permeability was found in heterologously expressed HCN4 channels and made up 0.6% of the inward current evoked at -120 mV (Yu et al., 2004). Whole-cell recordings in dorsal root ganglia neurons revealed an  $I_{\text{HCN}}$ -induced increase of  $[\text{Ca}^{2+}]_i$ , which was associated with an elevation of the membrane capacitance. From this it has been suggested that  $\text{Ca}^{2+}$  ions have caused membrane fusion, thus possibly implicating it in neurotransmission (Yu et al., 2004).

*Physiological function attributed to VGCCs:* Synaptic transmission is one of the most prominent and well characterized physiological processes in which VGCCs are involved. We describe here an example highlighting the diversity of VGCCs based on the example of GABA release at distinct hippocampal inhibitory synapses.

Hippocampal pyramidal cells of the CA3 area receive GABAergic inputs from morphologically, immunocytochemically, and electrophysiologically distinct interneurons, which arise in different strata and show distinct innervation patterns (Freund and Buzsáki, 1996). GABAergic interneurons produce both perisomatic and dendritic inhibition, and determine the timing of AP discharge of hippocampal pyramidal neurons through their embedding in feed forward and feedback circuits (Freund and Buzsáki, 1996). Distinct subtypes of VGCC mediate GABA release in different interneurons (Poncer et al., 1997). Dual recordings from *stratum oriens* interneurons and postsynaptic CA3 pyramidal cells revealed that unitary IPSPs were blocked after bath application of 200 nM of the P/Q-type  $\text{Ca}^{2+}$  current ( $\text{Ca}_v2.1$ ) blocker  $\omega$ -agatoxin IVA. The bath application of the N-type  $\text{Ca}^{2+}$  current ( $\text{Ca}_v2.2$ ) blocker  $\omega$ -conotoxin MVIIA (1  $\mu\text{M}$ ) however, had nearly no effect on GABA induced IPSPs. Conversely, dual recordings from *stratum radiatum* interneurons and postsynaptic CA3 pyramidal cells revealed that IPSPs were blocked after bath application of  $\omega$ -conotoxin MVIIA, but remained unchanged after the application of  $\omega$ -agatoxin IVA. These

results show that GABAergic interneurons from different regions (*stratum oriens* and *radiatum*) express a defined type of VGCC at presynaptic release sites. Considering that all VGCCs, and in that particular example, Ca<sub>v</sub>2.1 and Ca<sub>v</sub>2.2 channels and the related currents, differ in their biophysical and kinetic properties, it is likely that the predominant expression of a given VGCC gives rise to interneuron-specific GABA release characteristics, such as different release rates and release timing (Hefft and Jonas, 2005).

### **3.2.1.2 Ligand-gated Ca<sup>2+</sup> conducting channels**

Ligand-gated, plasmamembrane-bound Ca<sup>2+</sup>-conducting channels represent an additional pathway for Ca<sup>2+</sup> entry into neurons. This family is made up of channels activated by the neurotransmitters acetylcholine and glutamate, acting as extracellular ligands, or by cyclic nucleotides, acting as intracellular ligands.

#### **3.2.1.2.1 Plasmamembrane-bound ligand-gated Ca<sup>2+</sup> conducting channels**

The three Ca<sup>2+</sup>-conducting channels, which are gated by extracellular ligands, are the nAChRs and the glutamate-gated channels: The NMDARs and the AMPARs.

Neuronal nAChRs are pentameric acetylcholine-activated ion channels composed out of four different types of subunits. Nicotinic AChR are involved in functional processes as diverse as cognition, learning and memory, arousal, and metabolism as well as in many pathological conditions such as epilepsy, Alzheimer's and Parkinson's disease, schizophrenia, Tourette's syndrome, anxiety, and depression (Paterson and Nordberg, 2000). Channel gating opens a cation-permeable pore that conducts not only Ca<sup>2+</sup>, but also Na<sup>+</sup> and K<sup>+</sup>, and induces a rapid plasma membrane depolarization (Rogers and Dani, 1995). Growing evidence indicates that neuronal nAChRs are not limited to postsynaptic locations, but are also present at pre-, peri-, and extrasynaptic locations of the CNS, where they modulate neurotransmitter release (Paterson and Nordberg, 2000). Two different classes of neuronal nAChRs are distinguished by their Ca<sup>2+</sup> permeability, their sensitivity to  $\alpha$ -BTX, and their structural properties. The first class is  $\alpha$ -BTX sensitive, contains the subunits  $\alpha$ 7- $\alpha$ 9 and exhibits a variable and high level ( $P_{Ca}/P_{Na} \sim 6-80$ ) Ca<sup>2+</sup> permeability. The second group is  $\alpha$ -BTX insensitive, contains the subunits  $\alpha$ 2- $\alpha$ 6 and exhibits low Ca<sup>2+</sup> permeability ( $P_{Ca}/P_{Na} \sim 0.2-3.8$ ) (Fucile, 2004). Furthermore, neuronal nAChRs exhibit a range of single-channel

conductances between 5 and 50 pS and of desensitization time constants between 100ms and 2 s, depending on the specific subunit and tissue expression. Both types of nAChRs are widely expressed in the CNS and the functional differences between these two groups and the different isoforms within them are far from being understood (Fucile, 2004). Nevertheless, this high degree of diversity suggests specific physiological roles for distinct neuronal nAChR subtypes.

The NMDARs are a glutamate-gated cationic channels with an important contribution to excitatory synaptic transmission in the CNS (Dingledine et al., 1999). These channels are one of the most eminent ion conducting proteins in neuroscience in terms of its versatility in  $\text{Ca}^{2+}$  signalling being implicated in many aspects of synaptic plasticity. N-methyl-D-aspartate receptors play a crucial role in controlling synaptic plasticity-dependent AMPAR trafficking, are involved in structural modifications of the neuron associated with synaptic plasticity, and play a decisive role in major forms of homeostatic synaptic plasticity (Carlisle and Kennedy, 2005; Derkach et al., 2007; Perez-Otano and Ehlers, 2005). The cation permeability through the cationic NMDAR is highly voltage-dependent. At resting membrane potentials, cation permeability, and therefore  $\text{Ca}^{2+}$  influx through activated NMDARs is largely inhibited by a  $\text{Mg}^{2+}$  ion blocking the ion channel pore. Depolarization positive to  $\sim -50$  mV ejects the  $\text{Mg}^{2+}$  ions out of the channel pore and allows  $\text{Ca}^{2+}$  conductance. N-methyl-D-aspartate receptors are 5 to 10 times more permeable to  $\text{Ca}^{2+}$  than to  $\text{K}^{+}$  or  $\text{Na}^{+}$  (Hille, 1992). In the nervous system at least 6 different NMDAR subunits have been cloned, NR1, NR2A-2D, and NR3A-3B (Cull-Candy et al., 2001). Each combination of the different subunits and their splice variants that form functional channels gives rise to distinct biophysical channel properties that are critical for the  $\text{Ca}^{2+}$  signals provide. The assembling of NR1, for example, with any of the four different NR2 subunits increases the current conductance from 5- to 60-fold compared to homomeric NR1 channels (Squire, 2002). Furthermore, the NR2 subunits have markedly different decay kinetics, with NR2A-containing NMDARs producing the fastest and NR2D-containing NMDARs the slowest EPSC. Slow decaying NMDAR-mediated currents are predominant during early phases of development, whereas during experience-dependent maturation of circuits they are gradually replaced by more rapidly decaying isoforms (Cull-Candy et al., 2001).

The glutamate-activated AMPARs form the third group of ligand-gated, plasmamembrane-bound  $\text{Ca}^{2+}$ -conducting channels. AMPARs are tetrameric, voltage-

independent ion channels composed of four subunits, GluR1-4. For these receptors, the incorporation of the GluR2 subunit reduces the channel's  $\text{Ca}^{2+}$  permeability, which leads to the mediation of negligible  $\text{Ca}^{2+}$  influx, whereas receptors lacking the GluR2 subunit are highly permeable and exhibit distinctly fast kinetics. For example, in Bergmann glial cells, where only 3% of the expressed subunits are GluR2 subunits, the  $\text{Ca}^{2+}/\text{Na}^+$  permeability ratio is  $\sim 2.8$  and the time courses of deactivation and desensitization are around  $\tau \sim 1.0$  ms and  $\tau \sim 3.2$  ms respectively. Conversely, in neocortical layer V pyramidal cells, where 75% of the expressed subunits are GluR2 subunits, the  $\text{Ca}^{2+}/\text{Na}^+$  permeability ratio is  $\sim 0.07$  and the time courses of deactivation and desensitization are  $\tau \sim 2.5$  ms and  $\tau \sim 11.2$  ms respectively (Liu and Zukin, 2007). The subunit composition of AMPARs changes during synaptic plasticity. For example, cerebellar parallel fiber-stellate cell synapses express AMPARs, which are devoid of the GluR2 subunit. High frequency (50 Hz) activation of these synapses leads to the insertion of GluR2 subunits with the consequence of a reduced  $\text{Ca}^{2+}$  influx and thereby to the induction of LTD. In contrast, the inhibition of synaptic activity has the opposite effect. (Liu and Zukin, 2007). This activity dependent change of channel composition, which leads to a change of  $\text{Ca}^{2+}$  permeability, represents a particular form of synaptic plasticity.

*Physiological function attributed to extracellular ligand-gated  $\text{Ca}^{2+}$  conducting channels:* Long-term synaptic plasticity is the most prominent and well characterized physiological process in which NMDAR-mediated  $\text{Ca}^{2+}$  signalling is involved (Malenka and Bear, 2004).  $\text{Ca}^{2+}$  signalling through these channels underlies the induction of these long-term changes in structure, morphology and physiology of synapses (Perez-Otano and Ehlers, 2005).

We describe here an example illustrating that modifications in NMDAR composition underlie changes in hippocampus dependent learning behaviour. In the adult hippocampus, NR2A- and NR2B-containing NMDARs are the major contributors to synaptic NMDAR currents. NR2B-containing channels differ from NR2A-containing channels in their slower deactivation time, their larger  $\text{Ca}^{2+}$  permeability and their coupling to intracellular signalling partners important for plasticity (Kopp et al., 2007). Aged rats have deficits in spatial learning behavior due to an age-related decrease of NR2B expression (Magnusson et al., 2002). Thus, in young rats with a deficit of NR2B in the hippocampus, the success in tests to assess spatial learning, such as the Morris water maze, and the generation of LTP are impaired (Clayton et al., 2002). Conversely, overexpression of NR2B in the hippocampus facilitates synaptic potentiation and increases success in spatial learning (Tang et al., 1999). These examples

impressively demonstrate that alterations in the composition of channel subunits, whether experimentally introduced or resulting from aging, importantly shape synaptic plasticity and hippocampus-dependent learning.

There are two major  $\text{Ca}^{2+}$  sources provided by  $\text{Ca}^{2+}$ -permeable channels gated by intracellular ligands, the TRP channels and the CNG channels.

TRP channels are a remarkably diversified class of  $\text{Ca}^{2+}$  sources composed of at least 28 channel subunit genes. TRP channels are cation-permeable channels that could be grouped into seven subfamilies (TRPA, TRPC, TRPV, TRPM, TRPA, TRPP, and TRPL) on the basis of amino acid sequence homology (Ramsey et al., 2006). TRP channels show some similarities to VGCCs in the general structure of the transmembrane domains, as both are consist of six (S1-S6) transmembrane segments and a pore region between S5 and S6. The  $\text{Ca}^{2+}$  conductance varies within the different TRP subtypes. Most of the TRP channels exhibit little preference for  $\text{Ca}^{2+}$  ( $P_{\text{Ca}}/P_{\text{Na}} = 1-10$ ). A minor group and some splice variants show either  $\text{Na}^+$  selectivity ( $P_{\text{Ca}}/P_{\text{Na}} < 0.05$ ) or  $\text{Ca}^{2+}$  selectivity ( $P_{\text{Ca}}/P_{\text{Na}} > 100$ ), such as TRPV5, TRPV6 and a splice variant of TRPM3 (TRP3 $\alpha$ 2) (Ramsey et al., 2006). Although many different physiological mechanisms have been implicated with TRP channel activity and the resulting  $\text{Ca}^{2+}$  influx, the physiological role of TRP channel-mediated  $\text{Ca}^{2+}$  signalling is still unknown (Clapham, 2003). More recently, TRP channels have been implicated in store-operated  $\text{Ca}^{2+}$  entry based on knock-down experiments, which have shown that the elimination or the reduction of TRP expression can decrease native store-operated  $\text{Ca}^{2+}$  entry; however, this has been shown for other  $\text{Ca}^{2+}$  conducting channels, such as the CNG channel CNG2, as well (Ramsey et al., 2006). Furthermore, no mammalian TRP channel has yet explicitly fulfilled the electrophysiological criteria for store-operated channels. For example, no TRP channel exhibits the required high  $\text{Ca}^{2+}$  selectivity ( $P_{\text{Ca}}/P_{\text{Na}} \sim 1000$ ) or low single channel conductance ( $< 0.1$  pS) (Clapham, 2003).

The repertoire of stimuli leading to TRP channels includes not only ligands, but also physical stimuli. Several of these TRP channels recruited by a single stimulus modality are now known to confer distinct sensations, such as temperature, touch, pain, and taste (Clapham, 2003). The established modes of activation are subdivided into three general categories (Ramsey et al., 2006). First, receptor-based activation requires the recruitment of PLC by  $G_q$ -protein-coupled receptors and receptor tyrosine kinases can modulate TRP channel activity via the hydrolysis of  $\text{PIP}_2$  into the second messengers DAG and  $\text{IP}_3$ . This

form of regulation has been described predominantly for TRPC channels, which are mainly expressed in the CNS. Second, in the ligand-induced activation, exogenous small organic molecules, such as capsaicin or icilin; endogenous lipids or products of lipid metabolism, such as DAG or IP<sub>3</sub>; purine nucleotides and their metabolites and inorganic ions, such as Ca<sup>2+</sup> and Mg<sup>2+</sup>, have been shown to activate TRP channels. This form of activation is typical for TRPC channels as well and for some TRPM channels. Third, in the activation through physical stimuli, TRP channels seem to be gated by changes in temperature and by mechanical stimuli. Temperature-dependent gating has been described in TRP channels of the V-, M- and P-type and gating after a mechanical stimulus has been found in TRPP channels (Clapham, 2003; Ramsey et al., 2006).

CNG channels are non-selective cation channels that are gated by cyclic nucleotides, such as cAMP and cGMP (Craven and Zagotta, 2006). In contrast to ligand-gated receptors gated by extracellular ligands, CNG channels do not desensitize in the presence of the ligand, which render them a potentially strong Ca<sup>2+</sup> provider. Vertebrate CNG channels are tetramers composed of various combinations of 6 different subunits (CNGA1-4, CNGB1 and CNGB3). Whereas CNGA1, CNGA2, and CNGA3 form homomeric channels in heterologous expression systems, CNGA4, CNGB1, and CNGB3 do not form functional homomeric channels, but can co-assemble with other subunits to form heteromers and therefore give rise to more diversity. Probably most native CNG channels are heteromeric compositions (Craven and Zagotta, 2006). The different combination of subunits allows the expression of tissue-specific CNG channels with unique properties according to its physiological role. For example: The relative Ca<sup>2+</sup> permeability varies between different cell types and tissues. Whereas the Ca<sup>2+</sup> permeability of CNG channels in retinal cones is  $P_{Ca}/P_K = 8$ , the Ca<sup>2+</sup> permeability in retinal rods is  $P_{Ca}/P_K = 1.7$  (Zufall et al., 1997). This diversity on a cellular level could be explained by the different subunit composition of CNG channels in rods (CNGA1 and CNGB1) and cones (CNGA3 and CNGB3) (Craven and Zagotta, 2006; Kaupp and Seifert, 2002).

Cyclic nucleotide-gated channels are best known for their role in phototransduction and olfactory signalling (Craven and Zagotta, 2006). In vertebrate rod photoreceptors, direct binding of intracellular cGMP leads to an inward current of Na<sup>+</sup> and Ca<sup>2+</sup>. In the dark, when cGMP-levels are high, CNG channels are permanently open and contribute to the so called dark current, which triggers the glutamatergic neurotransmitter signals to the retinal cells. The Ca<sup>2+</sup> influx during darkness is not only participating in the depolarization of the cell, but also

controlling the activity of numerous down-stream  $\text{Ca}^{2+}$ -sensitive proteins, such as guanylyl cyclase-activating protein, whose stimulation gives rise to a positive feedback loop by stimulating guanylyl cyclase that then catalyses cGMP synthesis (Squire, 2002). Furthermore, both the  $\text{Ca}^{2+}$ -mediated depolarization, which increases the open probability of the channel, and the change in  $[\text{Ca}^{2+}]_i$ , due to the formation of a  $\text{Ca}^{2+}/\text{CaM}$  complex whose binding to some of the CNG channels inhibits the channel's allosteric opening transition, can modulate CNG channel properties (Matulef and Zagotta, 2003).

Cyclic nucleotide-gated channels have also been found expressed in non-sensory neurons, such as in the hippocampus, the cerebellum, and the cortex (Kaupp and Seifert, 2002), where their roles are not as well understood as in phototransduction and olfactory signalling (Craven and Zagotta, 2006).

*Physiological function attributed to intracellular ligand-gated  $\text{Ca}^{2+}$  conducting channels:* Among the most extensively characterized physiological roles of TRP channel-mediated  $\text{Ca}^{2+}$  influx is its involvement in growth cone guidance (Ramsey et al., 2006). Changes in  $[\text{Ca}^{2+}]_i$  play an important role in growth cone guidance by regulating growth cone morphology, the cytoskeleton and the trafficking of membrane precursor vesicles. Axon extension is guided by guiding cues, such as BDNF and netrin-1. BDNF-induced growth cone attraction requires  $\text{Ca}^{2+}$  influx through TRPC channels in rat cerebellar granule cells (Li et al., 2005). Conversely, netrin-1-induced growth cone attraction requires  $\text{Ca}^{2+}$  influx through  $\text{Ca}_v1$  channels and  $\text{Ca}^{2+}$  release from intracellular  $\text{Ca}^{2+}$  stores (Hong et al., 2000). These papers suggest that different chemotactic cues require defined  $\text{Ca}^{2+}$  sources to trigger particular types of  $\text{Ca}^{2+}$  signalling. Using short interfering RNA techniques, Li and colleagues showed, furthermore, that out of three expressed TRPC channels (TRPC1, TRPC3 and TRPC6) in the growth cone, only TRPC3 and TRP6 are specifically required for BDNF-induced growth cone attraction of cerebellar granule cells. However, TRPC3 is not involved in neurite outgrowth (Ramsey et al., 2006). Therefore, it seems that the diversity of TRP channels allows for the generation of  $\text{Ca}^{2+}$  signals that are specific for distinct regulatory functions in the growth cone.

### 3.2.1.2.2 *Intracellular $\text{Ca}^{2+}$ release channels*

From the extracellular space, neurons have access to an infinite supply of  $\text{Ca}^{2+}$  that accesses the cells' interior on given defined stimuli. In addition to this abundant source,

intracellular  $\text{Ca}^{2+}$  stores within the endoplasmic/sarcoplasmic reticulum provide a more finite internal store for which  $\text{Ca}^{2+}$  itself is a principal activator. In addition to its well-known cell biological role in the synthesis and processing of proteins, phospholipids and leukotrienes, the ER is an intracellular  $\text{Ca}^{2+}$  store that controls  $\text{Ca}^{2+}$  homeostasis and yet is also able to boost externally generated  $\text{Ca}^{2+}$  signals. Accordingly, the ER is equipped with  $\text{Ca}^{2+}$  channels and transporters in its membrane and a set of  $\text{Ca}^{2+}$  binding proteins in its lumen, such as calreticulin and calnexin, which control diverse aspects of ER function.  $\text{Ca}^{2+}$  release from the ER, is controlled by two families of  $\text{Ca}^{2+}$  channels. The  $\text{Ca}^{2+}$ -gated RYR and the  $\text{IP}_3\text{R}$  (Fill and Copello, 2002; Foskett et al., 2007; Verkhratsky, 2005).

There are three RYRs, which are best known for their role in excitation-contraction coupling in muscle. However, all three isoforms are expressed in neurons, and reach particularly high densities in somata and terminals. RYRs share a tetrameric structure and are activated by  $[\text{Ca}^{2+}]_i$  within the range of 1-10  $\mu\text{M}$ , depending on the subunit composition of the channel (Fill and Copello, 2002; Verkhratsky, 2005). The biophysical properties of the RYRs exhibit fast activation kinetics ( $\tau \sim 0.5\text{-}1\text{ms}$ ) and large conductance (100-500 pS), rendering them powerful  $\text{Ca}^{2+}$  providers in spite of a limited  $\text{Ca}^{2+}$  selectivity ( $P_{\text{Ca}}/P_{\text{K}} \sim 6\text{-}7$ ) (Fill and Copello, 2002). RYRs are triggered by intracellular free  $\text{Ca}^{2+}$  provided from either plasmamembrane-bound  $\text{Ca}^{2+}$  channels or neighbouring endomembrane bound receptors, leading to a phenomenon called CICR (Verkhratsky, 2005).  $\text{Ca}^{2+}$ -induced  $\text{Ca}^{2+}$  release has been shown to occur in many regions of the CNS after physiologically relevant stimulation (Verkhratsky, 2005). A particularly well-known example is the synaptically evoked CICR in boutons of hippocampal neurons, where the CICR-mediated  $\text{Ca}^{2+}$  transient has been associated with the mediation of short-term plasticity (Emptage et al., 2001). This example shows that CICR is critically involved in spatial and temporal aspects, as well as the strength of  $\text{Ca}^{2+}$  signalling (see below) (Verkhratsky, 2005).  $\text{Ca}^{2+}$  release by RYRs is positively modulated by the second messenger cyclic ADP ribose, a nucleotide metabolite, which is typically produced after hypoxia (Verkhratsky, 2005). Furthermore, another important modulator is  $\text{Ca}^{2+}$  itself. Increasing  $[\text{Ca}^{2+}]_L$  enhances the sensitivity of RYRs and eventually also of  $\text{IP}_3\text{Rs}$  (Verkhratsky, 2005). This  $\text{Ca}^{2+}$ -dependent modulation adds to the diversity of RYR-dependent  $\text{Ca}^{2+}$  signalling by providing the ER with a kind of memory by accumulating and storing information of former  $\text{Ca}^{2+}$  transients (Verkhratsky, 2005).



Like RYRs, IP<sub>3</sub>Rs are endomembrane-bound, Ca<sup>2+</sup>-selective ion channels of the endoplasmic reticulum and the Golgi apparatus, which are sensitive to the second messenger IP<sub>3</sub> and to Ca<sup>2+</sup>. The generation of IP<sub>3</sub> is based on the stimulation of PLC via G-protein-linked, metabotropic receptors or tyrosine kinase-linked receptors. Hydrolysis of PIP<sub>2</sub> by PLC leads to the second messengers DAG and IP<sub>3</sub>. There is strong evidence in neurons that this mechanism is relevant for the generation of localized Ca<sup>2+</sup> signals during synaptic transmission or in the emergence of Ca<sup>2+</sup> waves that spread from dendrites to soma (Verkhatsky, 2005).

Three different subunits (IP<sub>3</sub>R1-3) with various splice variants assemble into hetero- or homotetrameric channels, with IP<sub>3</sub>R1 being the dominant isoforms expressed in neurons. IP<sub>3</sub>Rs are synergistically activated by IP<sub>3</sub> and Ca<sup>2+</sup>. Therefore, in addition to CICR triggered by the gating of RYRs, activation of IP<sub>3</sub>Rs may also be involved (Foskett et al., 2007). The effects of Ca<sup>2+</sup> on the IP<sub>3</sub>Rs are such that low levels (300-400 nM) activate, whereas high levels become inhibitory. The ability of Ca<sup>2+</sup> to stimulate its own release is regulated by IP<sub>3</sub>, whose presence is required to allow Ca<sup>2+</sup> to act. The role of IP<sub>3</sub> could thus be seen as a compound that enhances cytosol excitability, such that Ca<sup>2+</sup> can provoke a boosting of its own signal.

The activity of IP<sub>3</sub>Rs is modulated by many factors such as ATP, interluminal divalent cations, like Ca<sup>2+</sup> itself, phosphorylation through cyclic AMP-dependent PKA, PKC and PKG, tyrosine kinase, and CaM-dependent protein kinase, and a large number of interacting proteins including CaM (Foskett et al., 2007).

*Physiological function attributed to endomembrane-bound ligand-gated Ca<sup>2+</sup> conducting channels:* A well-known illustration for the physiological relevance of Ca<sup>2+</sup> release from internal stores is the induction of LTD by mGluR-driven IP<sub>3</sub>-induced Ca<sup>2+</sup> release in cerebellar PC. These neurons have the largest and most arborized dendritic arbour of all vertebrate neurons and are filled with an elaborate network of ER that extends throughout the dendrites into the synaptic spines. This ER shows a high density of IP<sub>3</sub>Rs in both its dendritic and spinous protrusions. Paired stimulation of afferent excitatory inputs onto PCs, the climbing fibres and parallel fibres, produces LTD of parallel fibre inputs. In animals deficient in mGluR1 or IP<sub>3</sub>Rs such LTD cannot be induced (Aiba et al., 1994; Inoue et al., 1998). Furthermore, reintroduction of mGluRs and photolytic intracellular release of caged IP<sub>3</sub> successfully restores LTD induction (Ichise et al., 2000; Khodakhah and Armstrong, 1997). It was convincingly demonstrated that, indeed, a burst of synaptic activation of parallel

fibers leads to a biphasic pattern of  $\text{Ca}^{2+}$  accumulation in PC dendrites, the faster one being mediated by ionotropic AMPARs, the slower one being abolished with drugs that block mGluRs or  $\text{IP}_3$ Rs. Thus, it appears that the conjoint activation of  $\text{IP}_3$ -coupled pathways with the gating of VGCCs, resulting from the suprathreshold climbing fiber input, is necessary for LTD induction. This example provides a representative case for the powerful role of  $\text{IP}_3$  release in the dynamics of  $\text{Ca}^{2+}$  signalling. However the precise role of  $\text{IP}_3$  in the induction of LTD remains to be resolved, because it has recently been reported that selective activation of mGluR1 is sufficient to induce LTD attenuating mGluR-induced slow EPSC and  $\text{IP}_3$ R-mediated increase of  $[\text{Ca}^{2+}]_i$  (Jin et al., 2007).

### 3.2.2 $\text{Ca}^{2+}$ sinks

#### 3.2.2.1 *The extrusion mechanisms*

The maintenance of  $\text{Ca}^{2+}$  homeostasis requires a powerful extrusion system to compensate for  $\text{Ca}^{2+}$  influx and to restore the resting  $[\text{Ca}^{2+}]_i$ . Two membrane-bound extrusion systems, the PMCA and the  $\text{Na}^+/\text{Ca}^{2+}$  exchangers, are essentially responsible for  $\text{Ca}^{2+}$  extrusion in neurons (Guerini et al., 2005). Their function consists not only “cleaning up” excessive  $\text{Ca}^{2+}$ , but also further shaping the amplitude and time course of  $\text{Ca}^{2+}$  signals.

The PMCA is a membrane-bound extrusion pump, which hydrolyses ATP to transport  $\text{Ca}^{2+}$  from the cytosol into the extracellular medium (Thayer et al., 2002). The PMCA has a high affinity to  $\text{Ca}^{2+}$  with a  $K_{1/2}$  starting from 0.2  $\mu\text{M}$  (Garcia and Strehler, 1999), but a limited transport capacity with a turnover rate in the order of 10-50  $\text{s}^{-1}$  (i.e. number of  $\text{Ca}^{2+}$  transported per unit time) (Strehler and Zacharias, 2001). This means that, under physiological conditions, during which  $[\text{Ca}^{2+}]_i$  is about 0.1  $\mu\text{M}$ , PMCA is permanently active. It has been suggested therefore, that PMCA functions as a fine-tuner of  $[\text{Ca}^{2+}]_i$ , already extruding  $\text{Ca}^{2+}$  at a sub-micromolar level, and therefore keeping the  $[\text{Ca}^{2+}]_i$  low (Guerini et al., 2005).

Four different isoforms (PMCA1-4) have been characterized, which are expressed in a tissue specific manner. PMCA1 and 4 are expressed in almost all tissues, whereas the isoforms 2 and 3 are predominantly expressed in a restricted manner in the nervous system. The complexity is increased by numerous alternative splice variants, which affect the

expression localization, modulation and biophysical properties of the pump (Strehler and Zacharias, 2001; Thayer et al., 2002). This varied diversity in cellular and subcellular expression as well as the diversity of the isoforms and their splice variants and the resulting differences in biophysical properties suggesting a cell and cell-compartment specific function of the different PMCA. Isoform or even splice-variant specific biophysical properties and physiological roles are very difficult or not yet possible to address *in vivo*. There are many reasons for this. For example: First, standard methods for the investigation of pump activity, such as patch clamping, do not allow for successful measurements due to the low turnover rate of the PMCA. Second, there are neither isoform nor splice variant specific pharmacological inhibitors available. Third, most cells express more than one type and splice variant of PMCA (Strehler and Zacharias, 2001).

The extrusion rate of PMCA is  $[Ca^{2+}]_i$ -dependent in a hyperbolic manner. Under resting conditions, PMCA are characterized by a low binding affinity for  $Ca^{2+}$  ( $K_{1/2} \sim 10\text{-}20 \mu\text{M}$ ), which, however, rises  $\sim 100$ -fold ( $K_{1/2} \sim 0.2\text{-}0.5 \mu\text{M}$ ) after an increase of  $[Ca^{2+}]_i$  within a range of  $0.1 \mu\text{M}$  to  $1 \mu\text{M}$ . This  $Ca^{2+}$ -dependent regulation of PMCA function has been shown to occur via an autoinhibitory action of CaM at low  $[Ca^{2+}]_i$  (Garcia and Strehler, 1999). When  $[Ca^{2+}]_i$  increases, the formation of the  $Ca^{2+}$ -CaM-PMCA complex induces a conformational change that unmasks the active site of the pump (Guerini et al., 2005). The sensitivity to CaM differs between the different isoforms and their splice variants. PMCA2b ( $K_{1/2}=2.1 \text{ nM}$ ) exhibit, for example, an approximate 5 fold higher CaM affinity than PMCA4b ( $K_{1/2}=9.8 \text{ nM}$ ), and an approximate 4 fold higher affinity than PMCA2a ( $K_{1/2}=8.4 \text{ nM}$ ) (Strehler and Zacharias, 2001).

Due to its biophysical properties, such as low turnover rate and high  $Ca^{2+}$  affinity, PMCA were thought to “simply” maintain the resting level of  $[Ca^{2+}]_i$ . It has been show however, that PMCA play an active role in  $Ca^{2+}$  signalling, predominantly in the regulation of  $Ca^{2+}$  transients arising during cellular excitability (Strehler and Zacharias, 2001). Thus, PMCA activity is well-known for its role in sensory hair cell adaptation and its function in regulating excitatory synaptic transmission in hippocampal CA3 neurons (see below) (Garcia and Strehler, 1999). The important role of PMCA activity in sensory hair cell adaptation has been shown by an isoform-specific KO experiments that revealed that PMCA2 activity underlies the ability to hear. PMCA2 heterozygote mice are clearly hearing impaired (auditory brain stem response threshold 70-80 db compared to 30-45 db of WT mice) and PMCA2 null mice are deaf (Strehler and Zacharias, 2001).

In mammals two basic types of  $\text{Na}^+/\text{Ca}^{2+}$  exchangers have been described. The classical NCX exchange 3  $\text{Na}^+$  for each  $\text{Ca}^{2+}$  using the energy of the  $\text{Na}^+$  gradient set by the ATP-dependent  $\text{Na}^+/\text{K}^+$ -pump, whereas the second type of  $\text{Na}^+/\text{Ca}^{2+}$  exchangers, the NCKX is  $\text{K}^+$  dependent and co-exchanges one  $\text{Ca}^{2+}$  and one  $\text{K}^+$  for four  $\text{Na}^+$  ions.

The classical NCX have a lower affinity to  $\text{Ca}^{2+}$  ( $K_{1/2}$  0.6-6  $\mu\text{M}$ ), compared to the PMCAs, and the clearance rate increases exponentially with a rise in  $[\text{Ca}^{2+}]_i$  (Blaustein and Lederer, 1999). This comparatively greater efficacy of the NCXs enables them to handle the rapid extrusion (turn-over rate in range of 1000 to 5000 $\text{s}^{-1}$  for NCX1 (Blaustein and Lederer, 1999)) of large amounts of  $\text{Ca}^{2+}$ . It has been suggested therefore, that PMCAs and NCXs might work in a complementary way. Thus, PMCAs would control resting  $[\text{Ca}^{2+}]_i$  and extrude  $\text{Ca}^{2+}$  during rises in  $[\text{Ca}^{2+}]_i$  which are too low to activate NCXs, while NCXs would be responsible for the extrusion of large  $[\text{Ca}^{2+}]_i$  when PMCAs are saturated. In neurons, NCXs play a key role in the control of  $[\text{Ca}^{2+}]_i$  during synaptic transmission. Reduction of the  $\text{Na}^+$  gradient across the membrane, which has the consequence of a reduced NCX activity, increases the neurotransmitter release as many reports from mammalian peripheral and central synapses have shown. However the precise role of NCXs during vesicle release is not yet fully understood (Blaustein and Lederer, 1999).

Three isoforms (NCX1-3) are known to date, but whether there are biophysical differences between the three isoforms and their various splice variances is not yet clear. Therefore the diversity of NCXs is manifested in their different expression pattern and temporal variability of expression. All of the three NCX isoforms are expressed in the brain, but at different levels. NCX2 and NCX3 are expressed at high levels in the brain, whereas NCX1 is predominantly expressed in the heart (Guerini et al., 2005).

NCX expression shows strong activity-dependence. It has been reported that NCX2 genes are down-regulated within 30-60 minutes after depolarization of the membrane in developing cerebellar neurons (Guerini et al., 2005). The quick down-regulation of NCX2 has been shown to be dependent on the activity of the  $\text{Ca}^{2+}$ -dependent phosphatase calcineurin. This indicates that  $\text{Ca}^{2+}$  can directly modulate the amount of  $\text{Ca}^{2+}$  exchanger protein in the neuron (Guerini et al., 2005). Furthermore, the expression of the different isoforms changes during development. NCX3 becomes strongly up-regulated after chronic membrane depolarization during the process of maturation, while the total amount NCX1 remains unaltered. This has the consequence of an increased total amount of NCXs. These fast up- and

down regulations of particular NCX isoforms during development let one assume different physiological significances for the three isoforms.

K<sup>+</sup>-dependent Na<sup>+</sup>/Ca<sup>2+</sup> exchangers extrude one cytosolic Ca<sup>2+</sup> and K<sup>+</sup> in exchange for 4 Na<sup>+</sup>. In contrast to NCXs, NCKXs exhibit a higher affinity to Ca<sup>2+</sup> (for NCKX1-2: K<sub>1/2</sub> ~1-2 μM), and a lower maximum turnover rate (for NCKX1: 2 -115 s<sup>-1</sup>) (Blaustein and Lederer, 1999; Visser and Lytton, 2007). It is expected that, based on the sequence identity, the other NCKX isoforms exhibit the same biophysical properties (Visser and Lytton, 2007). K<sup>+</sup>-dependent Na<sup>+</sup>/Ca<sup>2+</sup> exchangers are therefore dedicated to reduce intracellular Ca<sup>2+</sup> to a low nanomolar concentration.

Five different isoforms (NCKX1-5) have been described so far with distinct expression patterns (Visser and Lytton, 2007). Although little differences in the biophysical properties are expected, the distinct expression pattern of the different isoforms suggests isoform-specific physiological significances.

It has been shown by several studies that NCKX-mediated Ca<sup>2+</sup> extrusion plays a prominent role in neuronal Ca<sup>2+</sup> clearance. In axon terminals of rat neurohypophysis, ~90% of Ca<sup>2+</sup> exchange based Ca<sup>2+</sup> clearance is K<sup>+</sup> dependent. A predominant contribution to Ca<sup>2+</sup> clearance by NCKX has also been demonstrated in the calyx of Held and in hippocampal CA1 neurons (Visser and Lytton, 2007).

*Physiological function attributed to the extrusion system.* We describe here how the diversity of PMCAs regulates excitatory synaptic transmission in hippocampal CA3 neurons. Alternative splicing at the C-terminal of a given PMCA isoform produces two functionally different variants: the splice variant “a” is more rapidly activated by Ca<sup>2+</sup> and extrudes Ca<sup>2+</sup> at a higher rate compared to the PMCA splice variant “b”, which exhibits long-lasting extrusion properties at high rates (Strehler and Zacharias, 2001). The spatially defined expression of a particular splice variant of a specific PMCA isoform is important for synaptic transmission (Jensen et al., 2007). Western blot analysis and immunohistochemical studies of hippocampal tissue, which expresses all PMCA isoforms (PMCA1-4), revealed that splice variant PMCA2a is selectively enriched at excitatory presynaptic terminals within the CA3 region. Electrophysiological experiments in CA3 hippocampal slices showed that the inhibition of PMCAs, either via increasing/lowering the pH, or through pharmacological blockade, enhances the frequency, but not the amplitude, of mEPSC. In contrast, although PMCA2a is present in some inhibitory presynaptic terminals within the hippocampal CA3, neither the

frequency nor the amplitude of mIPSCs changed after inhibition of PMCA (Jensen et al., 2007). Furthermore the paired-pulse ratio of evoked IPSCs, which is an indicator of presynaptic release probability, was not significantly altered after inhibition of PMCA. In contrast, the paired-pulse ratio of evoked EPSCs increased by an increment of the second EPSC, indicating an enhanced synaptic release, arbitrated by the PMCA-inhibition-mediated increase of presynaptic  $[Ca^{2+}]$ . These experiments nicely show that the compartmentalized expression of alternatively spliced PMCA isoforms is important for basic aspects of synaptic transmissions. In the example above a specific splice variant of a particular PMCA isoform (PMCA2a) is selectively enhanced in presynaptic terminals of predominantly excitatory synapses of the hippocampal CA3 region.

### 3.2.2.2 *The sequestration mechanisms*

Beside the two membrane-bound extrusion systems, which extrude  $Ca^{2+}$  out of the cell, three further mechanisms are known to remove  $Ca^{2+}$  from the cytosol. The SERCA pumps of the ER and the Golgi apparatus, the SPCA of the Golgi apparatus, and the mCU represent the sequestration mechanism absorbing  $Ca^{2+}$  from the cytosol into the particular organelle. All three organelles, the mitochondria, the ER, and the Golgi apparatus are known to be  $Ca^{2+}$  stores (Rizzuto, 2001).

Sarco-Endoplasmic Reticulum  $Ca^{2+}$  ATPase pumps are endomembrane-bound ATPases of the ER and the Golgi apparatus, which are closely related to the membrane-bound PMCA, since both belong to the P-type pumps, which are characterized by the formation of a phosphorylated intermediate as a part of the catalytic cycle (Verkhatsky, 2005). The ER acts simultaneously as a  $Ca^{2+}$  source, relying on the activation of the two  $Ca^{2+}$  channels RYRs and  $IP_3$ Rs, and a  $Ca^{2+}$  sink through SERCA-based sequestration of intracellular  $Ca^{2+}$  into the lumen (Berridge et al., 2000). Sarco-Endoplasmic Reticulum  $Ca^{2+}$  ATPase pumps are therefore an important element in the homeostatic regulation of  $[Ca^{2+}]_i$  in neurons and ensure the appropriate filling of the ER with  $Ca^{2+}$ .

Three isoforms (SERCA1-3) have been characterized with various splice variants, which differ in their expression pattern and their biophysical properties (Pozzan et al., 1994; Sepulveda et al., 2004). Two of the three isoforms, type 3 and type 2, are expressed in the brain. The splice variant SERCA2b is ubiquitously expressed in central neurons, whereas the splice variants SERCA2a and SERCA3 are principally restricted to the cerebellar PC

(Verkhatsky, 2005). Consistent with these expression patterns, SERCA2-deficient mice exhibit embryonic lethality, whereas mice deficient in the variant SERCA2a survive to adulthood, albeit with severe cardiac hypertrophy, and SERCA3 KO mice exhibit no apparent disease phenotype during maturation (Prasad et al., 2004).

Neuronal SERCA pumps act on a comparatively rapid ( $< 100$  ms) time scales and have a high affinity for  $\text{Ca}^{2+}$  ( $K_{1/2} \sim 0.1-1 \mu\text{M}$ ). It has been suggested therefore that SERCA pump activity is at about 50% of its maximal rate at resting  $[\text{Ca}^{2+}]_i$  (Pozzan et al., 1994). This enables the ER to sequester and accumulate  $\text{Ca}^{2+}$  rapidly, very efficiently and, in high concentrations ( $100 \mu\text{M}$ ). The activity of SERCA pumps is regulated by several mechanisms such as by phosphorylation, ER-immanent  $\text{Ca}^{2+}$  binding proteins and  $\text{Ca}^{2+}$  itself (Pozzan et al., 1994). In central neurons, a 10 time increase of  $[\text{Ca}^{2+}]_i$  results in a 5-fold increase of SERCA pump activity (Favre et al., 1996; Verkhatsky, 2005). More interestingly, the level of free  $[\text{Ca}^{2+}]_L$  plays an important role in the regulation of SERCA pump activity. The speed of  $\text{Ca}^{2+}$  uptake increases 5-7 times in response to a decrease in  $[\text{Ca}^{2+}]_L$ , whereas replenishment of the ER slows down the velocity of SERCA pump activity (Favre et al., 1996).

Secretory-pathway  $\text{Ca}^{2+}$ -ATPase are endomembrane-bound ATPases of the Golgi apparatus, which belong, as do SERCA and PMCA, to the P-type pumps. Little is known about the diversity and function of SPCA in mammals. Most studies so far have been done in yeast, *C. elegans* and expression systems (Wuytack et al., 2002). Two isoforms are known in man (SPCA1 and SPCA2) with two splice variants in SPCA1. SPCA activity appears to be important for shaping intracellular  $\text{Ca}^{2+}$  signalling in yeast and expression systems (Wuytack et al., 2002).

The mCU is the primary supplier of  $\text{Ca}^{2+}$  into the mitochondria (Duchen, 2000b; Gunter et al., 2000).  $\text{Ca}^{2+}$  uptake into the mitochondria depends strictly on the electrochemical gradient, which is maintained by the mitochondrial NCX (Gunter et al., 2000). It has been suggested that mCU is likely an inwardly rectifying  $\text{Ca}^{2+}$  selective ion channel, but the exact nature and molecular structure of the mCU is still elusive (Duchen, 2000b). Although little is known about the diversity of mCU in terms of isoforms, kinetics or expression, it is generally agreed that mitochondrial  $\text{Ca}^{2+}$  sequestration plays an important physiological role in shaping amplitude and duration of transient elevation of  $[\text{Ca}^{2+}]_i$  (Duchen, 2000a). The inhibition of mitochondrial  $\text{Ca}^{2+}$  sequestration, for example, accelerates the secretion of catecholamines

from adrenal chromaffin cells, which is dependent on a transient increase of  $[Ca^{2+}]_i$  (Thayer et al., 2002).

*Physiological function attributed to the sequestration mechanisms:* The link between SERCA-mediated  $Ca^{2+}$  uptake and physiological processes is best understood in cardiac cells (Berridge, 2003), but an important physiological role for SERCA-mediated  $Ca^{2+}$  sequestration in neuronal  $Ca^{2+}$  signalling has been documented in dendritic spines, the sites of synaptic communication and plasticity (Majewska et al., 2000). The concurrent generation of back-propagating APs and EPSP induces a supralinear rise of  $[Ca^{2+}]_i$  in dendritic spines, which underlies synaptic plasticity. The duration of the small time window, in which the neuron interprets the two signals as coincident is therefore crucial for the regulation of the generation of long-term plasticity. It has been shown that SERCA-mediated  $Ca^{2+}$  sequestration is crucially involved in the regulation of the time window during which spines are able to maintain high  $[Ca^{2+}]_i$ . The initiation of back-propagating APs in CA1 pyramidal neurons causes an increase of  $[Ca^{2+}]_i$  in their spines, which is larger (average ratio of the peak  $[Ca^{2+}]_i$  between spine and dendrite:  $\sim 2.1$ ) than the  $[Ca^{2+}]_i$  observed in the dendrite. The decay of this back-propagating APs-induced rise of  $[Ca^{2+}]_i$  has a monoexponential slow time course ( $\tau \sim 1261$  ms) in dendrites, whereas in spines a biexponential time course, with a initial fast ( $\tau \sim 141$  ms) and a subsequent slow ( $\tau \sim 1367$  ms) phase, has been found (Majewska et al., 2000). Based on previous studies showing a major role for SERCA pumps in  $Ca^{2+}$  clearance in dendrites of pyramidal neurons (Markram et al., 1995), the authors postulated that SERCA pumps contribute to the fast phase of the biexponential decay time course found in spines. Indeed, application of CPA, a selective blocker of SERCA pumps, lengthened the fast phase from  $\sim 118$  ms to  $\sim 611$  ms, whereas the slow phase followed the slow decay kinetics of dendrites (Majewska et al., 2000). These experiments show a crucial role of SERCA pumps in controlling the temporal continuance of  $Ca^{2+}$  in spines after a back-propagating AP-induced rise of  $[Ca^{2+}]_i$  and, therefore, in determining the duration of the time window in which generation of long-term plasticity is possible.



## 4 Aims of the thesis

This thesis deals with the specificity of  $\text{Ca}^{2+}$  signalling in the thalamus. It has long been recognized that an important thalamic function is to generate oscillatory activity during sleep. Most recently, it has been demonstrated that the lack of a gene encoding a low voltage-activated  $\text{Ca}^{2+}$  channel of the T-type family ( $\text{Ca}_v3$ ) leads to severe sleep disturbances. It is well known that  $\text{Ca}_v3$  channels are important for a particular form of neuronal discharge, the so-called LT bursts. However, a major unknown aspect of  $\text{Ca}^{2+}$  signalling in the thalamus is whether  $\text{Ca}^{2+}$  entering through  $\text{Ca}_v3$  channels adopts important signalling roles within thalamic neurons. How large are the  $\text{Ca}^{2+}$  signals generated by  $\text{Ca}_v3$  channels? Which role do they play in  $\text{Ca}^{2+}$  signalling through LT bursts? Do they act as gating molecules? Can we find evidence for a specificity of signalling, and, if yes, what are the mechanisms? What is the role of  $\text{Ca}^{2+}$  sinks in oscillatory activity? Can we attribute physiological relevance to this specificity, perhaps even at the behavioural level?

In my thesis, I have addressed all these questions by focusing on a thalamic nucleus that vigorously participates in oscillations during sleep, the *nucleus reticularis thalami*.

We hypothesized that defining the  $\text{Ca}^{2+}$  sources leading to SK channel activation in these neurons could be relevant to several levels of research related to sleep oscillations. First, it could help to elucidate the principles of  $\text{Ca}_v3$  channel-dependent  $\text{Ca}^{2+}$  signals in more detail, in particular in relation to the efficacy and specificity of the  $\text{Ca}^{2+}$  signalling that they provide. Second, it was previously shown that nRt oscillations are dynamic, in that they are either on-going, or intrinsically dampened. This observation points to a variable strength of SK channel activation, but the reasons for this variability are unclear. Third, we envisaged employing the well-documented animals lacking defined SK channel subtypes to get insight into the molecular basis and subcellular distribution of SK channels in nRt, and hence in their relative position to the  $\text{Ca}^{2+}$  sources. Fourth, we speculated that, by clarifying the mechanisms of SK channel gating in a sleep pacemaker nucleus, we could weigh the role of nRt oscillatory activity in generating the physiological hallmarks of sleep, the EEG waves. Finally, we had great hopes that, by elucidating the biophysical and molecular underpinnings of sleep-related neuronal activity, we could eventually define molecular targets that could interfere with the quality and the quantity of sleep, one of the major sources of health deterioration in modern society.

## 5 Results

### 5.1 Introduction to the paper

The past decades have witnessed a major interest in the role of LT bursts in the TC system in relation to the control of arousal states (Bezdudnaya et al., 2006; Crunelli et al., 2006), and to rhythmogenesis (Contreras, 2006; Llinás et al., 2005). In particular, it is well known that myriads of neurons in the TC system co-operate to produce synchronized, rhythmic network activity that underlies the characteristic EEG sleep waves (Contreras, 2006; Crunelli et al., 2006).

Recently, genetically modified mice lacking a  $\text{Ca}^{2+}$  channel subunit of the  $\text{Ca}_v3$  channel family were described as showing major disturbances in sleep patterns. These were accompanied by a reduced EEG power in two prominent frequency bands of NREMS, the delta (1-4 Hz) and the spindle (8-10 Hz) range (Anderson et al., 2005; Lee et al., 2004). These genetic studies hence establish a direct link between a unique form of neuronal discharge and sleep, and complement the classic electrophysiological demonstrations of the tight association of LT bursts with the functional brain state of sleep (Contreras, 2006).

#### 5.1.1 Mice lacking the gene encoding the $\text{Ca}_v3.1$ channel exhibit severe sleep disturbance

In these mice, the global, unconditional deletion of  $\text{Ca}_v3.1$  causes a prominent loss of low-frequency components in the EEG of naturally sleeping mice. To these belong the  $\delta$ -oscillations at 1-4 Hz, which are predominantly found and representative in the EEG during NREMS. Furthermore, spindle waves (7-14 Hz), which are typically found during lighter stages of sleep or, accompanied by  $\delta$ -waves, at the transition between NREMS and REMS, are significantly reduced (Lee et al., 2004). No differences between  $\text{Ca}_v3.1$  mutant and WT mice could be found in waves typical to REMS and wake states, such as  $\theta$ - (5-10 Hz) and  $\beta$ -waves (10-20 Hz) respectively. At the level of sleep behavior, mice lacking  $\text{Ca}_v3.1$  exhibited a reduced total amount of sleep time (786 min versus 856 min in WT). This deficit could be explained by the animals showing an increased number of brief awakenings (typically < 16

sec) and a reduction of time spent in NREMS (637 min versus 704 min in WT), while the time spent in REMS remained unaltered compared to WT mice. In mice with a thalamus-restricted KO of the Cav3.1 gene, a reduction of NREMS time was also observed (Anderson et al., 2005). In contrast to the EEG data shown by Lee et al., Anderson et al. report, but without showing the data, a decreased  $\delta$ -wave power during NREM in unconditional and thalamus-restricted KO. Thus, in both unconditional and thalamus-restricted KO mice more detailed experiments at the EEG level are required.

Altogether, these KO mice demonstrate a critical role for low-threshold  $\text{Ca}^{2+}$  channels. The data show the massive effect of the deletion of a single Cav3 isoform has on the level of sleep behaviour and EEG, and indicate a critical role for the thalamus in the generation of sleep rhythms. What is known about the role of thalamic Cav3 channels in the generation of NREMS rhythms?

### **5.1.2 The role of Cav3 channels in the generation of NREMS related rhythms**

The generation of NREMS related EEG waves relies on the synchronized, rhythmic network activity of the neurons of the TC system, which is composed of interconnected network loops between the neocortex, the thalamus and the nRt (Crunelli et al., 2006; Steriade, 2003). In the last decades of the 20<sup>th</sup> century, extracellular and intracellular recordings of sleeping animals have provided the cornerstones around which our view of the role of thalamic and cortical activities in sleep physiology was shaped. Subsequently, *in vitro* recordings from brain slice preparations, some of which were serendipitously recognized as generating spontaneous oscillatory activities, refined our understanding of the cellular and network interactions during sleep.

At the beginning of this remarkable history of TC physiology related to sleep, such extracellular and intracellular *in vivo* studies during the NREM sleep of natural sleeping animals demonstrated that thalamic neurons generated a peculiar form of bursts of APs that crowned a slower depolarizing potential (Hirsch et al., 1983; McCarley et al., 1983). Such burst discharges could be artificially triggered by the injection of hyperpolarizing current. *In vitro* electrophysiological experiments revealed that the slow depolarizing potential could be triggered by brief (~50 ms) depolarization of a relatively hyperpolarized membrane (membrane potential below ~-70 mV) or by the hyperpolarization of a membrane at resting

potential. The slow depolarizing potential was subsequently called the LT spike, because of its activation threshold at comparatively hyperpolarized membrane potentials ( $\sim -70$  mV). Bursts of APs are generated after the LT spike has reached the threshold of AP generation ( $\sim -55$  mV). Isolated LT spikes, obtained by the application of the  $\text{Na}^+$  channel blocker TTX, are abolished after the application of  $\text{Ca}^{2+}$  conductance inhibitors, such as  $\text{CoCl}_2$  or  $\text{CdCl}_2$  (Jahnsen and Llinás, 1984; Llinás and Jahnsen, 1982). The voltage dependence, the low activation threshold, and the pharmacological characteristics of the LT spike prompted the idea that a  $\text{Ca}^{2+}$  conductance underlies the generation of LT spikes (reviewed by (McCormick and Bal, 1997)). Indeed, voltage-clamp recordings from isolated thalamic cells clearly revealed the presence of a  $\text{Ca}^{2+}$  current with characteristics consistent with the conductance mediating the LT spike (Huguenard and Prince, 1992; Pape and McCormick, 1990). The flow of  $\text{Ca}^{2+}$  ions hence plays an important electrogenic role in the generation of burst discharges, which are found in thalamic neurons during natural NREMS.

These classical recordings also brought the understanding to the point that cellular oscillatory characteristics, such as the frequency and pattern of discharge, could be directly correlated with the frequency bands of the sleep EEG. Thus, *in vivo* recordings during NREMS show that TC neurons generate rhythmic burst discharges in a frequency range of 0.5-4 Hz, which correlates with the frequency band of  $\delta$ -waves in the EEG. Although the full cellular basis of the EEG  $\delta$ -waves is still a matter of controversy, with both thalamic and cortical activities involved (Buzsáki and Gage, 1989), the recent  $\text{Ca}_v3.1$  KO experiments provide substantial support in favor of a significant thalamic contribution to these sleep waves. The intrinsic burst mechanism of TC neurons is based on an interplay between a  $\text{Ca}_v3$  channel-mediated  $I_T$  and the  $I_{\text{HCN}}$ . At relatively a hyperpolarized membrane potential such as it is typical for TC neurons during NREMS (Hirsch et al., 1983),  $I_{\text{HCN}}$ , which typically activates at membrane potentials below  $-60$  mV, pushes the membrane potential towards the activation threshold of  $\text{Ca}_v3$  channels. The following additional influx of positive charges builds up a LT spike, which depolarizes the membrane towards the threshold for a burst of APs. Deactivation of  $I_{\text{HCN}}$  and inactivation of  $I_T$  leads to a hyperpolarization of the membrane, which de-inactivates  $I_T$  and activates  $I_{\text{HCN}}$  again (reviewed by (McCormick and Bal, 1997)). This important involvement of  $\text{Ca}_v3$  channels in the generation of intrinsic rhythmic burst discharges in TC neurons has been recently confirmed by KO experiments (Kim et al., 2001), in which the lack of  $\text{Cav}3.1$  leads to a full abolishment of cellular burst discharges, while tonic activity is spared.

In addition to the  $\delta$ -rhythm, we also have an elaborate cellular understanding of spindle wave generation (10-15 Hz). Rather than being based on the oscillatory activity of single neurons, these waves arise out of an interplay between TC neurons and their immediate neighbours the nRt neurons. Similar to TC neurons, nRt neurons generate bursts of APs. The nRt is a GABAergic structure, which covers the dorso-lateral part of the thalamus and is, therefore, interposed between the cortex and the thalamus. Nucleus reticularis neurons project to TC neurons. In contrast to the bursts of TC neurons, nRt bursts are followed typically by an AHP, which is generated by the activation of SK channels (Avanzini et al., 1989; Bal and McCormick, 1993). This AHP is strong enough to de-inactivate  $Ca_v3$  channels and therefore allows nRt neurons to autonomously generate sequences of bursts discharges. In contrast to TC neurons, the oscillatory activity of nRt cells is thus based on  $Ca^{2+}$  entry during LT bursts, rather than on an intrinsic pacemaker current, such as  $I_{HCN}$ . The spontaneous oscillatory activity of nRt neurons is much greater than that of TC neurons, due to the fact that these cells possess an  $I_T$  with a voltage range of activation that is more depolarized. This spontaneous oscillatory activity, and also its intrinsic dampening, is critical for the initiation and synchronization of spindle waves.

Thus, *in vivo* intracellular recordings revealed that during EEG spindle wave generation TC neurons receive rhythmic IPSPs at the frequency of 7-14 Hz, which correlated with the frequency band of spindle waves. Both *in vivo* and *in vitro* studies demonstrated that these rhythmic IPSPs result from an activation of GABAergic nRt neurons. The IPSP-mediated hyperpolarization activates  $I_{HCN}$  and de-inactivates  $Ca_v3$  channels, which open during the cessation of IPSP. The following LT spike-mediated burst of APs activates nRt neurons by a feedback loop again. The frequency of spindle waves correlates with the time required for closing the loop between the activation of a nRt neuron, the generation of inhibitory postsynaptic potential in TC neurons, the occasional rebound burst response of these neurons, and the generation of an excitatory response in the nRt cell, further eliciting rebound bursting (reviewed by (McCormick and Bal, 1997)). Thus,  $Ca_v3$  channels drive synaptic oscillations, which oscillate within a frequency band that correlates with those of EEG spindle waves.

### 5.1.3 Does Ca<sup>2+</sup> provided by Ca<sub>v</sub>3 have a signalling role in nRt neurons?

Given the versatility of Ca<sup>2+</sup> as an intracellular signalling compound, it is plausible to speculate that Ca<sup>2+</sup> entry through Ca<sub>v</sub>3 channels may not be restricted to its electrogenic function. However, in spite of a large body of work on LT bursts and Ca<sub>v</sub>3 channels both *in vivo* and *in vitro*, still remarkably little is known about the signalling function of T-type Ca<sup>2+</sup>. However, several studies strongly suggest that T-type Ca<sup>2+</sup> might be important for the temporal dynamics of sleep-related oscillatory activity. For example, it was found previously by Bal and McCormick that blocking I<sub>H<sub>CN</sub></sub> produced a block of the waxing and waning characteristics of spindle waves at frequencies of about once per 10 s (Bal and McCormick, 1996). This block was accompanied by a reduction in the duration of a refractory period between spindles, during which the propensity of neurons to generate rebound bursts is much reduced. Subsequently, it was found that the neuronal activity found during spindle waves itself is responsible for this refractory period, because it was associated with a Ca<sup>2+</sup>-dependent upregulation of I<sub>H<sub>CN</sub></sub> (Lüthi and McCormick, 1998). This Ca<sup>2+</sup> originated from the repetitive rebound bursting of TC neurons involved in spindle waves and is thought to be linked to the stimulation of a Ca<sup>2+</sup>-sensitive adenylyl cyclase. The resulting cAMP increase is then responsible for persistently activating I<sub>H<sub>CN</sub></sub>, which is carried by channels directly binding cAMP. Thus, although the contribution of I<sub>T</sub> was not directly specified, this work provided strong support for the idea that the bursting activity of neurons during sleep was accompanied by specific Ca<sup>2+</sup> signalling systems and the production of second messengers. Currently, it remains a matter of speculation whether the periodic stimulation of cAMP synthesis during spindle waves has any additional functional implications related to sleep function.

Additional evidence for T-type Ca<sup>2+</sup> signalling was recently reported from thalamic midline neurons, in which T-type Ca<sup>2+</sup> triggers CICR (Richter et al., 2005). Interestingly, CICR is not triggered in thalamic neurons involved in primary sensory relay nor in nRt neurons (Richter et al., 2005).

Finally, it was previously recognized that apamin-sensitive SK channels are activated during the generation of rhythmic burst discharges in nRt neurons (Avanzini et al., 1989; Bal and McCormick, 1993). Moreover, preliminary studies indicated that apamin infusion into the brain could affect sleep states (Benington et al., 1995; Gandolfo et al., 1996). Much is known about SK channel gating in diverse neuronal cell types. In particular, it has been shown that

SK channels are often selectively coupled to certain  $\text{Ca}^{2+}$  channels, thereby influencing particular types of neuronal discharge. For example, studies in dopaminergic midbrain neurons revealed a selective functional coupling of  $\text{Ca}_v3$  channels to SK channels, which prevents burst firing and maintains pacemaker precision in these neurons (Wolfart and Roper, 2002).

## **5.2 Publication 1**



**A competition between SK2 channels and SERCAs  
for Ca<sup>2+</sup> entry through T-type channels  
gates sleep-related oscillations in thalamic dendrites**

**Authors**

Lucius Cueni<sup>1</sup>, Marco Canepari<sup>1</sup>, Rafael Luján<sup>2</sup>, Yann Emmenegger<sup>3</sup>, Masahiko Watanabe<sup>4</sup>,  
Chris T. Bond<sup>5</sup>, Paul Franken<sup>3</sup>, John P. Adelman<sup>5</sup> and Anita Lüthi<sup>1</sup>

**Affiliations**

<sup>1</sup> Division of Pharmacology and Neurobiology, Biozentrum, University of Basel, 4056 Basel, Switzerland

<sup>2</sup> Departamento de Ciencias Medicas, Universidad de Castilla-La Mancha, 02006 Albacete, Spain

<sup>3</sup> Center for Integrative Genomics, University of Lausanne, Lausanne-Dorigny, Switzerland

<sup>4</sup> Department of Anatomy, Hokkaido University School of Medicine, Sapporo 060-8638, Japan

<sup>5</sup> Vollum Institute, OHSU, Portland, Oregon 97239, USA

**Running title**

T-type Ca<sup>2+</sup> channels in thalamic dendrites

**Contact**

e-mail: [anita.luthi@unibas.ch](mailto:anita.luthi@unibas.ch); phone: (+41) 61 267 22 46; fax: (+41) 61 267 22 08

Number of characters (including spaces): 72'812

Number of Figures: 8

Supplemental Data and Figure Files: 1

Supplemental Movie: 1

**Acknowledgments:** We thank Proff. M. Tafti, K. Vogt and Dr. N. Wanaverbecq for constructive input, and A. Reisch for carrying out preliminary electrophysiological experiments. We thank Prof. Dr. B. Gähwiler and Drs. L. Acsády, A. Destexhe, U. Gerber, C. Kopp and D. Ulrich for stimulating discussions and helpful comments on the manuscript. This work was supported by grants from the Swiss National Science Foundation (A.L.), the NIH (P.F., J.P.A.) and the Spanish Ministry of Education and Science (R.L.). The authors declare no conflict of interest.

## Summary

**T-type  $\text{Ca}^{2+}$  currents underlie rhythmic burst discharges during neuronal oscillations typical for sleep. However,  $\text{Ca}^{2+}$ -dependent effectors selectively regulated by T-type  $\text{Ca}^{2+}$  currents remain unknown. We show that in the dendrites of *nucleus reticularis thalami* (nRt),  $[\text{Ca}^{2+}]_i$  increases are dominated by T-type  $\text{Ca}^{2+}$  currents and shape rhythmic bursting by creating a competition between  $\text{Ca}^{2+}$ -dependent SK-type  $\text{K}^+$  currents and  $\text{Ca}^{2+}$  uptake pumps. Via selective activation of dendritically located SK2 channels, oscillatory bursting is generated along major dendritic segments. The sequestration of  $\text{Ca}^{2+}$  by sarco/endoplasmic reticulum  $\text{Ca}^{2+}$ -ATPases (SERCAs), together with cumulative T-type  $\text{Ca}^{2+}$  channel inactivation, antagonizes SK2 channel activation and dampens oscillations. Mice lacking the SK2 channel gene demonstrate a >3-fold reduction in low-frequency rhythms in the electroencephalogram of non-rapid-eye-movement sleep. The interplay of T-type  $\text{Ca}^{2+}$  channels, SK2 channels, and SERCAs in nRt dendrites comprises a specialized organization handling  $\text{Ca}^{2+}$  entry through T-type  $\text{Ca}^{2+}$  channels to regulate oscillatory dynamics related to sleep.**

## Introduction

Neurons in the thalamocortical system co-operate to produce synchronized, rhythmic network activity that underlies slow waves characteristic of sleep electroencephalograms (EEGs) (Crunelli et al., 2006; Steriade, 2003). Rhythmogenesis is accompanied by low-threshold (LT) burst discharges in thalamic neurons which are carried by  $\text{Ca}_v3$   $\text{Ca}^{2+}$  channels and give rise to low-voltage-activated, T-type,  $\text{Ca}^{2+}$  currents (Perez-Reyes, 2003). Mice lacking the  $\text{Ca}_v3.1$  channel subunit fail to produce bursts in thalamocortical neurons and show reduced EEG power in prominent frequency bands of non-rapid-eye-movement sleep (NREMS) (Shin et al., 2006).

Although  $\text{Ca}^{2+}$  ions entering through T-type  $\text{Ca}^{2+}$  currents are the electrical charge carriers underlying LT bursts, the associated intracellular  $\text{Ca}^{2+}$  ( $[\text{Ca}^{2+}]_i$ ) dynamics and their role in sleep physiology remain largely unknown. To understand the role of T-type  $\text{Ca}^{2+}$  currents in sleep-related oscillations, elementary quantitative information about  $\text{Ca}^{2+}$  influx through T-type  $\text{Ca}^{2+}$  currents, their contribution to  $[\text{Ca}^{2+}]_i$  during a LT burst and their function in intracellular signalling is required. T-type  $\text{Ca}^{2+}$  channels have a lower unitary conductance than other types of  $\text{Ca}^{2+}$  channels and inactivate more rapidly (Perez-Reyes, 2003), suggesting that they might make only a minor contribution to total  $\text{Ca}^{2+}$  influx during neuronal discharges. However, in thalamic neurons, T-type  $\text{Ca}^{2+}$  currents are large (Perez-Reyes, 2003), and computational studies suggest that a high channel density is important for oscillatory LT bursts (Destexhe et al., 1996). Moreover, LT burst-dependent  $\text{Ca}^{2+}$  signalling shapes the temporal evolution of sleep-related oscillations *in vitro* (Blethyn et al., 2006; Pape et al., 2004), but the specific roles of  $\text{Ca}^{2+}$  entering through T-type  $\text{Ca}^{2+}$  channels and how they affect the sleep EEG have not been determined.

We hypothesized that targets selectively regulated by T-type  $\text{Ca}^{2+}$  currents would be important for controlling sleep-related cellular oscillations and could have implications for sleep physiology. We focused on the *nucleus reticularis thalami* (nRt), a thin inhibitory network interposed between thalamocortical projection neurons and the cortex that is important for information transfer and arousal control (Fuentelba and Steriade, 2005; Pinault, 2004). Lesioning the nRt leads to the disappearance of sleep-related spindle oscillations and produces attention neglect (Fuentelba and Steriade, 2005; Pinault, 2004). Prominent and well-characterized forms of rhythmic bursting in the nRt accompany the major forms of low-frequency EEG oscillations, in particular  $\delta$ -oscillations (1 - 4 Hz), spindle waves (10 - 15 Hz) and slow oscillations ( $< 1$  Hz) (Amzica et al., 1992; Domich et al., 1986; Steriade et al., 1993), but the nRt also generates bursts in response to sensory stimuli (Cotillon and Edeline,

2000). T-type  $\text{Ca}^{2+}$  channels in nRt are composed of  $\text{Ca}_v3.2$  and  $\text{Ca}_v3.3$  subunits (Talley et al., 1999) and are heavily expressed along the somatodendritic axis (Joksovic et al., 2005). In contrast to the  $\text{Ca}_v3.1$ -mediated bursts of thalamocortical neurons, nRt bursts are typically followed by an afterhyperpolarization (AHP) generated by small-conductance  $\text{Ca}^{2+}$ -dependent SK-type  $\text{K}^+$  currents (Avanzini et al., 1989; Bal and McCormick, 1993), and recruit additional, although molecularly unidentified,  $\text{Ca}^{2+}$ - and  $\text{Na}^+$ -dependent cationic conductances (Bal and McCormick, 1993; Blethyn et al., 2006). Therefore,  $\text{Ca}^{2+}$ -dependent ionic mechanisms in nRt cells are responsible for time-varying oscillatory bursting patterns that are, at least partly, dependent on  $\text{Ca}^{2+}$  entry through T-type  $\text{Ca}^{2+}$  currents. Dynamics and synchrony of these oscillatory activities are sculpted by synaptic input within thalamocortical loops, via brainstem afferents, and by reciprocal connections between nRt cells (Fustealba and Steriade, 2005; Pinault, 2004).

Our study reveals that  $\text{Ca}^{2+}$  influx through T-type  $\text{Ca}^{2+}$  channels during a single LT burst leads to a marked  $[\text{Ca}^{2+}]_i$  increase in nRt dendrites, in which SK2-containing SK channels are strongly expressed and are activated rapidly and selectively. Sarco/endoplasmic  $\text{Ca}^{2+}$  ATPases (SERCAs) compete with SK2 channels for available  $\text{Ca}^{2+}$  and attenuate the strength of nRt oscillations. In mice lacking the gene encoding SK2 channels (SK2<sup>-/-</sup>), NREMS EEG power density is dramatically reduced in the  $\delta$  and spindle frequencies. Altogether, our findings suggest that  $\text{Ca}^{2+}$  influx through T-type  $\text{Ca}^{2+}$  channels, acting through competing targets, underlies endogenous nRt oscillations that are linked to characteristic frequency bands of NREMS.

## Results

### Selective coupling between T-type $\text{Ca}^{2+}$ and SK currents in nRt cells

We first examined the role of T-type  $\text{Ca}^{2+}$  currents in the activation of SK currents using whole-cell electrophysiological recordings. We used  $\text{Cs}^+$ -based patch electrodes to restrict  $\text{K}^+$  permeability and to optimize voltage-clamp conditions in recordings from intact nRt cells (Sun et al., 2001). Under these conditions, T-type  $\text{Ca}^{2+}$  currents were detected as rapid inward currents following 0.5 s step hyperpolarizations (by -40 mV from a holding potential of -55 to -60 mV) that were reduced by the T-type  $\text{Ca}^{2+}$  channel blocker mibefradil (10-50  $\mu\text{M}$  applied for 10 min) (from  $-494 \pm 101$  pA to  $-72 \pm 34$  pA,  $n = 7$ ,  $p < 0.02$ ; Figure 1A inset) (Perez-Reyes, 2003). Cells included in this analysis showed T-type  $\text{Ca}^{2+}$  currents with properties that fulfilled previously established criteria for acceptable voltage control in intact nRt cells (see Supplemental Experimental Procedures). We next recorded with  $\text{K}^+$ -based electrodes to

permit unrestricted activation of  $K^+$ , including SK currents. Under these conditions, the response recorded between -67 and -62 mV at the offset of the hyperpolarizing step (-40 mV, 125 ms) was biphasic: the T-type  $Ca^{2+}$  current was typically followed by a small outward current (~10-200 pA above baseline), which was blocked by the selective SK channel blocker apamin (100 nM) (Figure 1A). The apamin-sensitive current, obtained by subtracting currents before and after apamin application, had an amplitude of  $349 \pm 59$  pA ( $n = 5$ ; Figure 1B) and decayed with a biexponential time course. The fast component had a time constant of  $\tau_1 = 30.1 \pm 2.6$  ms ( $n = 5$ ), while the slow component decayed with  $\tau_2 = 834 \pm 227$  ms ( $n = 5$ ) and contributed  $17.3 \pm 4.2$  % to the total current amplitude. The latency from the peak of the T-type  $Ca^{2+}$  current to the peak of the apamin-sensitive current was  $14.1 \pm 0.3$  ms ( $n = 5$ ; Figure 1C). Thus, digital subtraction yields a large SK current in nRt cells, and the voltage-clamp approach appeared suitable for characterizing the mechanism of its activation (see Supplemental Experimental Procedures).

To determine whether  $Ca^{2+}$  entry through T-type  $Ca^{2+}$  currents was required for SK current activation, the effects on the apamin-sensitive current of including the  $Ca^{2+}$  chelators 1,2-Bis(2-aminophenoxy)ethane-*N,N,N',N'*-tetraacetic acid (BAPTA, 1-5 mM) in the patch pipette were determined. When BAPTA was present, no apamin-sensitive current could be elicited ( $5.9 \pm 3.2$  pA,  $n = 9$ ,  $p < 0.001$  compared to BAPTA-free conditions; Figure 1D), although T-type  $Ca^{2+}$  currents remained unaltered (currents amounted to  $426 \pm 49$  pA at the offset of the hyperpolarizing step,  $p > 0.05$ ). Furthermore, apamin-sensitive currents persisted in the presence of the  $Na^+$  channel blocker tetrodotoxin (TTX, 0.5  $\mu$ M) ( $366 \pm 34$  pA vs.  $423 \pm 54$  pA,  $n = 3$ ,  $p > 0.05$ ; Figure 1E), but were largely blocked in mibefradil (50  $\mu$ M applied for 10 min, remaining apamin-sensitive current amplitude  $-11 \pm 4$  pA,  $n = 4$ ,  $p < 0.002$ ; Figure 1F).

The role of rapid SK current activation was explored by quantifying the decay phase of T-type  $Ca^{2+}$  currents. Since these show a biphasic inward-outward waveform before apamin, and a monophasic decay in apamin, we compared the initial current decay slope between the two conditions (see Supplemental Experimental Procedures). Apamin strongly reduced the decay slope, making it comparable to that found with  $Cs^+$ -based electrodes (Figure 1G). Thus, apamin-sensitive SK channels underlie the outward  $K^+$  current following the T-type  $Ca^{2+}$  currents, and the repolarizing effect of the SK current accelerates the decay of the T-type current, consistent with its role in promoting oscillations.

High-voltage-activated (HVA)  $Ca^{2+}$  currents may also activate SK currents in the nRt (Debarbieux et al., 1998). Indeed, apamin-sensitive currents ( $194 \pm 24$  pA,  $n = 11$ ), evoked

following depolarizing voltage steps (from -67 to -37 mV for 10 - 125 ms), were reduced by the Ca<sub>v</sub>2 channel blocker  $\omega$ -conotoxinMVIIC ( $\omega$ -CTXMVIIC, ~1  $\mu$ M) ( $18.7 \pm 6.4$  % of the control amplitude, n = 5, p < 0.02; Figure 1H). Therefore, it was important to determine the distinct contributions of T-type and HVA Ca<sup>2+</sup> currents to SK current activation during a LT burst. Upon transient hyperpolarization, nRt cells recorded in the whole-cell patch configuration presented 2 - 5 oscillatory high-frequency (150 - 250 Hz) LT burst discharges, typically of 2 - 10 action potentials at around 4 - 10 Hz (Supplemental Experimental Procedures). Bath application of TTX (0.5  $\mu$ M) blocked the action potentials, isolating the LT Ca<sup>2+</sup> spike, but only marginally reduced the number of LT spikes (in ctrl:  $3.0 \pm 0.3$  bursts, in TTX:  $2.6 \pm 0.2$  bursts, n = 6, p < 0.05), and the amplitude of the AHP was largely preserved (data not shown) (Bal and McCormick, 1993). In contrast, apamin abolished oscillations and unmasked a plateau potential (n = 6; Figure 1I). Finally, the SK channel gating enhancer 1-ethyl-2-benzimidazolinone (1-EBIO, 0.1 mM), which increases the apparent Ca<sup>2+</sup> sensitivity of SK channels but does not alter their maximal activation (Pedarzani et al., 2001), potentiated oscillatory activity (Figure S1A-D). These pharmacological experiments suggest that a coupling between T-type Ca<sup>2+</sup> and SK currents is the central event underlying the oscillatory activity in nRt neurons.

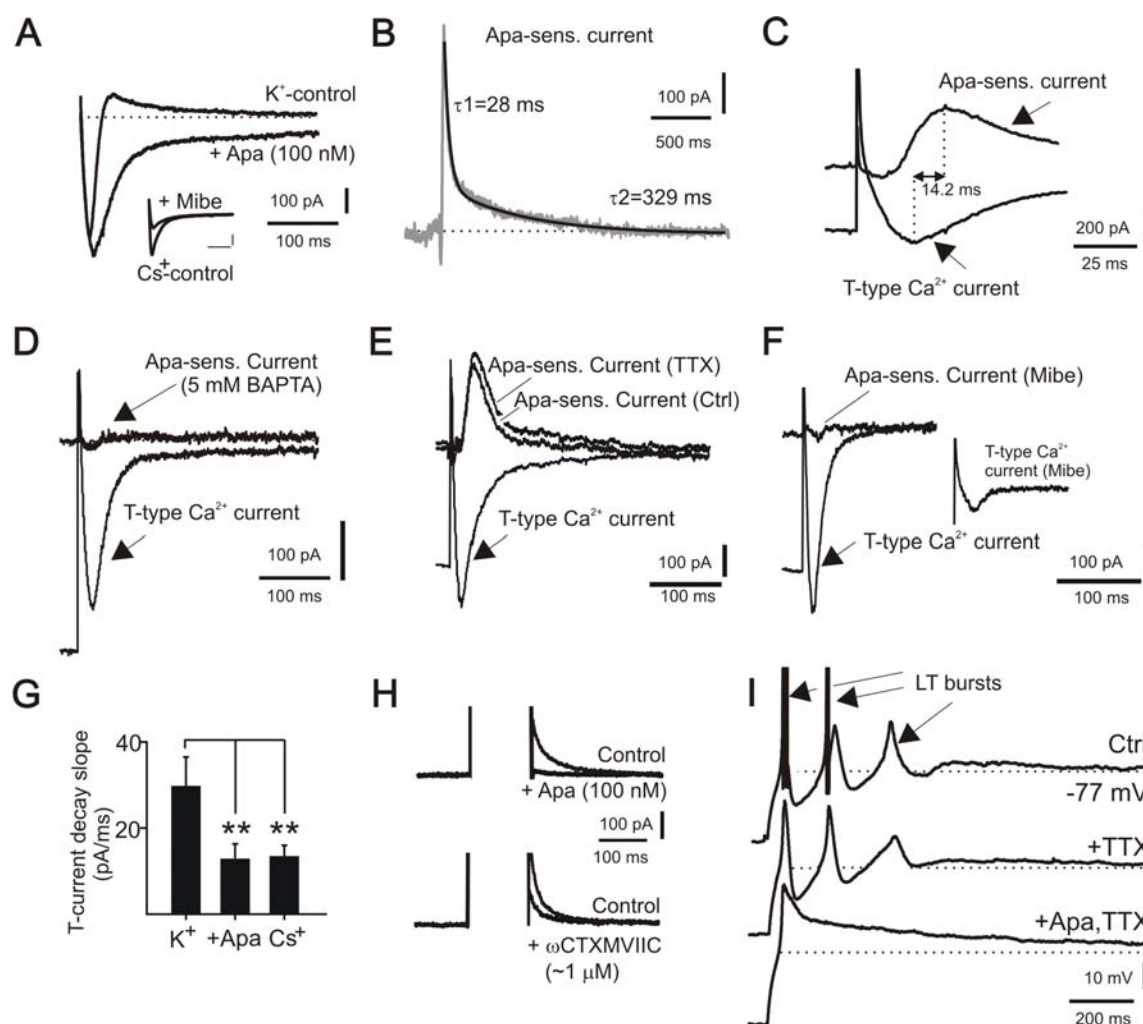


Figure 1. SK channels are selectively gated by T-type  $\text{Ca}^{2+}$  channels and control oscillatory discharges in the nRt

- (A) Membrane current responses elicited after a hyperpolarizing voltage command (from  $-60$  to  $-100$  mV, 500 ms) in  $\text{K}^+$ -based solutions ( $\text{K}^+$ -control). A small outward current followed the inwardly directed T-type  $\text{Ca}^{2+}$  current, that was abolished by the SK channel blocker apamin (+Apa, 100 nM). Note that apamin also decelerated T-type  $\text{Ca}^{2+}$  current decay. *Inset*: The T-type  $\text{Ca}^{2+}$  current, evoked with  $\text{Cs}^+$ -based patch solution ( $\text{Cs}^+$ -control) blocking  $\text{K}^+$  channels, is strongly reduced by mibefradil (+Mibe, 50  $\mu\text{M}$ ). Scale bars for inset: 100 pA, 100 ms.
- (B) Digital isolation of the apamin-sensitive current, obtained from the same cell as in A. Dark line shows a biexponential fit to the trace, described by time constants  $\tau_1$  and  $\tau_2$ . A small inward current component preceding the apamin-sensitive current typically remained in the subtracted trace because the lack of SK current led to a small increase in the peak of the T-type  $\text{Ca}^{2+}$  current (see A). The correlation coefficient of the fit was  $0.91 \pm 0.01$  for  $n = 6$  cells.
- (C) Overlay of the T-type  $\text{Ca}^{2+}$  current (in the presence of apamin) and the apamin-sensitive current (Apa-sens. current). Same cell as in A. Double-headed arrow and

- vertical dotted lines delineate the peak-to-peak latency between T-type  $\text{Ca}^{2+}$  current and apamin-sensitive current.
- (D) Apamin-sensitive current was not detectable in the presence of 5 mM BAPTA in the recording pipette, while the T-type  $\text{Ca}^{2+}$  current remained unaltered.
  - (E) Apamin-sensitive currents before and during TTX application are shown overlaid, together with the inward T-type  $\text{Ca}^{2+}$  current in TTX+apamin.
  - (F) Apamin-sensitive current in mibefradil (50  $\mu\text{M}$ ) and T-type  $\text{Ca}^{2+}$  current in control conditions. Inset shows T-type  $\text{Ca}^{2+}$  current in mibefradil. Scale bars apply for all traces.
  - (G) The decay slope of the T-type  $\text{Ca}^{2+}$  current, obtained by its linear fitting (Supplemental Experimental Procedures), in  $\text{K}^+$ -based solution and in the presence of apamin or intracellular  $\text{Cs}^+$ . \*\* denotes  $p < 0.01$ . Data are means  $\pm$  SEM of 6 cells for Ctrl and apamin, and of 13 cells for  $\text{Cs}^+$ .
  - (H) Apamin-sensitive current, activated by depolarizing voltage steps (30 mV, 125 ms, upper traces) to gate high-voltage-activated (HVA)  $\text{Ca}^{2+}$  currents, and effects of the  $\text{Ca}_v2$  channel blocker  $\omega$ -conotoxin MVIIC (+  $\omega$ -CTXMVIIC, lower traces).
  - (I) Whole-cell recordings of nRt discharge patterns after brief negative current injections (-100 pA, 400 ms). Under control conditions (Ctrl), an oscillation with three LT bursts (arrows) was elicited. Application of tetrodotoxin (+ TTX, 0.5  $\mu\text{M}$ ) abolished action potentials, but left the oscillation largely intact. Subsequent apamin application (+ Apa, 100 nM) uncovered a slowly decaying plateau potential. Dotted lines, resting membrane potential.

### T-type $\text{Ca}^{2+}$ currents dominate $\Delta[\text{Ca}^{2+}]_i$ in dendrites during a LT burst

To identify the mechanism underlying a presumed selective coupling between T-type  $\text{Ca}^{2+}$  currents and SK currents, the change in intracellular free  $\text{Ca}^{2+}$  concentration ( $\Delta[\text{Ca}^{2+}]_i$ ) generated by a LT burst was imaged in cells filled with the  $\text{Ca}^{2+}$  dye magfura-2 (3 mM). This low-affinity  $\text{Ca}^{2+}$  indicator ( $K_d \sim 25 \mu\text{M}$ , see Experimental Procedures) is best-suited to this study because it permits us to real-time image  $\Delta[\text{Ca}^{2+}]_i$  in the micromolar range (Ogden et al., 1995). We focused on signals in the dendrites, because dendritic T-type  $\text{Ca}^{2+}$  currents are essential for LT bursting (Destexhe et al., 1996; Joksovic et al., 2005). Figure 2A shows a dye-filled nRt cell, with the bipolar-shaped, thin dendritic arborization partially visible. The  $\Delta[\text{Ca}^{2+}]_i$  evoked by a LT burst could be measured up to  $\sim 150 \mu\text{m}$  from the soma with only minor differences in amplitude and kinetics at different dendritic sites (Figure 2B). Therefore,  $\Delta[\text{Ca}^{2+}]_i$  was determined from fluorescence signals averaged over the entire imaged dendrite (100 - 150  $\mu\text{m}$  from soma). The  $\Delta[\text{Ca}^{2+}]_i$  associated with the LT burst reached peak levels of  $713 \pm 71 \text{ nM}$  ( $n = 6$  dendrites from 6 different nRt neurons in 3 independent experiments), and decayed with a time constant of  $56 \pm 9 \text{ ms}$  (fitted in  $n = 5$  experiments). At 0.1 mM ethylene glycol tetraacetic acid (EGTA),  $\Delta[\text{Ca}^{2+}]_i$  measured with magfura-2 was undistinguishable from that without EGTA ( $\Delta[\text{Ca}^{2+}]_i = 775 \pm 82 \text{ nM}$ ,  $\tau = 46 \pm 8 \text{ ms}$ ,  $n = 4$ ,  $p >$



0.05). Mibefradil (50  $\mu\text{M}$ ) reduced these transients by  $90.2 \pm 3.6\%$  (to  $87 \pm 57$  nM,  $n = 3$ ,  $p < 0.05$ ; Figure 2B). The delay between the  $\Delta[\text{Ca}^{2+}]_i$  and the AHP, measured as a peak-to-peak latency, was  $37 \pm 6$  ms (range 21 - 46 ms,  $n = 4$ ; Figure 2C). Taking into account that AHP time-to-peak is the convolution of T-type  $\text{Ca}^{2+}$  current decay, SK current activation and the charging of cell capacitance ( $\tau \sim 12 - 22$  ms), this value is consistent with the electrophysiologically determined peak-to-peak latency between T-type  $\text{Ca}^{2+}$  currents and SK currents ( $\sim 14$  ms, see Figure 1C) and supports our ability to measure robust  $\text{Ca}^{2+}$  currents with imaging techniques.

We next determined the relative importance of  $\text{Ca}^{2+}$  specifically provided by the T-type  $\text{Ca}^{2+}$  current over the  $\text{Ca}^{2+}$  currents activated during action potentials. Neurons were depolarized to values between -55 and -45 mV to generate a train of 5 - 30 action potentials without an underlying LT spike. Tonic discharge rates reached frequencies around 150 - 220 Hz within the first 3 - 5 action potentials before undergoing adaptation, close to those reached during burst discharges (150 - 250 Hz). Under these conditions,  $\Delta[\text{Ca}^{2+}]_i$  was markedly smaller ( $15.9 \pm 5.4$  nM per action potential,  $n = 5$ ,  $p < 0.01$ ; Figure 2D) than  $\Delta[\text{Ca}^{2+}]_i$  associated with the LT burst.

This difference could be due to a larger  $\text{Ca}^{2+}$  influx through T-type  $\text{Ca}^{2+}$  channels compared to HVA channels, or because the sources of  $\Delta[\text{Ca}^{2+}]_i$  were associated with different local endogenous buffering. To distinguish between these possibilities, the total  $\text{Ca}^{2+}$  entering during a LT burst was measured with the high-affinity  $\text{Ca}^{2+}$  indicator bis-fura-2 (1 mM). In these recordings, the dye-bound  $\text{Ca}^{2+}$  ( $\Delta[\text{DCa}^{2+}]_i$ , see Experimental Procedures and (Canepari et al., 2004)) was  $135 \pm 22$   $\mu\text{M}$  ( $n = 4$ ) for a single LT burst and  $1.35 \pm 0.18$   $\mu\text{M}$  ( $n = 4$ ) per action potential (Figure 2E). Taken together, a LT burst generates a large  $[\text{Ca}^{2+}]_i$  increase in nRt cell dendrites due to  $\text{Ca}^{2+}$  influx through T-type  $\text{Ca}^{2+}$  currents, while an action potential crowning the burst contributes only  $\sim 1\%$ . With a single-channel conductance of 1 pS and a dendritic diameter of 5 - 8  $\mu\text{m}$ , a T-type  $\text{Ca}^{2+}$  conductance density of  $\sim 0.6 - 1$  mS/cm<sup>2</sup> is required to achieve these signal amplitudes. Furthermore, these measurements provide an estimate of the buffer capacity  $\sim 200$ , which is similar for HVA- and T-type  $\text{Ca}^{2+}$  currents. Thus, both electrophysiological and imaging data demonstrate an overwhelming dominance of  $\text{Ca}^{2+}$  provided by the T-type  $\text{Ca}^{2+}$  currents in nRt dendrites during a LT burst.

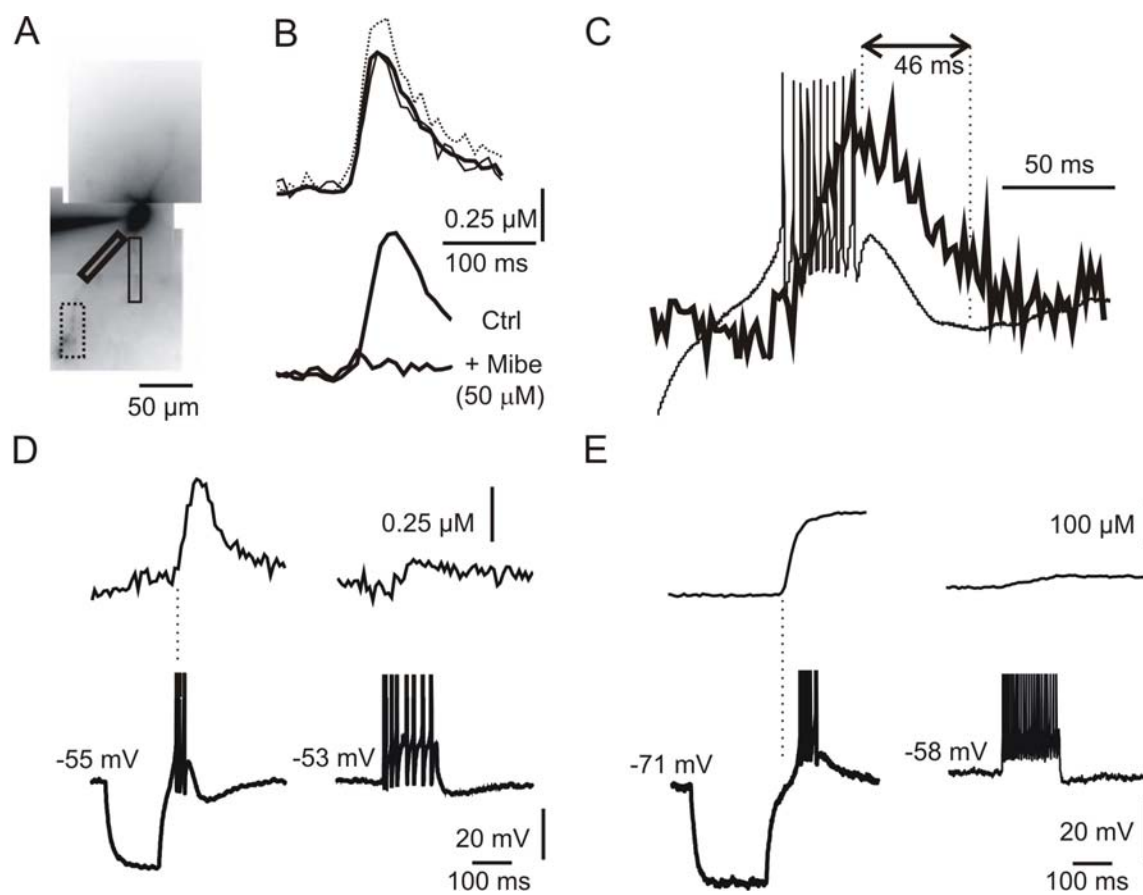


Figure 2. T-type  $\text{Ca}^{2+}$  channels dominate dendritic  $[\text{Ca}^{2+}]_i$  increases during LT bursts

- (A) Reconstruction of a mag-fura2-filled nRt cell (3 mM). Boxes depict areas over which fluorescent signals were measured and averaged.
- (B) Upper traces:  $\Delta[\text{Ca}^{2+}]_i$  acquired at 125 Hz in the areas of the boxes in A, elicited by a LT burst. Traces are superimposed, showing their overlapping time course throughout the first  $\sim 150 \mu\text{m}$  of the dendrite. Lower traces: Effects of Mibefradil (+ Mibe, 50  $\mu\text{M}$ , bath-applied for 10 min) on the  $\text{Ca}^{2+}$  transient induced by a LT burst (Ctrl).
- (C) Overlay of the LT burst (thin line) and the  $\Delta[\text{Ca}^{2+}]_i$  acquired at 500 Hz (thick line), illustrating the delay (double-headed arrow) between the peak of the  $[\text{Ca}^{2+}]_i$  transient and the AHP. Same cell as in A, B.
- (D) For another cell,  $[\text{Ca}^{2+}]_i$  increases produced by both a LT burst (left traces) and tonic action potentials (evoked by 100 pA d.c., right traces) are shown. Dotted line denotes the onset of the  $[\text{Ca}^{2+}]_i$  transient, which is delayed with respect to the LT burst, consistent with the low  $\text{Ca}^{2+}$  affinity of mag-fura2.
- (E) In a cell filled with bis-fura-2 (1 mM),  $\Delta[\text{DCa}^{2+}]_i$  evoked by a LT burst (left traces) and tonic action potential discharge (right traces) was determined. Note the lack of a burst-associated AHP, in contrast to the cell in D recorded with mag-fura2. For this high-affinity  $\text{Ca}^{2+}$  dye, the transient starts closer to the onset of the LT burst (dotted line).

**SK2 channels mediate the SK currents in nRt cells**

The apparently selective coupling of T-type  $\text{Ca}^{2+}$  channels to SK channels could be supported if SK channels were expressed at subcellular sites at which  $\text{Ca}^{2+}$  entry through T-type  $\text{Ca}^{2+}$  channels is dominant. Previous *in situ* hybridization results revealed that both SK1 and SK2 channel subunits are expressed in nRt (Stocker and Pedarzani, 2000). To determine which channel isoforms carry the SK current, we examined SK1<sup>-/-</sup> or SK2<sup>-/-</sup> mice (Bond et al., 2004). The nRt cell morphology, basic cellular properties, and whole-cell T-type  $\text{Ca}^{2+}$  current properties important for repetitive bursting were similar in cells from SK2<sup>-/-</sup>, SK1<sup>-/-</sup> and wild-type (WT) SK2<sup>+/+</sup> littermate animals (Supplemental Experimental Data). However, in SK2<sup>-/-</sup> animals, the oscillatory discharge was arrested and replaced by a single, slowly decaying depolarization (in 27 / 27 cells tested; Figure 3A), with a distinct lack of burst-associated AHPs. In contrast, SK1<sup>-/-</sup> cells showed unaltered discharge behaviour compared to WT littermates in all 39 cells studied (Figure 3B). Moreover, SK2<sup>-/-</sup>, but not SK1<sup>-/-</sup>, nRt neurons lacked an apamin-sensitive current following both the T-type and the HVA  $\text{Ca}^{2+}$  currents (Figure 3A-C). Finally, the slope of the T-type  $\text{Ca}^{2+}$  current decay in SK2<sup>-/-</sup> neurons (n = 20) was not significantly different from the values obtained after apamin application ( $p > 0.05$ ; see Figure 1G), but smaller than in WT and in SK1<sup>-/-</sup> cells (Figure 3C). Finally, application of 1-EBIO failed to induce an outward current following the T-type  $\text{Ca}^{2+}$  current in SK2<sup>-/-</sup> cells (Figure S1E and S1F). Low-threshold bursting properties of thalamocortical neurons, including sag potentials, burst amplitudes, and burst discharge frequencies, appeared unaltered in the SK2<sup>-/-</sup> mice (n = 4) compared to wild-type animals (n = 5, data not shown). Thus, within the thalamic network, the lack of SK2 channels selectively compromises oscillatory bursting in nRt neurons.

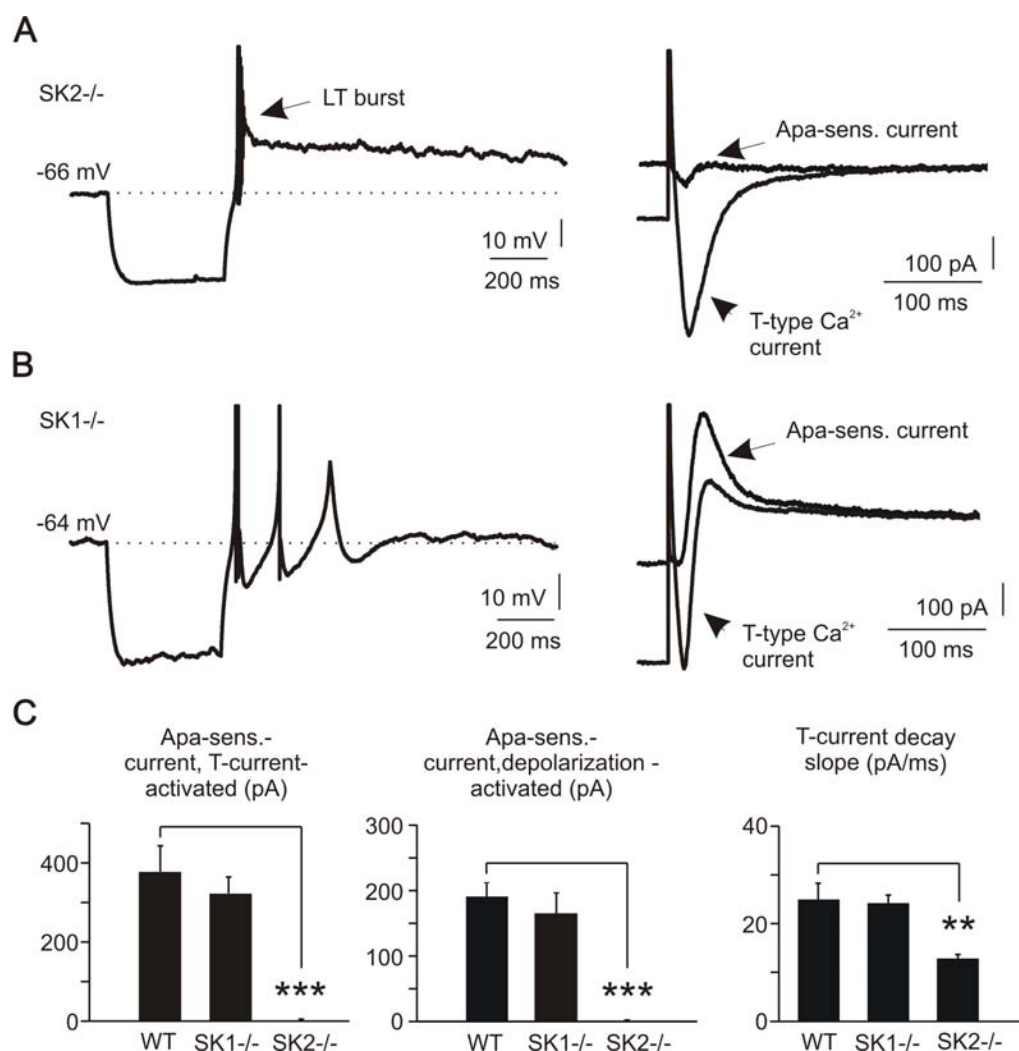


Figure 3. SK2-containing SK channels mediate oscillatory LT bursts and apamin-sensitive currents in nRt cells

- (A) Membrane voltage responses to negative current injections (-100 pA, 400 ms, left) and apamin-sensitive (Apa-sens.) currents (right), in nRt cells of SK2<sup>-/-</sup> mice. Note that a LT burst and a T-type Ca<sup>2+</sup> current (T-current) were clearly present.
- (B) Same as A, for a cell derived from a SK1<sup>-/-</sup> mouse.
- (C) Pooled data showing the amplitudes of apamin-sensitive currents evoked after T-type Ca<sup>2+</sup> current (left), after HVA Ca<sup>2+</sup> current (depolarization-activated, +30 mV, 60-125 ms) (middle), and the slope of the T-type Ca<sup>2+</sup> current decay (right) for SK1<sup>-/-</sup>, SK2<sup>-/-</sup> and wild-type (WT) littermate controls. Data are presented as means ± SEM of 4-20 cells. \*\* denotes  $p < 0.005$ , \*\*\*  $p < 0.001$ .

### Selective expression of SK2 channels in nRt cell dendrites

High-resolution immunohistochemical techniques were applied to determine the subcellular localization of SK2 protein in nRt neurons (Figure 4). Immunoreactivity for SK2

was found throughout the dorsoventral extension of the nRt (Figure 4A-C), consistent with previous observations at the mRNA level (Stocker and Pedarzani, 2000). The SK2 immunoreactivity was predominantly located in the neuropil surrounding the spindle-shaped cell bodies (Figure 4C), and was absent in SK2<sup>-/-</sup> animals (Figure 4D). The subcellular localization of SK2 subunits was further refined using pre-embedding immunogold electron microscopy (Figure 4E-I). Few immunogold particles were observed in cell bodies, and most of them were associated with the rough endoplasmic reticulum (ER); almost no immunoparticles were found at the somatic plasma membrane ( $0.87 \pm 0.32$  immunogold/ $\mu\text{m}^2$ ) (Figure 4E). Most SK2 immunoparticles were located in dendrites along the extrasynaptic plasma membrane of dendritic shafts ( $10.87 \pm 2.11$  immunogold/ $\mu\text{m}^2$ ,  $p < 0.01$  compared to somatic density; Figure 4F-I). Notably, immunoparticles were often found close to excitatory synapses (146 immunoparticles within 200 nm from the edge of postsynaptic density of 50 excitatory profiles), but never close to inhibitory synapses (0 immunoparticles for 25 inhibitory profiles), suggesting that they may detect  $\text{Ca}^{2+}$  entry resulting from glutamatergic synaptic transmission (Ngo-Anh et al., 2005). A large portion of total labelling (1181 immunoparticles out of 1737; 68%) was also found associated with intracellular membranes, potentially reflecting protein trafficking. Thus, SK2 channel density is highest in dendrites, where  $\text{Ca}^{2+}$  influx occurs almost exclusively through T-type  $\text{Ca}^{2+}$  channels during a LT burst.

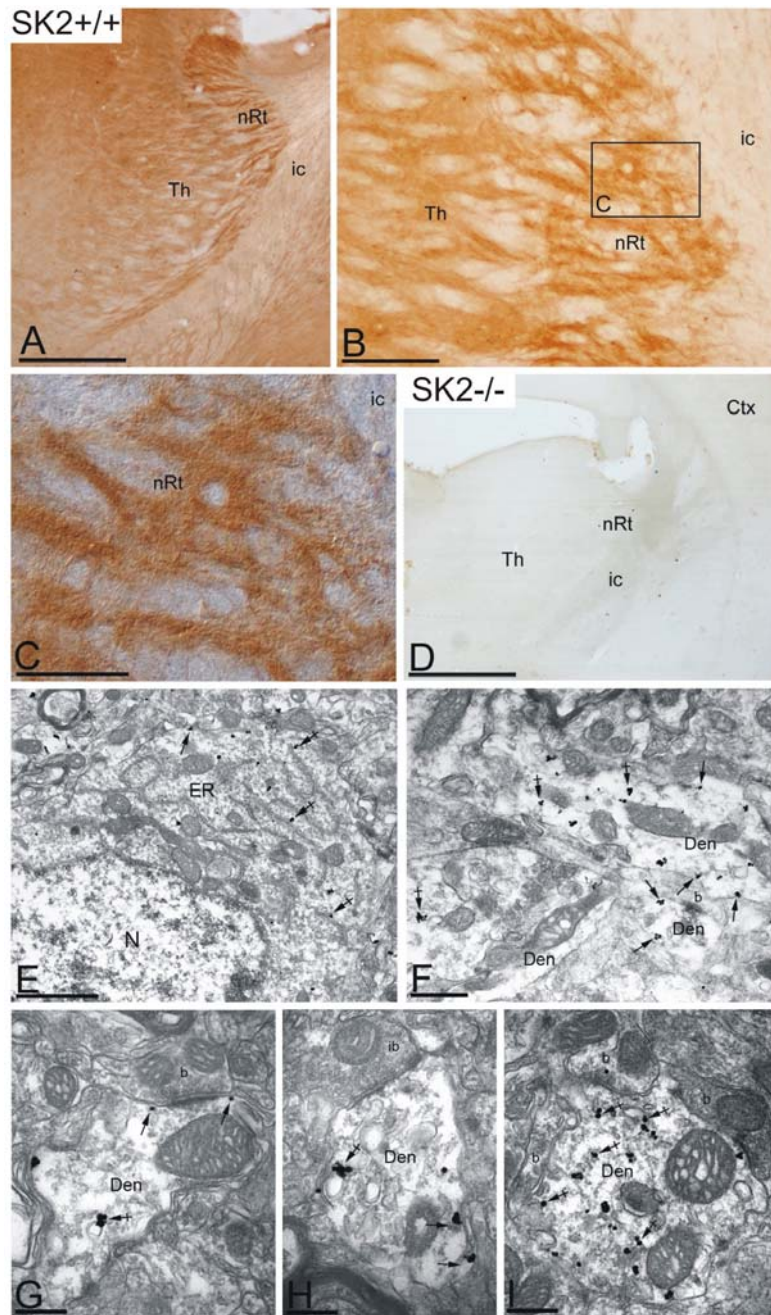


Figure 4. SK2 channel subunits are selectively expressed in nRt dendrites

- (A-D) Immunoreactivity for SK2 protein in nRt-containing sections of WT animals (SK2<sup>+/+</sup>) at three different magnifications (A-C), and of SK2<sup>-/-</sup> animals (SK2<sup>-/-</sup>, D), as revealed by a pre-embedding immunoperoxidase method at the light microscopic level. Box in B denotes area presented in C. Scale bars: A,D, 1 mm; B, 0.2 mm; C, 0.1 mm. Ctx, cortex, Th, Thalamus, ic, internal capsule.
- (E-I) Immunoreactivity for SK2 at ultrastructural level, using electron microscopy. Arrows, immunogold particle in somatic and dendritic membranes; Crossed arrows, gold labeling in intracellular membranes. Den, Dendrite, ER, Endoplasmic Reticulum, N, Nucleus, b, bouton, ib, inhibitory bouton. Scale bars in E-I, 0.2  $\mu$ m.

### **Weakening of nRt oscillations through T-type channel $\text{Ca}^{2+}$ channel inactivation**

Are there regulatory mechanisms that vary the strength of T-type  $\text{Ca}^{2+}$  channel/SK2 channel coupling? This question was motivated by the well-documented observation that, albeit single nRt bursts show a stereotyped discharge pattern (Domich et al., 1986): their temporal succession exhibits a complex time course in which consecutive bursts gradually weaken and are replaced by tonic discharges, or in which switching between active and silent states occurs (Bal and McCormick, 1993; Blethyn et al., 2006; Domich et al., 1986; Fuentealba et al., 2005). Cationic conductances have been advocated to explain these deviations from on-going rhythmic bursting (Crunelli et al., 2006; Pape et al., 2004). Here, we assessed whether variable T-type  $\text{Ca}^{2+}$ -to-SK2 channel coupling might contribute to a diversification of nRt discharge patterns by quantifying  $\text{Ca}^{2+}$  signals during repetitive LT bursts in *magfura-2* filled cells. Up to three bursting cycles of a dampened oscillation were imaged (Figure 5A), each of which was accompanied by rapid elevations of  $[\text{Ca}^{2+}]_i$  that largely decayed ( $< 10\%$  of the peak) before the generation of the next transient ( $n = 5$  cells). These  $[\text{Ca}^{2+}]_i$  transients showed a striking decrement in amplitude from one oscillatory cycle to the next ( $n = 5$ ,  $p < 0.001$ ; Figure 5B), indicating that fewer T-type  $\text{Ca}^{2+}$  channels open in successive cycles of the oscillation (Movie S1). Consistent with this, the rising slope of successive  $[\text{Ca}^{2+}]_i$  transients became shallower, while decay time constants increased (Figure 5C), indicating a gradual temporal blurring in the synchronicity of T-type  $\text{Ca}^{2+}$  channel activation. Moreover, the integrated area beneath the  $[\text{Ca}^{2+}]_i$  transients was proportional to the amplitude of the LT spikes throughout all three oscillatory cycles ( $p < 0.0001$ ; Figure 5D) and repeated voltage-gating of T-type  $\text{Ca}^{2+}$  currents at frequencies comparable to those of dampened oscillations resulted in cumulative current inactivation (Figure S2).

We tested whether these decremental  $[\text{Ca}^{2+}]_i$  transients weakened activation of SK2 currents. T-type  $\text{Ca}^{2+}$  currents during cumulative inactivation lacked rapid outward currents and showed a decelerated decay slope (Figure S2), consistent with diminished SK2 current amplitudes (see Figure 1G). Moreover, the SK channel gating enhancer 1-EBIO selectively lengthened interburst intervals later in oscillations, while not significantly altering the first interburst interval (Figure S1 and Supplemental Data). Taken together, these data show that use-dependent inactivation mechanisms limit activation of T-type  $\text{Ca}^{2+}$  currents during repetitive oscillations, thereby leading to smaller  $[\text{Ca}^{2+}]_i$  signals and attenuated SK2 channel activation.

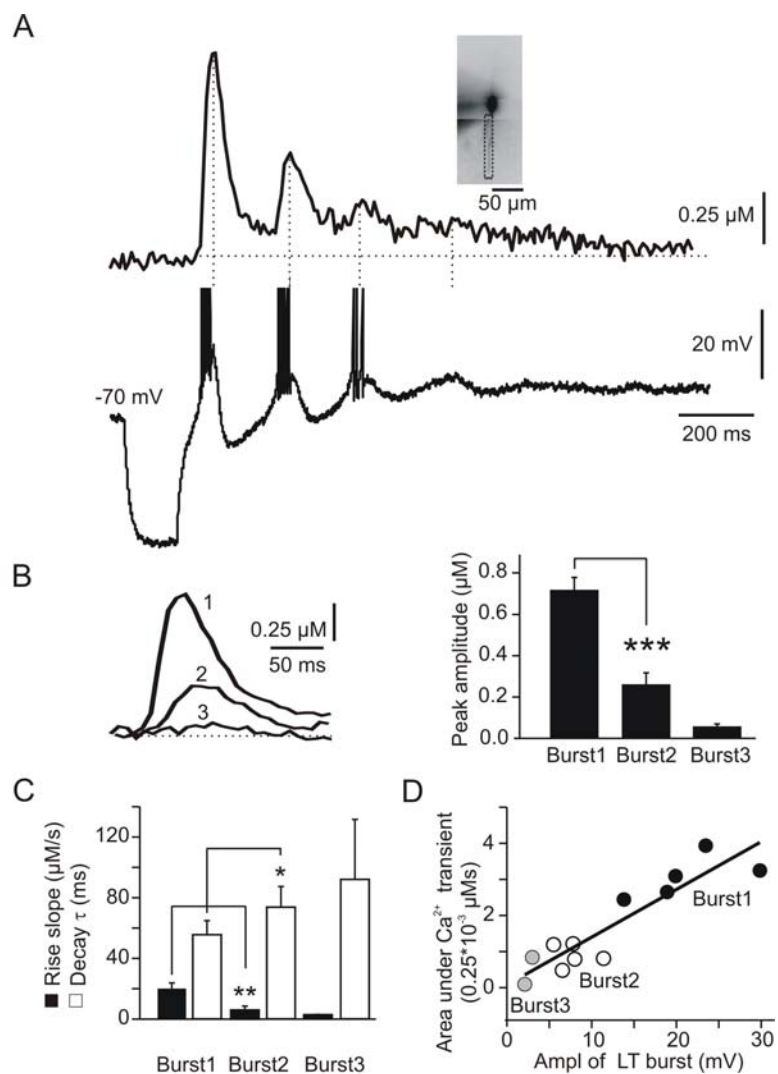


Figure 5. Repetitive LT bursting is accompanied by a decrease in the amplitude of  $\Delta[\text{Ca}^{2+}]_i$

- (A) Combined recording of electrophysiological and fluorescent signals during the generation of repetitive LT bursting.  $\Delta[\text{Ca}^{2+}]_i$  was acquired at 125 Hz in a dendritic segment shown in the inset (boxed area).
- (B) Overlay of the first three  $[\text{Ca}^{2+}]_i$  transients shown in A, labeled as 1, 2, 3. Histogram illustrates means  $\pm$  SEM of the peak  $\Delta[\text{Ca}^{2+}]_i$  reached in 5 cells for bursts 1 and 2, and in 2 cells for burst 3. \*\*\* denotes  $p < 0.001$
- (C) Quantification of the time course of the transients by rising slope (filled bars, in  $\mu\text{M/s}$ ) and decay time constant (open bars, in ms). Data are presented as means  $\pm$  SEM, with \*\* denoting  $p < 0.005$ , and \* denoting  $p < 0.02$ .
- (D) Plot of the LT burst amplitude against the area underneath the  $\text{Ca}^{2+}$  transient, showing the linear correlation. The LT burst amplitude was determined from burst threshold to the peak of the T-type  $\text{Ca}^{2+}$  current-induced depolarization. Data points were pooled for all bursts from 5 cells. The squared correlation coefficient for the linear regression was 0.834, and  $p < 0.0001$ .



### Strengthening of nRt oscillations through blockade of endoplasmic Ca<sup>2+</sup> sequestration

The gating of SK currents is regulated by the handling of internal Ca<sup>2+</sup> in diverse neurons (Bond et al., 2005; Stocker, 2004) and may be strengthened by Ca<sup>2+</sup>-induced Ca<sup>2+</sup> release triggered via T-type Ca<sup>2+</sup> currents (Cui et al., 2004; Richter et al., 2005). To assess whether similar mechanisms regulate T-type Ca<sup>2+</sup> channel/SK2 channel coupling in nRt cells, we studied the effects of decreasing Ca<sup>2+</sup>-induced Ca<sup>2+</sup> release through antagonizing SERCAs. Within ~ 5 min of bath application of the SERCA inhibitor, cyclopiazonic acid (CPA, 10  $\mu$ M), the amplitude of the outward SK2 current following T-type Ca<sup>2+</sup> currents was markedly enhanced (from  $14 \pm 30$  pA to  $91 \pm 33$  pA,  $n = 10$ ,  $p < 0.001$ ; Figure 6A). Digital subtraction was carried out in a subgroup of 7 cells to confirm that the apamin-sensitive current increased significantly in CPA ( $n = 7$ ;  $p < 0.02$ ; Figure 6B). Thapsigargin (4  $\mu$ M in the patch pipette), a less-selective inhibitor of SERCAs, also produced an increase in the outward current from  $51 \pm 12$  pA to  $153 \pm 33$  pA ( $n = 7$ ,  $p < 0.03$ ). In the presence of CPA, apamin-sensitive currents showed a biexponential decay similar to control ( $p > 0.4$  for both fast and slow time constants), but the slow component now contributed  $29.7 \pm 7.6\%$  of the total current ( $n = 7$ ;  $p < 0.05$  compared to slow current components before CPA application; Figure 6C), suggesting a prolonged presence of Ca<sup>2+</sup> ions able to activate SK2 channels. Blocking SERCAs thus potentiates SK2 currents, contrary to an expected decrease if Ca<sup>2+</sup>-induced Ca<sup>2+</sup> release was involved. In these cells, the amplitude of the T-type Ca<sup>2+</sup> current was largely preserved in the presence of 10  $\mu$ M CPA (~10% decrease, Ctrl T-type Ca<sup>2+</sup> current peak amplitude:  $-510 \pm 88$  pA, CPA T-type Ca<sup>2+</sup> current peak amplitude:  $-456 \pm 80$  pA,  $n = 7$ ,  $p < 0.05$ ) and the decay time remained unaltered in comparison to cells exposed to apamin only ( $\tau_{\text{decay}} = 31.3 \pm 3.1$  ms,  $n = 7$ ;  $p > 0.05$ ). The potentiated apamin-sensitive current could thus not be explained by altered voltage-gating of T-type Ca<sup>2+</sup> currents.

The effects of SERCA antagonism on SK2 currents could reflect increased steady [Ca<sup>2+</sup>]<sub>i</sub> levels or SK2 channel modifications, such as dephosphorylation of bound calmodulin (Bildl et al., 2004) rather than an action on T-type Ca<sup>2+</sup>/SK2 channel coupling. To address this possibility, we tested whether CPA affected SK2 currents activated via Ca<sup>2+</sup> entry through HVA channels of the Ca<sub>v</sub>2 type (see Figure 1H). Notably, CPA produced a small but non-significant reduction of the apamin-sensitive SK2 currents ( $n = 7$ ,  $p = 0.055$ ; Figure 6D). Similar results were obtained when the depolarizing voltage step was shortened to 60 ms to reduce Ca<sup>2+</sup> influx (data not shown), showing that limiting the duration of Ca<sup>2+</sup> entry did not alter the polarity of CPA actions. Moreover, CPA (10  $\mu$ M) had no effect on currents activated after a hyperpolarizing command in nRt neurons of SK2<sup>-/-</sup> mice, but potentiated the outward

currents in nRt neurons of SK1<sup>-/-</sup> mice (Figure 6E and G) and revealed a slowly decaying apamin-sensitive current component (Figure 6F). Thus, SERCA's role is to selectively clear the Ca<sup>2+</sup> flowing through T-type Ca<sup>2+</sup> channels and to antagonize SK2 channel activation. Indeed, T-type Ca<sup>2+</sup> channels, SK2 channels and SERCAs appear to be grouped into a Ca<sup>2+</sup> signalling domain, in which SK2 channels and SERCA stand in competition for available Ca<sup>2+</sup> entered through T-type Ca<sup>2+</sup> channels.

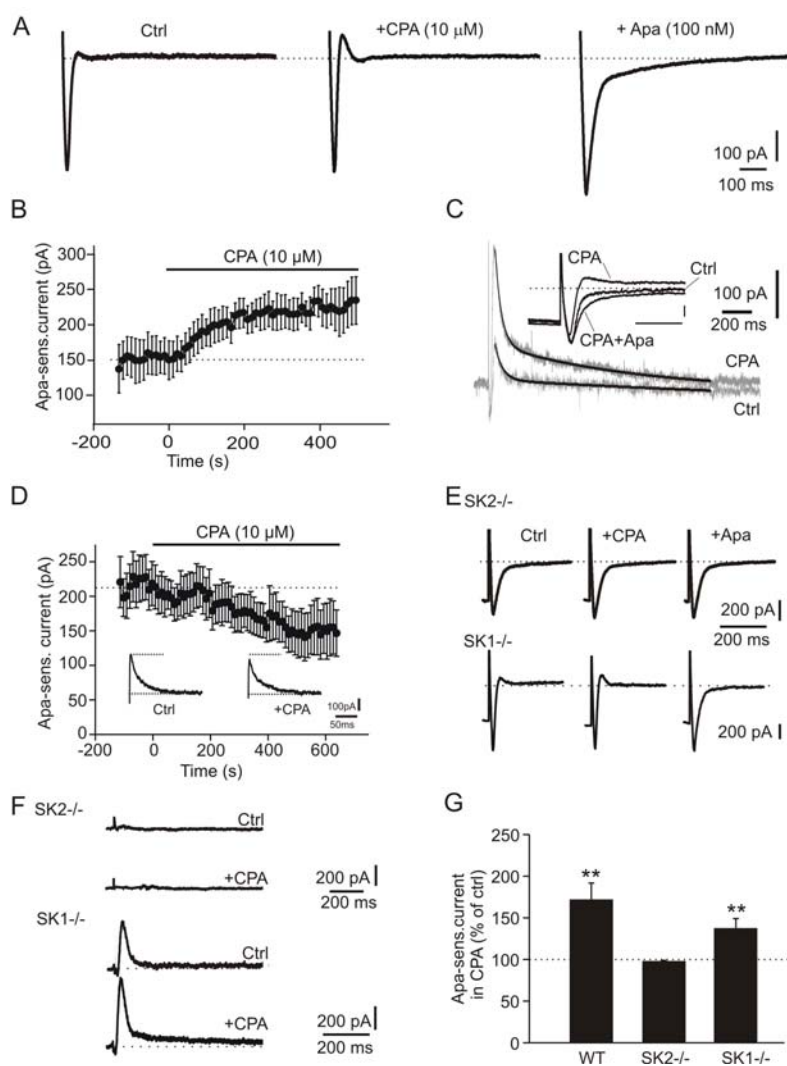


Figure 6. Sarco/endoplasmic Ca<sup>2+</sup>-ATPases (SERCAs) specifically limit SK2 channel gating by T-type Ca<sup>2+</sup>, but not by HVA Ca<sup>2+</sup> currents

(A) Representative cell showing current responses to membrane hyperpolarization (-40 mV, 125 ms) in control (Ctrl), in cyclopiazonic acid (CPA, 10 μM), and after addition of apamin (+ Apa, 100 nM).

- (B) The time course of the apamin-sensitive current, evoked after membrane hyperpolarization, before and during CPA application. Dotted line, average current before CPA. Data are means  $\pm$  SEM of 7 cells.
- (C) Apamin-sensitive currents before (Ctrl) and after CPA application (CPA), obtained by digital subtraction of traces recorded in apamin. Black lines depict biexponential fits, with time constants  $\tau_1 = 33$  ms and  $\tau_2 = 429$  ms in Ctrl, and  $\tau_1 = 41$  ms and  $\tau_2 = 946$  ms in CPA. In the presence of CPA, the slow current component contributed 32.6% of the total apamin-sensitive current, whereas in Ctrl it was 19.6%. Inset shows an overlay of the current traces that were used for digital subtraction. Note that the inward T-type  $\text{Ca}^{2+}$  current overlaid in all experimental conditions, but its decay was accelerated in CPA and decelerated in CPA + apamin (CPA + Apa). The small decrease in peak current amplitude in CPA is attributable to the potentiated outward SK current. Scale bars, 100 pA, 200 ms.
- (D) Time course of apamin-sensitive currents, evoked by depolarization (30 mV, 125 ms), before and during CPA application. Dotted line, average current before CPA. Data are means  $\pm$  SEM of 7 cells.
- (E) As in A, with recordings obtained from cells of SK2<sup>-/-</sup> and SK1<sup>-/-</sup> animals. Note the lack of effects of CPA and apamin on cells from the SK2<sup>-/-</sup> animals, whereas these were preserved in SK1<sup>-/-</sup> cells.
- (F) Apamin-sensitive currents, obtained by digital subtraction of currents shown in E. Dotted lines denotes 0 pA. Note the enhanced slow current component in CPA in the cell from a SK1<sup>-/-</sup> mouse.
- (G) Histogram showing the CPA-induced changes in apamin-sensitive currents relative to baseline in wild-type (WT, n = 9), SK2<sup>-/-</sup> (n = 5) and SK1<sup>-/-</sup> (n = 10) cells. In SK2<sup>-/-</sup>, the current obtained as apamin-sensitive before CPA was < 1 pA. \*\* denotes  $p < 0.01$ .

We evaluated whether such competitive interaction plays a role in rhythmic nRt discharges. Under control conditions, the number of bursts showed a bell-shaped dependence on the resting membrane potential preceding a hyperpolarizing current injection (-100 pA, 400 ms) (Figure 7A and B). Bath application of CPA (10  $\mu\text{M}$ ) induced a prolongation of the AHPs following the LT bursts (n = 9; Figure 7A), and lengthened the time spent bursting. The increased bursting was most pronounced at the peak of the bell-shaped curve, while bursting was not affected for current injections initiated at the margins of the burst voltage window (Figure 7B and C). The membrane potential responses to the hyperpolarizing current steps remained unaltered (in control:  $-22.8 \pm 3.3$  mV and  $-24.4 \pm 2.2$  mV from  $-72$  and  $-77$  mV; in CPA:  $-24.2 \pm 2.3$  mV and  $-26.4 \pm 2.1$  mV; n = 9;  $p > 0.05$ ). The effects of CPA were also tested on cells using whole cell perforated patch-clamp recordings that faithfully preserve the intracellular  $\text{Ca}^{2+}$  homeostasis. In this configuration, nRt neurons showed more bursts as well as more variable burst discharge patterns (Figure 7D). The CPA effects were evident as a marked prolongation of the bursting pattern (n = 5 different nRt cells).

In a computational model of a single-compartment cell incorporating previously described phenomenological models of T-type  $\text{Ca}^{2+}$  currents, SK currents and SERCAs

(Supplemental Data), basic aspects of nRt oscillatory dynamics and their regulation by SERCA could be reproduced (Figure S3). This model provides additional support to the conclusion that we have identified three major interacting partners controlling the dynamics of nRt cell oscillations.

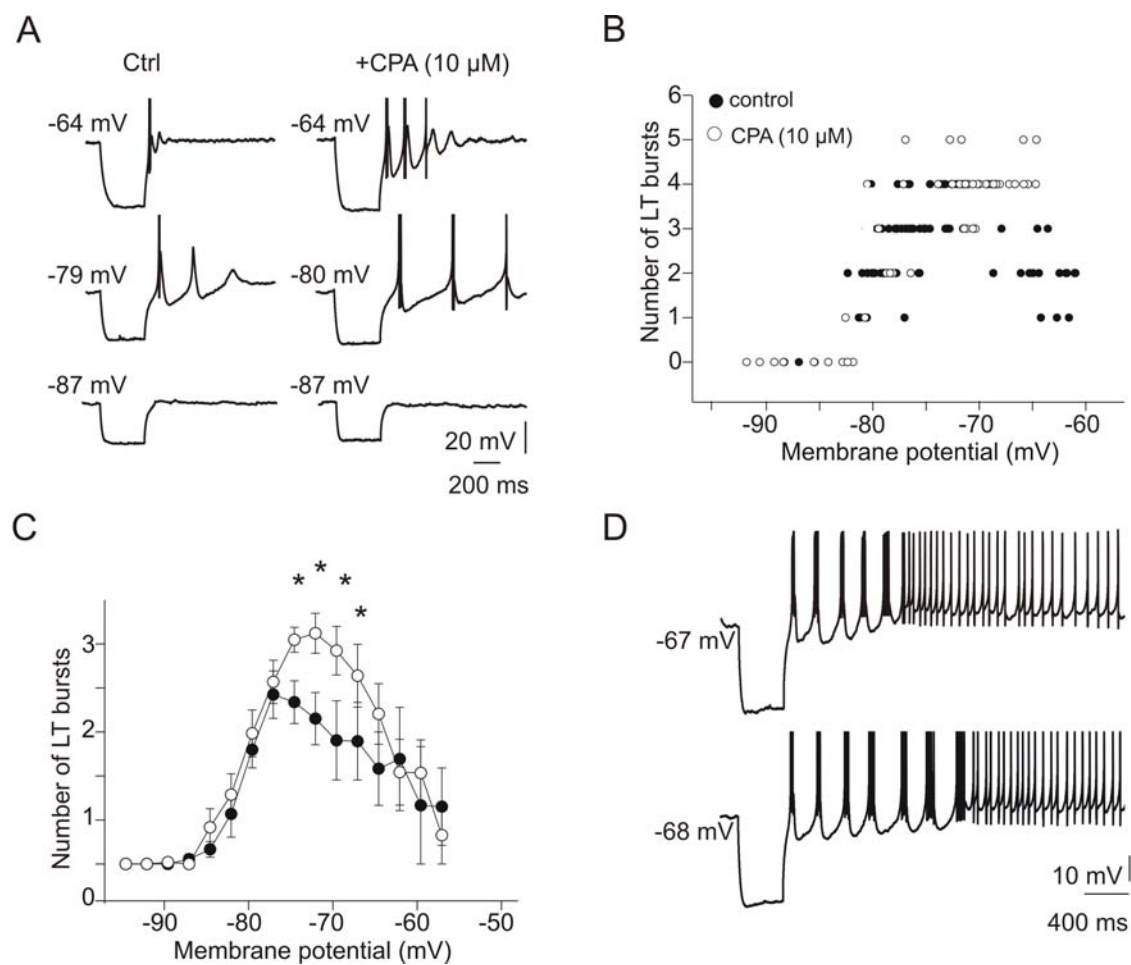


Figure 7. SERCAs modulate the strength of nRt oscillations

- (A) Discharge patterns of a representative nRt cell before (Ctrl) and after CPA application, evoked by negative current injection (-100 pA, 125 ms). Cell was held at different membrane potentials, indicated to the left of each trace.
- (B) Number of LT burst discharges in the cell presented in A, plotted against holding potential. Black circles represent burst discharge number before, open circles after CPA application.
- (C) As B, showing pooled data for 8 cells with voltage bins of 2.5 mV. Data are presented as means  $\pm$  SEM, \* denotes  $p < 0.05$ .
- (D) Effect of CPA on a cell in perforated-patch mode. The bursting mode was strengthened in CPA (bottom trace) compared to the control situation (top trace).

**NREM sleep in SK2<sup>-/-</sup> mice shows reduced EEG power and increased fragmentation**

In the *in vivo* situation, oscillatory burst discharges in nRt accompany characteristic slow waves found in the EEG during NREMS (Crunelli et al., 2006; Steriade, 2003). To explore whether the cellular mechanisms identified here are relevant for slow-wave sleep oscillations, we studied the sleep EEG in SK2<sup>-/-</sup> mice (Bond et al., 2004). EEG spectral profiles between 0 - 35 Hz were examined in freely behaving SK2<sup>-/-</sup> (n = 6) and SK2<sup>+/+</sup> (n = 7) mice during NREMS, REMS and while awake. Normally, NREMS is characterized by low-frequency and high-amplitude oscillations in the EEG (Figure 8A), and the thalamic contributions to these is well established (for review, see (Crunelli et al., 2006; Steriade, 2003)). The REMS EEG is, in contrast, dominated by theta (5 - 10 Hz) oscillations to which the hippocampus makes an important contribution (for review, see (Buzsáki, 2002)). Various frequency components contribute to the waking EEG, including theta activity. In the SK2-null mice, we found that the EEG of all arousal states showed a reduction in power, consistent with the expression of SK2 in numerous brain regions, including the hippocampus and brainstem (Stocker and Pedarzani, 2000). However, we noted that the lack of SK2 channels compromised the NREMS EEG to the greatest extent. An almost 4-fold decrease was observed in the delta (1 - 4 Hz) frequency range, and a more than 3-fold reduction in the sleep spindle (10 - 15 Hz) band (Figure 8B). The reduced contribution of slow oscillations to the NREMS EEG persisted even after taking the differences in overall EEG amplitude into account (Figure S4A). For waking and REMS, a pronounced reduction was observed in the 10 Hz range (Figure 8B). This decrease was due mainly to a slowing of EEG theta oscillations (Figure S4A), consistent with a contribution of SK2 channels to the waveform of hippocampal discharges at theta frequencies (Kramár et al., 2004). Finally, SK2<sup>-/-</sup> mice showed a diminished surge of the sleep spindle activity that is characteristic of the transition from NREMS to REMS (Figures 8D and S4B) (Franken et al., 1998; Gottesmann, 1996).

Additionally, SK2<sup>-/-</sup> mice showed greater NREMS fragmentation, such as more frequent brief awakenings from NREMS and a higher number of short NREMS periods (Figure 8C and Table S1). These are behavioral signs indicative of decreased sleep depth, consistent with the reduction of EEG delta activity (Franken et al., 1999). This suppression of prominent low-frequency components of the NREMS EEG, accompanied by sleep disturbances, suggests that SK2 channel activity contributes to generating some of the physiological hallmarks of NREMS.

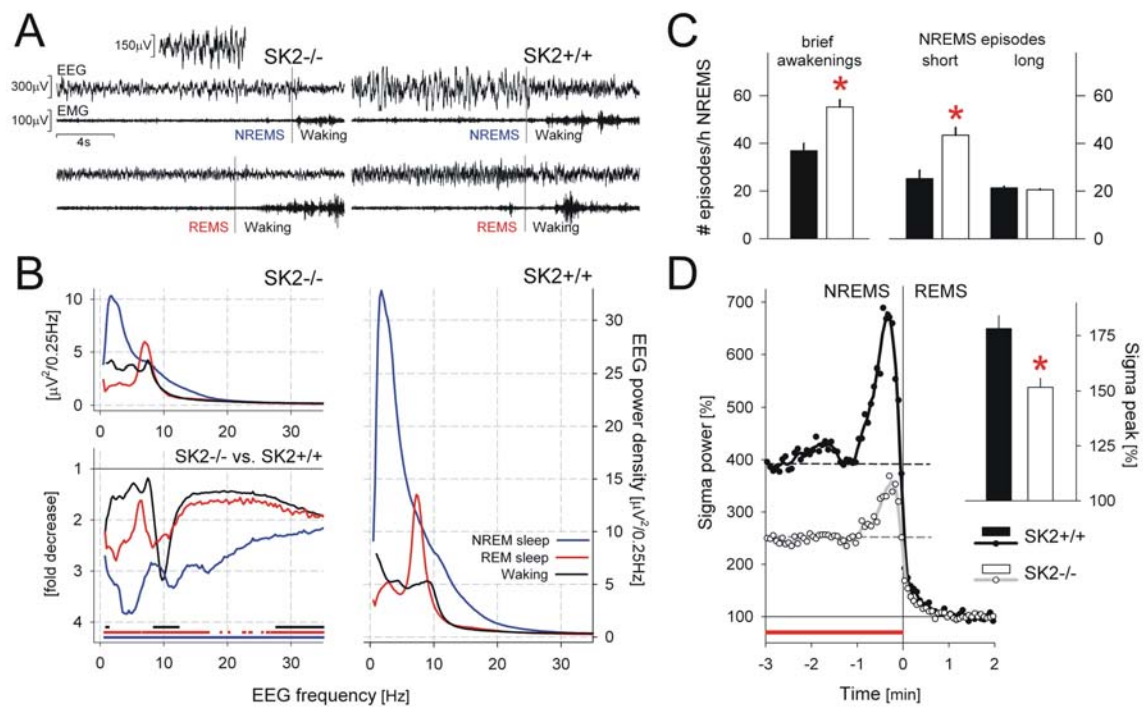


Figure 8. Lack of SK2 greatly impacts the sleep EEG and NREM sleep (NREMS) fragmentation

- (A) Examples of 20 s EEG and EMG traces for SK2<sup>-/-</sup> (left) and SK2<sup>+/+</sup> (right panels) mice at the NREMS to waking (upper) and REMS to waking (lower panels) transitions. Despite the pronounced reduction in EEG amplitude, NREMS preserved its characteristic EEG signature (see insert at 2-fold amplification) ensuring the reliable determination of this state also in SK2<sup>-/-</sup> mice. The same scaling for EEG and EMG amplitude was used across traces except for insert (see scale bars). Examples were taken from two simultaneously recorded mice approximately 1 h after lights-on.
- (B) Quantification of the spectral composition of the EEG during NREMS, REMS, and waking confirmed an important reduction in EEG activity in SK2<sup>-/-</sup> (upper left) and SK2<sup>+/+</sup> (right panel) mice. Genotype differences (lower left panel) were most pronounced during NREMS at frequencies below 15 Hz. Horizontal bars mark frequency bins in which EEG power density significantly differed between genotypes (post-hoc  $t$ -tests,  $P < 0.05$ ). Color codings of bars match those of the spectra for each behavioral state.
- (C) Sleep fragmentation measured as the number of waking episodes shorter or equal to 16 s (one or two 4 s epochs) and the number of short NREMS episodes ( $< 1$  min) were increased in SK2<sup>-/-</sup> mice (open bars) while the number of longer NREMS episodes ( $> 1$  min) did not differ. Number of episodes was expressed per hour of NREMS to correct for eventual differences in NREMS time. Asterisks mark significant differences between genotypes (post-hoc  $t$ -tests,  $P < 0.05$ ). Bars mark means + SEM.
- (D) Time course of EEG activity in the spindle frequency band (i.e., sigma power; 10–15 Hz) at the NREM to REMS transitions. The prevailing level of sigma power during NREMS as well as its surge prior to REMS onset (see inset; maximum values reached were expressed as % of prevailing level; see dashed horizontal lines) were both

reduced. Power density was expressed relative to the level reached in REMS during which spindle oscillations are absent. See Figure S4 for details on the analyses and for changes in other frequency bands. Bottom bar denotes 4 s epochs in which sigma power was significantly reduced in SK2<sup>-/-</sup> mice; asterisk indicates significant genotype difference in sigma peak power (post-hoc *t*-tests,  $P < 0.05$ ).

## Discussion

We used a diverse repertoire of technical approaches to study the coupling between T-type Ca<sup>2+</sup> currents and the Ca<sup>2+</sup>-activated SK2 K<sup>+</sup> currents and its role in oscillatory activity of nRt neurons. We found that thalamic T-type Ca<sup>2+</sup> currents, beyond their role as burst generators, produce marked intracellular Ca<sup>2+</sup> elevations that adopt specific intracellular signalling roles. The interaction between T-type Ca<sup>2+</sup> channels and SK2 channels is based on their spatial co-expression in a substantial portion of nRt dendrites. In these dendrites, T-type Ca<sup>2+</sup> and SK2 channels, together with SERCAs, form an efficient signalling triad. Ca<sup>2+</sup> entry through T-type Ca<sup>2+</sup> channels activates SK2 channels and SK2 channel activity is attenuated by SERCA-mediated sequestration of that same pool of Ca<sup>2+</sup> ions. EEG analysis showed that global deletion of the SK2 channel gene produced a most marked decrement in the frequency bands that correlate with rhythmic burst discharges of thalamic neurons, including those from the nRt (Crunelli et al., 2006; Steriade, 2003). We propose that through the dual coupling of T-type Ca<sup>2+</sup> channels to SK2 channels and SERCAs, nRt dendrites are endowed with a dendritic Ca<sup>2+</sup> signalling triad that contributes to the amplification of thalamic oscillations into large-scale EEG waves.

### T-type Ca<sup>2+</sup> channels in nRt dendrites

T-type Ca<sup>2+</sup> current-dependent Ca<sup>2+</sup> signals account for the overwhelming majority of [Ca<sup>2+</sup>]<sub>i</sub> in nRt dendrites. At the high time resolution of our Ca<sup>2+</sup> imaging system (up to 2 ms), no marked differences in the dynamics of these signals along the imaged dendrite section were detected, suggesting that T-type Ca<sup>2+</sup> channels are homogeneously distributed along proximal dendritic membranes. A dominance of Ca<sup>2+</sup> entry through T-type Ca<sup>2+</sup> currents has also been reported for the dendrites of cerebellar unipolar brush cells (Diana et al., 2007), for dendrodendritic synapses of olfactory bulb granule cells (Egger et al., 2003), and for the neuritic tree of invertebrate heart interneurons (Ivanov and Calabrese, 2000). However, it stands in contrast to the thalamocortical neurons, in which both T-type and HVA Ca<sup>2+</sup> currents increase [Ca<sup>2+</sup>]<sub>i</sub> in dendrites during bursting (Kuisle et al., 2006; Munsch et al., 1997). The nRt may thus belong to a small group of nuclei with neuronal dendrites

specialized in the handling of  $\text{Ca}^{2+}$  entry through T-type  $\text{Ca}^{2+}$  channels and in compartmentalizing targets for these, such as ion channels, sequestration machinery, and sites of vesicular release (Egger et al., 2003; Ivanov and Calabrese, 2000). Cells in the nRt express mRNA for both  $\text{Ca}_v3.2$  and  $\text{Ca}_v3.3$  isoforms (Talley et al., 1999) and T-type  $\text{Ca}^{2+}$  currents show distinct kinetic properties according to their subcellular localization, characterized by rapidly inactivating somatic, and more slowly decaying dendritic currents (Joksovic et al., 2005). Both  $\text{Ca}_v3.2$  and  $\text{Ca}_v3.3$  subtypes contribute to dendritic  $\text{Ca}^{2+}$  currents in nRt (Joksovic et al., 2006). However, it appears likely that the properties conferred by the  $\text{Ca}_v3.3$  isoform make a significant contribution to the  $[\text{Ca}^{2+}]_i$  transients observed here. Heterologously expressed  $\text{Ca}_v3.3$  channels exhibit slow components of inactivation and recovery from inactivation (Frazier et al., 2001; Uebachs et al., 2006) and once activated, generate spontaneous plateau potentials and large  $[\text{Ca}^{2+}]_i$  increments (Chevalier et al., 2006). Similarly, in the absence of SK2 channels, nRt bursting is followed by long-lasting plateau potentials, reminiscent of those generated by  $\text{Ca}_v3.3$  channels. Furthermore, the dampening of nRt oscillations is caused by fading T-type  $\text{Ca}^{2+}$  channel recruitment, as imaging, electrophysiological, and modelling studies are consistent with a use-dependent cumulative inactivation of T-type  $\text{Ca}^{2+}$  channels and a drop-out of channels in burst generation. How, in detail, the inactivation and recovery characteristics of currents generated by  $\text{Ca}_v3.3$  or  $\text{Ca}_v3.2$  channels (Frazier et al., 2001; Uebachs et al., 2006) shape the activation of SK2 currents remains to be determined. In addition, synaptic activity during network oscillations, in particular  $\text{Ca}^{2+}$  influx through N-methyl-D-aspartate (NMDA) receptors may further contribute to  $[\text{Ca}^{2+}]_i$  in nRt dendrites and regulate synaptically located SK2 channels (Ngo-Anh et al., 2005). This possibility remains to be explored, both in terms of synergistic effects of glutamatergic receptor currents and T-type  $\text{Ca}^{2+}$  currents in SK2 current activation, as well as how  $\text{Ca}^{2+}$  influx through NMDA receptors could additionally regulate SK2 channel function at synaptic sites.

Our work unifies a number of previous theoretical and experimental aspects of nRt rhythmogenesis. An essential role of dendrites for nRt function has been recognized (Destexhe et al., 1996; Huguenard and Prince, 1992), and is underscored here by demonstrating the dendritic ionic specializations required for rhythmogenesis.  $[\text{Ca}^{2+}]_i$  elevations appear synchronously in proximal dendrites, suggesting a uniform and high expression of T-type  $\text{Ca}^{2+}$  channels. The estimated T-type  $\text{Ca}^{2+}$  channel conductance density is consistent with previous values used in computational studies (Destexhe et al., 1996), and suggests that T-type  $\text{Ca}^{2+}$  channel density in proximal dendrites is high enough to play an



active role in dendritic  $\text{Ca}^{2+}$  electrogenesis. These properties are combined with additional distinctive features of nRt dendrites (Pinault, 2004). Their fine and extended arborizations give rise to a high surface-to-volume ratio that generates large transmembrane current flow, guaranteeing robust switching between the oscillatory ‘up’ and ‘down’ states. Together with the electrical connectivity via gap junctions and long-range reciprocal interactions (Pinault, 2004), nRt dendrites appear uniquely equipped to form a plexus of vigorously oscillating membrane surfaces.

### **SK2 channels in nRt dendrites**

Heterologously expressed SK2 channels need ~6-8 ms to gate in saturating  $[\text{Ca}^{2+}]_i$  (Pedarzani et al., 2001; Xia et al., 1998) and, in CA1 hippocampal cells, presumed single SK channels open within 15 ms following HVA  $\text{Ca}^{2+}$  channel activation, which are colocalized within 50-150 nm (Marrion and Tavalin, 1998). In nRt cells, the peak  $[\text{Ca}^{2+}]_i$  levels reached in the dendrites (~0.7  $\mu\text{M}$ ) are close to what is needed to maximally activate SK2 channels (Köhler et al., 1996; Pedarzani et al., 2001). Moreover, the latency to SK current activation was ~14 ms from the peak of the T-type  $\text{Ca}^{2+}$  current, indicating a close-to-maximal rate of exposure of SK2 channels to the  $\text{Ca}^{2+}$  entered through T-type  $\text{Ca}^{2+}$  channels. In imaging experiments, the AHP generated by SK channels peaked within ~37 ms after  $[\text{Ca}^{2+}]_i$  was maximal. Although this value is determined by the convolution of ion current flow and charge of membrane capacitance (see Results), it is also consistent with the idea that SK2 channel activation occurs at a very fast rate. These estimates underscore the idea that dendrites of nRt cells are functionally specialized to ensure a rapid  $\text{Ca}^{2+}$ -activated  $\text{K}^+$  signalling via colocalization with a high density of  $\text{Ca}^{2+}$  sources.

After their strong activation by a single LT burst, SK2 channels exert a threefold role in nRt oscillations. First, the AHPs generated by SK2 channels in nRt neurons are permissive for repetitive LT burst generation because they allow T-type  $\text{Ca}^{2+}$  channels to recover from inactivation and to generate the next LT burst. Second, we found that SK2 channels accelerate LT burst termination, because blocking them with apamin or intracellular  $\text{Cs}^+$ , or via genetic deletion, reduced the T-type  $\text{Ca}^{2+}$  current decay slope by more than two-fold and led to pronounced, slowly decaying plateau potentials. Thus, T-type  $\text{Ca}^{2+}$  channels and SK2 channels form a  $\text{Ca}^{2+}$ -mediated feedback loop.  $\text{Ca}^{2+}$  entry through T-type  $\text{Ca}^{2+}$  currents activates SK2 currents and the repolarizing effect of these terminates the T-type  $\text{Ca}^{2+}$  currents that supply their  $\text{Ca}^{2+}$  source. Such rapid current decay perhaps prevents a slow form of inactivation (Frazier et al., 2001) and is consistent with previous descriptions of SK currents

in the context of terminating plateau potentials (Bond et al., 2005; Cai et al., 2004). The coupling between T-type  $\text{Ca}^{2+}$  and SK currents can even prevent bursting, when SK currents activate rapidly enough to effectively terminate T-type  $\text{Ca}^{2+}$  currents before their full activation (Wolfart and Roper, 2002). Third, our data suggest that decremental activation of SK2 currents may also be involved in the cessation of nRt oscillations. Such dampening was previously attributed to slowly activating,  $\text{Ca}^{2+}$ -dependent cationic currents (Bal and McCormick, 1993; Blethyn et al., 2006; Pape et al., 2004), but the question remained open to what extent these additional currents were instrumental for oscillatory dampening, and, if so, what were their biophysical and molecular properties. Our imaging experiments show little temporal summation of  $[\text{Ca}^{2+}]_i$  during repetitive LT bursts and thus provide little support for a scenario of an accruing activation of  $\text{Ca}^{2+}$ -dependent cationic currents during repetitive LT bursts. Instead, we found that T-type  $\text{Ca}^{2+}$  currents diminish during repetitive activation and produce smaller  $[\text{Ca}^{2+}]_i$  elevations. This was accompanied by a lack of associated rapid outward currents and a shallower decay, consistent with decreased SK2 current activation. Finally, the analysis of the effects of 1-EBIO further suggests that SK2 current activation is submaximal in later oscillatory cycles. For these reasons, we propose that a mechanism invoking T-type  $\text{Ca}^{2+}$  and SK2 channel coupling may, in large part, account for dampened nRt oscillations.

### **Role of SERCAs in regulating the coupling between T-type $\text{Ca}^{2+}$ currents and SK2 currents**

SERCAs are an important element in the homeostatic regulation of  $[\text{Ca}^{2+}]_i$  in neurons and ensure the appropriate filling of the ER with  $\text{Ca}^{2+}$ , which can become available via  $\text{Ca}^{2+}$ -induced  $\text{Ca}^{2+}$  release, to regulate ion channels. In contrast to this well-established role of intracellular  $\text{Ca}^{2+}$  stores in neuronal excitability, the possibility that SERCAs actively control neuronal rhythmicity via their sequestering function has not been described, although SERCA-mediated  $\text{Ca}^{2+}$  uptake is well-known for enhancing performance of cardiac cells (Misquitta et al., 1999). Remarkably, SERCAs act specifically on T-type  $\text{Ca}^{2+}$  current-dependent  $\text{Ca}^{2+}$  entry, strongly suggesting that they are colocalized with T-type  $\text{Ca}^{2+}$  and SK2 channels, but not with HVA  $\text{Ca}^{2+}$  channels. SERCAs have an affinity for  $\text{Ca}^{2+}$  of 0.27 - 0.4  $\mu\text{M}$  (Lytton et al., 1992) and, in Purkinje cells at room temperature, remove  $\text{Ca}^{2+}$  at a rate of up to  $\sim 0.6 \mu\text{M/s}$  for  $[\text{Ca}^{2+}]_i$  in the low micromolar range (Fierro et al., 1998). These are parameters ranges consistent with the idea of SERCAs acting as competitors with SK2 channels for available free  $\text{Ca}^{2+}$  ions. The competition is supported by our observation that

apamin-sensitive currents are potentiated in total amplitude and in a slowly decaying current component when SERCAs are blocked, indicating a higher and more prolonged  $[Ca^{2+}]_i$  in the vicinity of SK2 channels. Moreover, interburst AHPs are lengthened and the number of bursts increased in CPA. On the one hand, SERCAs may contribute to shorten the exposure of SK2 channels to  $Ca^{2+}$  during the AHP, thereby limiting T-type  $Ca^{2+}$  channel recovery and promoting oscillatory dampening. This possibility is consistent with a greater slow tail component in SK2 currents when SERCAs are blocked. On the other hand, the fact that SK2 currents are also potentiated at their peak suggests that SERCAs may act rapidly to antagonize SK2 channel-induced deactivation of T-type  $Ca^{2+}$  channels, thereby effectively potentiating T-type  $Ca^{2+}$  channel activation and SK2 channel exposure to  $[Ca^{2+}]_i$ . Further  $Ca^{2+}$  imaging experiments will be required to understand the detailed consequences of SERCA activity on dendritic  $[Ca^{2+}]_i$  signals and on SK2 channel function.

### **The role of nRt SK2 channels in low-frequency EEG waves of NREMS**

*In vivo*, burst discharges in nRt are most prominent during periods of EEG synchronization, such as during NREMS, while tonic firing predominates during waking and REMS (Domich et al., 1986; Fuentealba and Steriade, 2005). We note in particular that EEG power is reduced most strongly during NREMS in SK2<sup>-/-</sup> mice, suggesting that SK2 channels play a role in boosting oscillatory activities underlying low-frequency sleep oscillations. This may indicate a link between the observed oscillatory bursting deficits in nRt cells and the EEG alterations. However, at present we cannot exclude other explanations since EEG rhythms result from interplay between thalamic and cortical networks and are strongly regulated by ascending brainstem afferents (Steriade et al., 2003). Indeed, in the absence of SK2 channels, low-frequency oscillations in the EEG persist, albeit they are strongly weakened, consistent with the nRt not being the only site of rhythm generation (Steriade, 2003). The reduction of the EEG power in SK2-null mice could be caused by multiple disturbances in thalamic and cortical networks, and of alterations in corticothalamic communication (for earlier works, see (Benington et al., 1995; Gandolfo et al., 1996)). In addition, there may be compensatory effects due to the lack of SK2 channels. Although nRt is clearly implicated in some NREMS oscillations (Fuentealba and Steriade, 2005), a substantial experimental effort in recordings *in vivo* would be needed to elucidate the detailed role of SK2 channels in nRt dendrites in the neuronal networks underlying NREMS EEG oscillations. Nevertheless, our work suggests that assessing the roles of SK2 channels in thalamocortical networks could help to identify targets for improving NREMS continuity

and/or depth, in disorders in which NREMS quality is impacted such as in primary insomnia or insomnias associated with psychiatric or neurological disorders.

## Experimental Procedures

### Electrophysiological Recordings

Horizontal slices (400  $\mu\text{m}$  for extracellular recordings, 300  $\mu\text{m}$  for patch-clamp recordings) were prepared from WT, SK1<sup>-/-</sup> or SK2<sup>-/-</sup> mice and corresponding +/+ littermates (1.5 - 2 month-old for extracellular recordings, 17 - 23 days for patch-clamp recordings), as described previously (Kuisle et al., 2006) and approved by the Veterinäramt of the Canton Basel-Stadt. Extracellular and patch-clamp recording were obtained according to well-established procedures at 33.5 - 35°C (Supplemental Experimental Procedures). Data were analyzed off-line using pClamp 9.2. and Igor Pro V.5.0.5. software and are indicated as means  $\pm$  standard error (SEM).

### Genotyping

Homozygous SK2<sup>-/-</sup> and SK1<sup>-/-</sup> mice were obtained from crossings of heterozygotic pairs, bred to the genetic background of the WT C57Bl/6J animals, and were genotyped as described (Bond et al., 2004).

### Ca<sup>2+</sup> imaging experiments

The internal solution for whole-cell recordings was supplemented with magfura-2 (3 mM) or bis-fura-2 (1 mM,  $K_d = 0.525 \mu\text{M}$ ), but no EGTA, unless otherwise specified. Fluorescence was excited with a 150 W ultrastable Xenon Arc lamp (Cairn Research, UK) at  $387 \pm 6 \text{ nm}$  and detected with a NeuroCCD-SM camera (RedShirt, USA) at  $510 \pm 45 \text{ nm}$  and sampled either at 125 or 500 frames/s. The field was 125  $\mu\text{m}$  x 125  $\mu\text{m}$  (80 pixels x 80 pixels). Bleaching was taken into account by subtracting trials without electrophysiological stimulation. The brightest dendrite was selected for recordings. Four sequences were averaged to improve the signal-to-noise ratio. For experiments with magfura-2, fluorescence signals were converted into changes of free Ca<sup>2+</sup> concentration defined as  $\Delta[\text{Ca}^{2+}]_i = K_d \cdot (F_{\min} - F) / (F - F_{\max})$  where F is the fluorescence intensity (after correction for the slice auto-fluorescence) and  $F_{\min}$  and  $F_{\max}$  are the fluorescence intensities at 0 and at saturating Ca<sup>2+</sup>, respectively. The value for  $K_d$  was determined experimentally (see Supplemental Experimental Procedures). Bis-fura-2-mediated signals were converted into dye-bound Ca<sup>2+</sup> defined as  $\Delta[\text{DCa}^{2+}] =$

$1mM * (F_{min} - F) / (F_{min} - F_{max})$  (Canepari et al., 2004). In the conversions of fluorescence signals either into  $\Delta[Ca^{2+}]_i$  or  $\Delta[DCa^{2+}]$ ,  $F_{min}$  was approximated with the initial resting fluorescence whereas  $F - F_{max}$  and  $F_{min} - F_{max}$  were approximated with  $F$  and  $F_{min}$  respectively.

### **Immunohistochemistry and electron microscopy**

Sections were treated for light and electron microscopy immunolabeling as described previously (Luján et al., 1996) (Supplemental Experimental Procedures). Affinity-purified rabbit and guinea pig antibodies to SK2 were raised against amino acid residues 536 - 574 of the mouse SK2 (Accession No. NM080465), and diluted at 1 - 2  $\mu\text{g/ml}$ .

### **EEG Monitoring and Analyses**

For EEG recordings, adult (2.5 - 4 months-old), female SK2 +/+ (n = 7) and SK2-/- (n = 6) mice were used. Mice were equipped with EEG and electromyogram (EMG) electrodes according to standard procedures (see Supplementary Experimental Procedures). Continuous EEG and EMG recordings were obtained for 24 h (n = 5) or 48 h (n = 8). Offline, the behavioral states waking, NREMS, and REMS were determined by visual inspection of the EEG and EMG signals for consecutive 4 s intervals. The spectral content of the EEG was estimated using a discrete fourier transformation routine. For further details on recording and analysis, see Supplemental Experimental Procedures.

### **Computational modeling**

For details of the model, see Supplemental Experimental Procedures. Equations were solved in Mathematica V.5.0 using Runge-Kutta integration.

### **Statistical analysis**

Two-tailed paired and unpaired t-test were used for within and between group comparisons, respectively. For multiple comparisons between data obtained from wild-type, SK1- and SK2-deficient animals, Tukey's HSD or Dunnett's T3 post-hoc test was used after significance was reached in a one-way analysis of variance with factor "genotype" and homogeneity of variances was tested with Levene's test.  $p < 0.05$  was considered statistically significant. Analyses were carried out using SPSS V. 14. See legends to the Figure S4 and Table S1 for further details on statistical analyses.

## References

- Amzica, F., Nuñez, A., and Steriade, M. (1992). Delta frequency (1-4 Hz) oscillations of perigeniculate thalamic neurons and their modulation by light. *Neuroscience* *51*, 285-294.
- Avanzini, G., de Curtis, M., Panzica, F., and Spreafico, R. (1989). Intrinsic properties of nucleus reticularis thalami neurones of the rat studied *in vitro*. *J Physiol* *416*, 111-122.
- Bal, T., and McCormick, D.A. (1993). Mechanisms of oscillatory activity in guinea-pig nucleus reticularis thalami *in vitro*: a mammalian pacemaker. *J Physiol* *468*, 669-691.
- Benington, J.H., Woudenberg, M.C., and Heller, H.C. (1995). Apamin, a selective SK potassium channel blocker, suppresses REM sleep without a compensatory rebound. *Brain Res* *692*, 86-92.
- Bildl, W., Strassmaier, T., Thurm, H., Andersen, J., Eble, S., Oliver, D., Knipper, M., Mann, M., Schulte, U., Adelman, J.P., and Fakler, B. (2004). Protein kinase CK2 is coassembled with small conductance Ca<sup>2+</sup>-activated K<sup>+</sup> channels and regulates channel gating. *Neuron* *43*, 847-858.
- Blethyn, K.L., Hughes, S.W., Tóth, T.I., Cope, D.W., and Crunelli, V. (2006). Neuronal basis of the slow (<1 Hz) oscillation in neurons of the nucleus reticularis thalami *in vitro*. *J Neurosci* *26*, 2474-2486.
- Bond, C.T., Herson, P.S., Strassmaier, T., Hammond, R., Stackman, R., Maylie, J., and Adelman, J.P. (2004). Small conductance Ca<sup>2+</sup>-activated K<sup>+</sup> channel knock-out mice reveal the identity of calcium-dependent afterhyperpolarization currents. *J Neurosci* *24*, 5301-5306.
- Bond, C.T., Maylie, J., and Adelman, J.P. (2005). SK channels in excitability, pacemaking and synaptic integration. *Curr Opin Neurobiol* *15*, 305-311.
- Buzsáki, G. (2002). Theta oscillations in the hippocampus. *Neuron* *33*, 325-340.
- Cai, X., Liang, C.W., Muralidharan, S., Kao, J.P., Tang, C.M., and Thompson, S.M. (2004). Unique roles of SK and K<sub>v</sub>4.2 potassium channels in dendritic integration. *Neuron* *44*, 351-364.
- Canepari, M., Auger, C., and Ogden, D. (2004). Ca<sup>2+</sup> ion permeability and single-channel properties of the metabotropic slow EPSC of rat Purkinje neurons. *J Neurosci* *24*, 3563-3573.
- Chevalier, M., Lory, P., Mironneau, C., Macrez, N., and Quignard, J.F. (2006). T-type Ca<sub>v</sub>3.3 calcium channels produce spontaneous low-threshold action potentials and intracellular calcium oscillations. *Eur J Neurosci* *23*, 2321-2329.
- Cotillon, N., and Edeline, J.M. (2000). Tone-evoked oscillations in the rat auditory cortex result from interactions between the thalamus and reticular nucleus. *Eur J Neurosci* *12*, 3637-3650.
- Crunelli, V., Cope, D.W., and Hughes, S.W. (2006). Thalamic T-type Ca<sup>2+</sup> channels and NREM sleep. *Cell Calcium* *40*, 175-190.
- Cui, G., Okamoto, T., and Morikawa, H. (2004). Spontaneous opening of T-type Ca<sup>2+</sup> channels contributes to the irregular firing of dopamine neurons in neonatal rats. *J Neurosci* *24*, 11079-11087.
- Debarbieux, F., Brunton, J., and Charpak, S. (1998). Effect of bicuculline on thalamic activity: a direct blockade of I<sub>AHP</sub> in reticularis neurons. *J Neurophysiol* *79*, 2911-2918.
- Destexhe, A., Contreras, D., Steriade, M., Sejnowski, T.J., and Huguenard, J.R. (1996). *In vivo*, *in vitro*, and computational analysis of dendritic calcium currents in thalamic reticular neurons. *J Neurosci* *16*, 169-185.
- Diana, M.A., Otsu, Y., Maton, G., Collin, T., Chat, M., and Dieudonne, S. (2007). T-type and L-type Ca<sup>2+</sup> conductances define and encode the bimodal firing pattern of vestibulocerebellar unipolar brush cells. *J Neurosci* *27*, 3823-3838.
- Domich, L., Oakson, G., and Steriade, M. (1986). Thalamic burst patterns in the naturally sleeping cat: a comparison between cortically projecting and reticularis neurones. *J Physiol* *379*, 429-449.

- Egger, V., Svoboda, K., and Mainen, Z.F. (2003). Mechanisms of lateral inhibition in the olfactory bulb: efficiency and modulation of spike-evoked calcium influx into granule cells. *J Neurosci* 23, 7551-7558.
- Fierro, L., DiPolo, R., and Llanò, I. (1998). Intracellular calcium clearance in Purkinje cell somata from rat cerebellar slices. *J Physiol* 510 ( Pt 2), 499-512.
- Franken, P., Malafosse, A., and Tafti, M. (1998). Genetic variation in EEG activity during sleep in inbred mice. *Am J Physiol* 275, R1127-R1137.
- Franken, P., Malafosse, A., and Tafti, M. (1999). Genetic determinants of sleep regulation in inbred mice. *Sleep* 22, 155-169.
- Frazier, C.J., Serrano, J.R., George, E.G., Yu, X., Viswanathan, A., Perez-Reyes, E., and Jones, S.W. (2001). Gating kinetics of the  $\alpha 1I$  T-type calcium channel. *J Gen Physiol* 118, 457-470.
- Fuentealba, P., and Steriade, M. (2005). The reticular nucleus revisited: intrinsic and network properties of a thalamic pacemaker. *Prog Neurobiol* 75, 125-141.
- Fuentealba, P., Timofeev, I., Bazhenov, M., Sejnowski, T.J., and Steriade, M. (2005). Membrane bistability in thalamic reticular neurons during spindle oscillations. *J Neurophysiol* 93, 294-304.
- Gandolfo, G., Schweitz, H., Lazdunski, M., and Gottesmann, C. (1996). Sleep cycle disturbances induced by apamin, a selective blocker of  $Ca^{2+}$ -activated  $K^{+}$  channels. *Brain Res* 736, 344-347.
- Gottesmann, C. (1996). The transition from slow-wave sleep to paradoxical sleep: evolving facts and concepts of the neurophysiological processes underlying the intermediate stage of sleep. *Neurosci Biobehav Rev* 20, 367-387.
- Huguenard, J.R., and Prince, D.A. (1992). A novel T-type current underlies prolonged  $Ca^{2+}$ -dependent burst firing in GABAergic neurons of rat thalamic reticular nucleus. *J Neurosci* 12, 3804-3817.
- Ivanov, A.I., and Calabrese, R.L. (2000). Intracellular  $Ca^{2+}$  dynamics during spontaneous and evoked activity of leech heart interneurons: low-threshold Ca currents and graded synaptic transmission. *J Neurosci* 20, 4930-4943.
- Joksovic, P.M., Bayliss, D.A., and Todorovic, S.M. (2005). Different kinetic properties of two T-type  $Ca^{2+}$  currents of rat reticular thalamic neurones and their modulation by enflurane. *J Physiol* 566, 125-142.
- Joksovic, P.M., Nelson, M.T., Jevtovic-Todorovic, V., Patel, M.K., Perez-Reyes, E., Campbell, K.P., Chen, C.C., and Todorovic, S.M. (2006).  $Ca_v3.2$  is the major molecular substrate for redox regulation of T-type  $Ca^{2+}$  channels in the rat and mouse thalamus. *J Physiol* 574, 415-430.
- Köhler, M., Hirschberg, B., Bond, C.T., Kinzie, J.M., Marrion, N.V., Maylie, J., and Adelman, J.P. (1996). Small-conductance, calcium-activated potassium channels from mammalian brain. *Science* 273, 1709-1714.
- Kramár, E.A., Lin, B., Lin, C.-Y., Arai, A.C., Gall, C.M., and Lynch, G. (2004). A novel mechanism for the facilitation of theta-induced long-term potentiation by brain-derived neurotrophic factor. *J Neurosci* 24, 5151-5161.
- Kuisle, M., Wanaverbecq, N., Brewster, A.L., Frere, S.G., Pinault, D., Baram, T.Z., and Lüthi, A. (2006). Functional stabilization of weakened thalamic pacemaker channel regulation in rat absence epilepsy. *J Physiol* 575, 83-100.
- Luján, R., Nusser, Z., Roberts, J.D., Shigemoto, R., and Somogyi, P. (1996). Perisynaptic location of metabotropic glutamate receptors mGluR1 and mGluR5 on dendrites and dendritic spines in the rat hippocampus. *Eur J Neurosci* 8, 1488-1500.
- Lytton, J., Westlin, M., Burk, S.E., Shull, G.E., and MacLennan, D.H. (1992). Functional comparisons between isoforms of the sarcoplasmic or endoplasmic reticulum family of calcium pumps. *J Biol Chem* 267, 14483-14489.

- Marrion, N.V., and Tavalin, S.J. (1998). Selective activation of  $\text{Ca}^{2+}$ -activated  $\text{K}^+$  channels by co-localized  $\text{Ca}^{2+}$  channels in hippocampal neurons. *Nature* 395, 900-905.
- Misquitta, C.M., Mack, D.P., and Grover, A.K. (1999). Sarco/endoplasmic reticulum  $\text{Ca}^{2+}$  (SERCA)-pumps: link to heart beats and calcium waves. *Cell Calcium* 25, 277-290.
- Munsch, T., Budde, T., and Pape, H.C. (1997). Voltage-activated intracellular calcium transients in thalamic relay cells and interneurons. *Neuroreport* 8, 2411-2418.
- Ngo-Anh, T.J., Bloodgood, B.L., Lin, M., Sabatini, B.L., Maylie, J., and Adelman, J.P. (2005). SK channels and NMDA receptors form a  $\text{Ca}^{2+}$ -mediated feedback loop in dendritic spines. *Nat Neurosci* 8, 642-649.
- Ogden, D., Khodakhah, K., Carter, T., Thomas, M., and Capiod, T. (1995). Analogue computation of transient changes of intracellular free  $\text{Ca}^{2+}$  concentration with the low affinity  $\text{Ca}^{2+}$  indicator fura2/AM during whole-cell patch-clamp recording. *Pflügers Arch* 429, 587-591.
- Pape, H.C., Munsch, T., and Budde, T. (2004). Novel vistas of calcium-mediated signalling in the thalamus. *Pflügers Arch* 448, 131-138.
- Pedarzani, P., Mosbacher, J., Rivard, A., Cingolani, L.A., Oliver, D., Stocker, M., Adelman, J.P., and Fakler, B. (2001). Control of electrical activity in central neurons by modulating the gating of small conductance  $\text{Ca}^{2+}$ -activated  $\text{K}^+$  channels. *J Biol Chem* 276, 9762-9769.
- Perez-Reyes, E. (2003). Molecular physiology of low-voltage-activated T-type calcium channels. *Physiol Rev* 83, 117-161.
- Pinault, D. (2004). The thalamic reticular nucleus: structure, function and concept. *Brain Res Brain Res Rev* 46, 1-31.
- Richter, T.A., Kolaj, M., and Renaud, L.P. (2005). Low voltage-activated  $\text{Ca}^{2+}$  channels are coupled to  $\text{Ca}^{2+}$ -induced  $\text{Ca}^{2+}$  release in rat thalamic midline neurons. *J Neurosci* 25, 8267-8271.
- Shin, H.S., Lee, J., and Song, I. (2006). Genetic studies on the role of T-type  $\text{Ca}^{2+}$  channels in sleep and absence epilepsy. *CNS&Neurol Disorders - Drug Targets* 5, 629-638.
- Steriade, M. (2003). The corticothalamic system in sleep. *Front Biosci* 8, d878-d899.
- Steriade, M., Contreras, D., Curró Dossi, R., and Nuñez, A. (1993). The slow (< 1 Hz) oscillation in reticular thalamic and thalamocortical neurons: scenario of sleep rhythm generation in interacting thalamic and neocortical networks. *J Neurosci* 13, 3284-3299.
- Stocker, M. (2004).  $\text{Ca}^{2+}$ -activated  $\text{K}^+$  channels: molecular determinants and function of the SK family. *Nat Rev Neurosci* 5, 758-770.
- Stocker, M., and Pedarzani, P. (2000). Differential distribution of three  $\text{Ca}^{2+}$ -activated  $\text{K}^+$  channel subunits, SK1, SK2, and SK3, in the adult rat central nervous system. *Mol Cell Neurosci* 15, 476-493.
- Sun, Q.Q., Huguenard, J.R., and Prince, D.A. (2001). Neuropeptide Y receptors differentially modulate G-protein-activated inwardly rectifying  $\text{K}^+$  channels and high-voltage-activated  $\text{Ca}^{2+}$  channels in rat thalamic neurons. *J Physiol* 531, 67-79.
- Talley, E.M., Cribbs, L.L., Lee, J.H., Daud, A., Perez-Reyes, E., and Bayliss, D.A. (1999). Differential distribution of three members of a gene family encoding low voltage-activated (T-type) calcium channels. *J Neurosci* 19, 1895-1911.
- Uebachs, M., Schaub, C., Perez-Reyes, E., and Beck, H. (2006). T-type  $\text{Ca}^{2+}$  channels encode prior neuronal activity as modulated recovery rates. *J Physiol* 571, 519-536.
- Wolfart, J., and Roeper, J. (2002). Selective coupling of T-type calcium channels to SK potassium channels prevents intrinsic bursting in dopaminergic midbrain neurons. *J Neurosci* 22, 3404-3413.
- Xia, X.M., Fakler, B., Rivard, A., Wayman, G., Johnson-Pais, T., Keen, J.E., Ishii, T., Hirschberg, B., Bond, C.T., Lutsenko, S., *et al.* (1998). Mechanism of calcium gating in small-conductance calcium-activated potassium channels. *Nature* 395, 503-507.



**Supplemental Data**

**A competition between SK2 channels and SERCAs  
for Ca<sup>2+</sup> entry through T-type channels  
gates sleep-related oscillations in thalamic dendrites**

Lucius Cueni, Marco Canepari, Rafael Luján, Yann Emmenegger, Masahiko Watanabe, Chris T. Bond, Paul Franken, John P. Adelman and Anita Lüthi

## **1) Supplemental Experimental Procedures**

### **Electrophysiological recordings**

*Recording solutions and data acquisition.* For patch-clamp recordings, the bath was constantly perfused with fresh medium at a rate of 2.5-4 mlmin<sup>-1</sup> that contained (in mM): 131 NaCl; 2.5 KCl; 1.25 NaH<sub>2</sub>PO<sub>4</sub>; 1.2 MgCl<sub>2</sub>; 2 CaCl<sub>2</sub>; 26 NaHCO<sub>3</sub>, 18 dextrose, 1.7 L(+)-ascorbic acid. The caudal portion of the nRt was localized before pipette positioning using a low-power (10 x) objective, and a high-power water immersion objective (40 x) and near-infrared differential interference contrast optics were used for visualizing cells. Patch pipettes were pulled from borosilicate glass tubing (TW150F-4, outer diameter 1.5 mm, World Precision Instruments) on a vertical two-step puller (PP-83, Narishige) and filled with the following solution (in mM): 130 KMeSO<sub>4</sub>, 10 KCl, 10 HEPES, 0.1 mM EGTA, 2 MgCl<sub>2</sub>, 2 K-ATP, 0.2 Na-GTP, 10 phosphocreatine, adjusted to 290 mOsm with sucrose, pH 7.25. The low concentration of EGTA increases the intracellular Ca<sup>2+</sup> buffering capacity by ~1000 and hence clamps steady-state Ca<sup>2+</sup> levels to low values, while not affecting [Ca<sup>2+</sup>]<sub>i</sub> transients generated by LT bursts (see Results). The resistance of the electrodes was 2.1-3.8 MΩ and yielded series resistances in the range between 10-20 MΩ. Series resistance was constantly monitored throughout the experiments and increases > 20% were not accepted. For MeSO<sub>4</sub>- and gluconate-based pipettes, a liquid junction potential of -17 mV and -10 mV was taken into account, respectively. Data from voltage- and current-clamp recordings were collected through an Axopatch 200B amplifier (Molecular Devices), filtered at 2 kHz and acquired at 5 kHz using pClamp 9.2. software (Molecular Devices). To isolate T-type Ca<sup>2+</sup> currents, Cs<sup>+</sup>-based intracellular solutions were used, in which KMeSO<sub>4</sub> was replaced by CsGluconate and

KCl by CsCl, and hyperpolarizing voltage commands were applied (from -60 to -100 mV, 500 ms). Cells included in this analysis showed T-type  $\text{Ca}^{2+}$  currents with properties that fulfilled previously established criteria for acceptable voltage control in intact nRt cells, including a smooth activation and decay ( $\tau_{\text{decay}} = 28.1 \pm 3.2$  ms at -55 to -60 mV at 35 °C,  $n = 12$ ) and a steady-state inactivation curve with a  $V_{50}$  of  $-79.3 \pm 0.3$  mV and a slope of  $5.0 \pm 0.2$  mV ( $n = 12$ ), close to values published previously for acutely dissociated cells (Huguenard and Prince, 1992). In  $\text{K}^+$ -based recordings, neurons were generally clamped around their resting membrane potentials ( $\sim -67$  -  $-80$  mV) and SK currents, evoked after hyper- (-40 mV, 125 ms) or depolarizing voltage steps (+ 30 mV, 125 ms), were quantified between -62 and -67 mV. T-type  $\text{Ca}^{2+}$  current decay slope was determined by a linear fit to the 15 ms time interval after current peak, during which decay is linear (e.g. Figure 1A, C).

*Analysis of apamin-sensitive currents.* SK currents were obtained by digital subtraction of currents recorded in the presence of apamin (100 nM), and are presented as apamin-sensitive currents. In our experiments, SK currents were recorded at a constant holding voltage following a hyperpolarizing step to gate T-type  $\text{Ca}^{2+}$  currents. Apamin subtraction was carried out by digitally subtracting averaged traces (typically 2 - 5 sweeps) obtained following bath application of 100 nM apamin. We assessed the quality and stability of voltage-clamp control in these recordings with  $\text{K}^+$ -based electrodes in several ways. First, we tested whether the apamin-sensitive currents, obtained by digital subtraction, remained stable for the period required to perform application of pharmacological substances via the bath or through the recording pipette (ca. 10 min). Apamin-sensitive currents were unchanged after this time ( $109.2 \pm 7.9$  % of control amplitude,  $n = 4$ ,  $p > 0.4$ ). Second, we took care to only carry out the subtraction when all recording conditions, such as input resistance, series resistance and capacitive currents remained unaltered before and after apamin application. We noted that some small inward T-type  $\text{Ca}^{2+}$  currents ( $< 15\%$  of total current) remained which were due to a slight, apamin-induced increase in the peak of the T-type  $\text{Ca}^{2+}$  current. This likely resulted from apamin-induced decelerated decay of the T-type  $\text{Ca}^{2+}$  current (see e.g. Figure 1A, B). However, these currents were small ( $< \sim 50$  pA) and decayed rapidly compared to the time course of the apamin-sensitive outward current. These remaining currents will thus lead to an overestimation of the latency between peak T-type and peak SK current, an error which does not affect the interpretation of the tight temporal coupling between the two currents. Third, the decay time constant of the T-type  $\text{Ca}^{2+}$  currents was  $32.3 \pm 1.2$  ms ( $n = 6$ ) in apamin, close to the value obtained with  $\text{Cs}^+$ -based electrodes ( $p > 0.05$ ).

This suggests that, in the cells selected, voltage-clamp was comparable to the situation in which  $K^+$  currents were blocked. Finally, we noted that the peak-to-peak latency between T-type  $Ca^{2+}$  currents and apamin-sensitive currents showed little variability in the 5 cells included in the analysis ( $14.1 \pm 0.3$  ms, range 12.9 - 14.8 ms), further pointing to a stable time course of T-type  $Ca^{2+}$  currents and reproducible voltage-clamp across experiments. From these tests, we concluded that our experimental conditions were such that voltage-clamp of T-type  $Ca^{2+}$  currents at -62 to -67 mV was stable enough to allow for reliable activation of apamin-sensitive currents. However, we also noted that our T-type  $Ca^{2+}$  current amplitudes were comparatively small, which indicated that we clamped only a portion of the whole-cell currents (Joksovic et al., 2005; Sun et al., 2001), likely those contained in soma and proximal dendrites.

*Whole-cell and perforated patch recordings in current-clamp mode.* Dampened oscillations were obtained after brief membrane hyperpolarization (-100 pA, 400 ms). Cells recorded in the whole-cell patch configuration presented 2 - 5 oscillatory high-frequency (150 - 250 Hz) LT burst discharges of typically 2 - 10 action potentials around 4 - 10 Hz, similar to findings *in vivo* and *in vitro* (Avanzini et al., 1989; Bal and McCormick, 1993; Blethyn et al., 2006; Steriade et al., 1993). The discharge frequency decreased from ~10 Hz when current pulses were injected at -60 mV to ~4 - 6 Hz around -78 mV, similar to the oscillations obtained by microelectrode recordings *in vitro*. Note that the properties of action potentials and associated rapid AHPs may be distorted due to the electronic design of the Axopatch 200B amplifier. Perforated patch-clamp recordings were achieved via including gramicidin at 2.8  $\mu$ M in the prefiltered patch pipette solution, which was then sonicated for 30 s. Gramicidin was prepared freshly in a 2.8 mM stock solution in dimethylsulfoxide. The pipette tip was initially filled with gramicidin-free solution by brief immersion and backfilled with gramicidin-containing patch pipette solution. Minimal pressure was applied to the patch pipette only while crossing the surface of the bath and before cell contact. The cell-attached configuration, with a seal resistance  $> 0.7$  G $\Omega$  was obtained by applying negative pressure to the patch pipette. Perforation was assessed in voltage-clamp by monitoring current responses to 10 mV hyperpolarizing steps. When current transients reached values  $>90$  pA, the recording configuration was switched to current-clamp and the experiment was started.

*Drugs.* Drugs (1-EBIO, mibefradil, apamin, TTX,  $\omega$ -CTXMVIIC, CPA) were maintained in 200-1000-fold concentrated stock concentrations and applied to the bath at the

concentrations indicated. In some experiments, 1-EBIO, apamin and  $\omega$ -CTXMVIIC were applied focally through a local puffing pipette attached to a picospritzer (World Precision Instruments). Thapsigargin was included at 4  $\mu$ M in the patch pipette through back-filling, as described for gramicidin. In control pipette solutions, apamin-sensitive current remained unaltered ( $239 \pm 41$  pA after 1.5 min,  $261 \pm 19$  pA after 8-10 min,  $n = 4$ ,  $p > 0.4$ ).

### **Ca<sup>2+</sup> imaging experiments**

*Calibration of fluorescent signals.* Ca<sup>2+</sup> signals were evaluated after calibration of dye affinities with solutions containing known free [Ca<sup>2+</sup>] using established procedures. The K<sub>d</sub> of magfura-2 with Mg<sup>2+</sup> at pH 7.3 and 34 °C, measured using EGTA-buffered solutions ([Ca<sup>2+</sup>] ~ 1 - 30  $\mu$ M), was  $25 \pm 5$   $\mu$ M (standard deviation from least-squares interpolation). This estimate was similar to that reported by (Hyrc et al., 2000) and slightly smaller than that reported by (Naraghi, 1997) and (Ogden et al., 1995), presumably because these measurements were done at 22 - 24 °C. The K<sub>d</sub> of bis-fura-2 with Mg<sup>2+</sup>, not relevant for the estimate of [DCa<sup>2+</sup>], was considered to be that reported by Molecular Probes (0.525  $\mu$ M). The buffer capacity of the cell, defined as  $K = [BCa^{2+}]/[Ca^{2+}]$  where [BCa<sup>2+</sup>] is the transient Ca<sup>2+</sup> bound to the endogenous cell buffer, was estimated as  $\Delta[DCa^{2+}]/\Delta[Ca^{2+}]_i$ . This estimate is based on the approximation that 3 mM magfura-2 (buffer capacity ~120) does not significantly alter the physiological  $\Delta[Ca^{2+}]$  and that in the presence of 1 mM bis-fura-2 (buffer capacity ~1900) all the Ca<sup>2+</sup> that enters the cell binds to the dye.

### **Immunohistochemical procedures**

*Preparation of tissue sections.* Three P21 mice were deeply anaesthetised by intraperitoneal injection of ketamine-xylazine 1 : 1 (0.1 mL / kg body weight) and perfused through the ascending aorta for 13 - 18 min, first with 0.9% saline for 1 min followed by freshly prepared ice-cold fixative containing 4% paraformaldehyde, 0.05% glutaraldehyde and ~0.2% picric acid made up in 0.1 M phosphate buffer (PB; pH 7.4). After perfusion, brains were removed from the skull and immersed in the same fixative for 2 hours. Tissue blocks containing the nRt were dissected and washed thoroughly in 0.1 M phosphate buffer for several hours. Coronal 60  $\mu$ m thick sections were then cut on a Vibratome (Leica V1000) and collected in 0.1 M phosphate buffer.

*Light microscopy.* A similar procedure to that described earlier was used (Luján et al., 1996). Briefly, free-floating sections were incubated in 10% normal goat serum (NGS, Vector Laboratories, USA) diluted in Tris-buffered saline (TBS) for 1 h. Sections were then incubated for 48 h in a solution of a primary antibody against SK2 at a final protein concentration of 1 - 2  $\mu\text{g}/\text{ml}$  each, diluted in TBS containing 1% NGS. After washes in TBS, the sections were incubated for 2 h in biotinylated goat anti-rabbit or goat anti-guinea pig IgGs (Vector Laboratories) diluted 1 : 50 in TBS containing 1% NGS. They were then transferred into avidin-biotin-peroxidase complex (ABC kit, Vector Laboratories) diluted 1 : 100 and left for 2 h at room temperature. Peroxidase enzyme activity was revealed using 3,3'-diaminobenzidine tetrahydrochloride (DAB; 0.05% in TB, pH 7.4) as the chromogen and 0.01%  $\text{H}_2\text{O}_2$  as substrate. Finally, the sections were air-dried and coverslipped prior to observation with a photomicroscope (DMRS, Leica) equipped with differential interference contrast optics.

*Electron microscopy.* For ultrastructural analysis, the silver-enhanced immunogold technique was used and immunogold particles along the plasma membrane and at intracellular sites of morphologically identifiable somata, dendritic shafts and axon terminals were assessed. We quantified the percentage of immunoparticles located along the plasma membrane of nRt dendrites. We also measured the density of immunoparticles (number of immunoparticles/ $\mu\text{m}^2$ ). The immunoparticle density was calculated in particle/effective membrane area in EM pictures (in particle/ $\mu\text{m}^2$ ) over plasma membrane compartments and was statistically compared to the non-specific labelling densities (also given in particle/ $\mu\text{m}^2$ ). Background labelling, assessed by determining particle density over nucleus, mitochondria and myelin, was  $0.05 \pm 0.01$  immunogold/ $\mu\text{m}^2$ .

## **EEG Monitoring and Analyses**

*Animals used.* Adult female SK2<sup>+/+</sup> (n = 7) and SK2<sup>-/-</sup> (n = 6) mice were used in this study. Mice were kept individually in polycarbonate cages (31 x 18 x 18cm) with food and water available *ad libitum*, and maintained on a 12 h light – 12 h dark cycle (lights-on at 9:00 AM) at an ambient temperature of 24.5 - 25.5 °C. Body (SK2<sup>+/+</sup>:  $19.4 \pm 0.7$  g; SK2<sup>-/-</sup>:  $21.2 \pm 0.6$  g) and brain (SK2<sup>+/+</sup>:  $452 \pm 8$  mg; SK2<sup>-/-</sup>:  $449 \pm 13$  mg) weight did not differ between genotypes. Age at time-of-recording was 17 weeks for 4 of the SK2<sup>-/-</sup> mice; all others were 11-weeks old.

*Surgical implantation.* EEG and EMG electrodes were implanted under deep anaesthesia with a mixture of ketamine and xylazine (i.p., 75 and 10 mg/kg, respectively, at a volume of 8  $\mu$ l/g). Two gold-plated miniature screws (diameter 1.1 mm) served as EEG electrodes and were screwed into the cranium over the right cerebral hemisphere, in a fronto-parietal position (according to (Franken et al., 1998)). Four additional anchor screws were implanted; one over the right hemisphere and three over the left hemisphere. Two semi-rigid gold wires served as EMG electrodes and were inserted between two neck muscles. The EEG and EMG electrodes were soldered to a connector and the anchor screws were cemented to the skull. Four to 8 days of recovery from surgery were allowed before animals were connected to the recording leads. A minimum of 6 adaptation days (or 10 including recovery from surgery) were scheduled before data collection.

*Analysis.* EEG and EMG signals were recorded continuously for 24 h (n = 5) or 48 h (n = 8) under undisturbed baseline conditions. The analogous signals were digitized at 2 kHz and subsequently stored at 200 Hz on hard disc. The EEG was subjected to a discrete-Fourier transformation yielding power spectra (range: 0.25 – 90 Hz, resolution: 0.25 Hz, window function: hamming) for consecutive 4 - s epochs. Hardware (EMBLA™) and software (Somnologica-3™) were purchased from Medcare/Flaga (Island). Based on the EEG and EMG signals, the animal's behavior was classified as REMS, NREMS, or wakefulness, for consecutive 4 - s epochs according to standard criteria (Franken et al., 1998). States were scored by visual inspection of the EEG and EMG signals displayed on a PC monitor. Four-second epochs containing EEG artifacts were marked, so they could be excluded from EEG spectral analyses. For each state, an EEG spectral profile was constructed by averaging all 4-s epochs scored as that state. Spectral changes at the NREM-to-REMS transition, calculation of theta peak frequency in the REMS and waking EEG and the fragmentation of NREMS were calculated as described previously (Franken et al., 2006; Franken et al., 1998, 1999).

### **Drugs and chemicals**

1-EBIO, apamin, thapsigargin and  $\omega$ -CTXMVIIC were obtained from Tocris, CPA from Alomone Labs, TTX from Latoxan, and magfura-2, bis-fura-2 from Molecular Probes. EGTA, BAPTA, Gramicidin D and standard salts for electrophysiological solutions were purchased from Sigma-Aldrich or Merck, L(+)-Ascorbic acid from VWR Prolabo and KMeSO<sub>4</sub> from ICN Biomedicals. Mibefradil was a kind gift of F. Hoffmann-La Roche Ltd, Basel Switzerland.

## 2) Supplemental Data, Figures and Table

### **Supplemental Figure S1: Effects of the SK channel gating enhancer 1-EBIO on oscillatory bursting of single units in nRt and on SK-currents in wild-type and SK2-/- mice.**

1-EBIO enhances the apparent affinity of native SK channels for  $\text{Ca}^{2+}$  (Pedarzani et al., 2001), and is expected to potentiate channel activation. Extracellular recordings were obtained in interface-style recording chambers with low-resistance ( $< 1 \text{ M}\Omega$ ) tungsten electrodes (Frederick Haer) and band-pass filtered between 0.3 kHz and 10 kHz using an extracellular amplifier (Warner Instruments) from slices perfused with (in mM): 131 NaCl, 2.5 KCl, 1.25  $\text{NaH}_2\text{PO}_4$ , 26  $\text{NaHCO}_3$ , 2  $\text{CaCl}_2$ , 1.2  $\text{MgCl}_2$ , 18 dextrose, 1.7 L(+)-ascorbic acid. A single-unit was identified by series of spontaneous tonic or bursts of action potentials. Bursts showed an accelerando-decelerando pattern in the action potential discharge frequency (Domich et al., 1986). Single electric shocks (50 - 200  $\mu\text{A}$ , 1 ms) were applied at 0.05 - 0.1 Hz via bipolar stimulation electrodes (Frederick Haer) placed in the internal capsule adjacent to the nRt. These stimuli typically silenced active units and then elicited repetitive burst discharges. The number of bursts was determined by the average of the bursts after 5-10 successive stimuli. Tonic action potential frequency was determined by counting action potentials in the first second after cessation of burst discharge.

Single units were identified in extracellular recordings by a stable action potential amplitude (20 - 100  $\mu\text{V}$ ) above baseline ( $\sim 2 - 5 \mu\text{V}$ ) and repetitive, high-frequency (220 - 500 Hz), burst discharges. An electric shock to the internal capsule transformed a tonically discharging into a repetitively bursting unit for 2 - 8 s, before tonic action potential discharge was resumed (Panels A, B). Local application of 1-EBIO ( $\sim 0.1 \text{ mM}$ ) provoked an almost three-fold increase in the number of LT bursts (Panel C) and a prolongation of the interburst intervals in the initial portion of the oscillation (Panel A), while the frequency of the tonic discharge remained unaffected (Panel D). Interestingly, the prolongation of the interburst intervals was significant for all but the first of 6 intervals measured (first 6 intervals in control:  $402 \pm 40 \text{ ms}$ ,  $338 \pm 34 \text{ ms}$ ,  $325 \pm 25 \text{ ms}$ ,  $296 \pm 26 \text{ ms}$ ,  $295 \pm 17 \text{ ms}$ ,  $277 \pm 18 \text{ ms}$ ; in 1-EBIO:  $482 \pm 53 \text{ ms}$ ,  $398 \pm 36 \text{ ms}$ ,  $344 \pm 33 \text{ ms}$ ,  $316 \pm 33 \text{ ms}$ ,  $320 \pm 24 \text{ ms}$ ,  $297 \pm 21 \text{ ms}$ ;  $p < 0.03$  for 2<sup>nd</sup> to 6<sup>th</sup> interval,  $p = 0.067$  for 1<sup>st</sup> interval), suggesting that, except for the first interburst interval, the SK channel gating by bursts is normally submaximal.. Bursting was abolished by local application of apamin (100 nM) (data not shown). 1-EBIO markedly



enhanced SK-currents in wild-type animals, while not having any effect on T-type  $\text{Ca}^{2+}$  current-dependent outward currents in SK2<sup>-/-</sup> cells (Panels E, F).

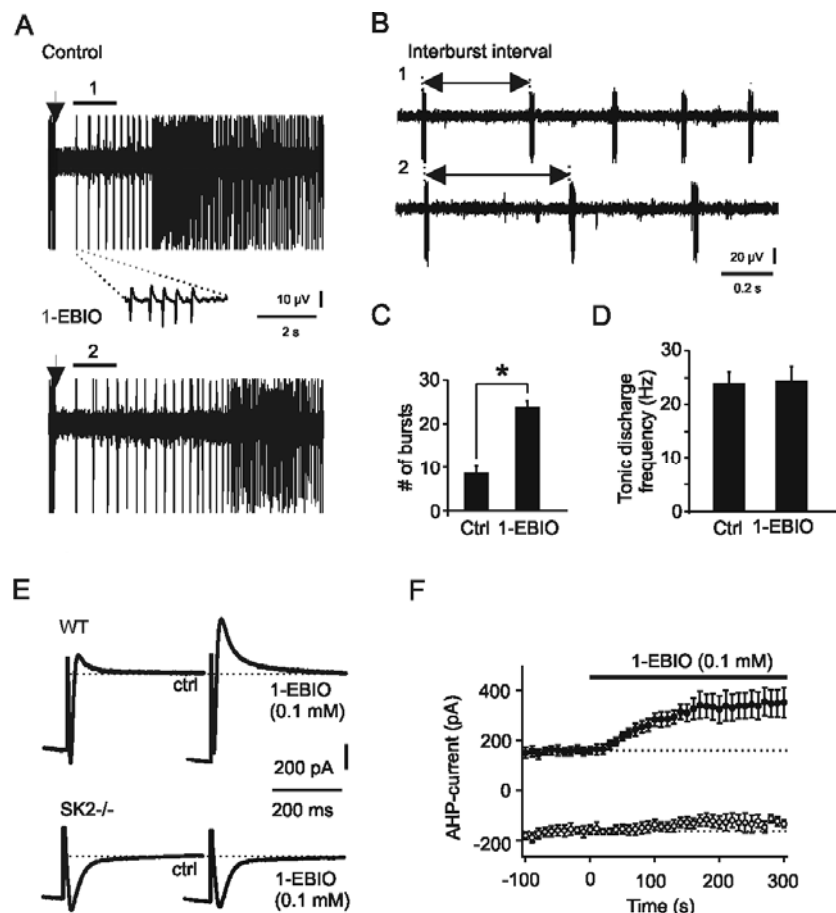


**Figure S1.** 1-EBIO, an SK channel enhancer, promotes bursting in nRt cells and its effects on SK-currents are absent in SK2<sup>-/-</sup> cells. **A** Extracellular recordings of a tonically discharging nRt cell, which is transformed into bursting by electrically stimulating synaptic inputs (200  $\mu\text{A}$ , 0.1 ms, arrow), before (Control) and after local application of 1-EBIO (~0.1 mM). Inset shows a single burst at an expanded time scale. The cell generates a series of burst discharges, before resuming tonic firing. In 1-EBIO, the number of burst discharges was increased. **B** Expanded portions of recordings numbered 1 and 2 in A. Double-headed arrows denote the interburst interval. **C** Average number of bursts discharged per stimulation, before and after 1-EBIO application. Data are presented as means  $\pm$  SEM of 10 units. \* denotes  $p < 0.05$ . **D** Average number of action potentials discharged in the first sec after resuming tonic firing. Data are presented as means  $\pm$  SEM of 7 units. **E** Bath-application of 1-EBIO (0.1 mM) onto voltage-clamped nRt cells from wild-type (WT) and SK2<sup>-/-</sup> mice. 1-EBIO promotes the generation of an outward afterhyperpolarization current (AHP-current) that follows the T-type  $\text{Ca}^{2+}$  current in WT, but not in SK2<sup>-/-</sup> cells. Cells were hyperpolarized to -120 mV for 125 ms, before being repolarized to -62 mV. Dotted lines denote steady-state holding current at -62 mV. **F** Graphic representation of the time course of 1-EBIO effects on AHP-current in recordings from WT (black circles,  $n = 5$ ) and SK2<sup>-/-</sup> cells (white circles,  $n = 5$ ). Dotted lines

represent the average of the last 5 responses before the start of 1-EBIO application. Note that the current values in SK2<sup>-/-</sup> animals are negative at the time point at which an AHP-current is generated in WT cells, due to the slower decay of T-type Ca<sup>2+</sup> currents in SK2<sup>-/-</sup> cells. 1-EBIO increased the current in WT ( $p < 0.005$ ), but not in SK2<sup>-/-</sup> cells ( $p > 0.05$ ). Data are presented as means  $\pm$  SEM of 5 cells per genotype.

### **Supplemental Figure S2. Cumulative use-dependent inactivation of T-current**

To assess for use-dependent decrease in T-current activation, a voltage-protocol that involves repeated depolarization-hyperpolarization cycles was used. This protocol mimics the rapid membrane potential changes occurring during dampened oscillations (Panel A) and allows to measure full T-type Ca<sup>2+</sup> current amplitudes at each cycle. Representative traces presented in Panel B illustrate that rapid inward currents were generated after each depolarizing upstroke (asterisks), which markedly diminished in amplitude in subsequent cycles, and reached steady-state levels after about three cycles. These inward currents were T-type Ca<sup>2+</sup> currents since they were largely blocked by mibefradil (50  $\mu$ M)(Panel C). In Panel D, averaged values of four experiments involving five depolarization-hyperpolarization cycles yielded a significant decrease of current response after 3 cycles (to  $45.6 \pm 10\%$ ,  $p < 0.05$ ), to  $30 \pm 8\%$  after 5 cycles ( $p < 0.05$  compared to third cycle). Also added to the plot in Panel D is a decrease in the decay slope of the T-type Ca<sup>2+</sup> current, which is a measure of the efficiency of T-type Ca<sup>2+</sup> / SK2 channel coupling. Taken together, whole-cell T-type Ca<sup>2+</sup> current in nRt cells showed use-dependent cumulative inactivation, accompanied by a decrement in SK channel recruitment. These gating properties are consistent with the observed accruing decrement of Ca<sup>2+</sup> signals during dampened oscillations.

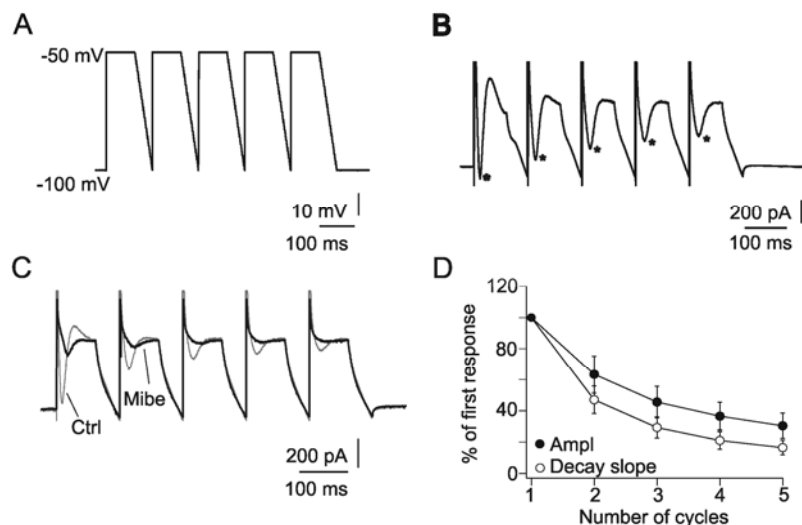


**Figure S2.** T-type Ca<sup>2+</sup> current in nRt cells shows use-dependent cumulative inactivation. **A** Voltage-clamp protocol involving five hyperpolarizing-depolarizing cycles, approaching the membrane potential events during a dampened oscillation. Depolarized phases were maintained for 80 ms to allow for full decay of T-type Ca<sup>2+</sup> current amplitudes. In this way, current amplitudes could be measured directly. **B** Representative current responses to the protocol illustrated in A. Note the rapid generation of an inward current at the onset of each depolarizing cycle (\*), reflecting activation of T-type Ca<sup>2+</sup> current, and its decrement in current amplitude from one cycle to the next. The T-type Ca<sup>2+</sup> current activated in the first cycle is followed by an outward current, which strongly weakens, reflecting weakened SK channel recruitment. **C** Overlay of current responses before (Ctrl, thin lines) and after Mibefradil (Mibe, thick lines) (50 μM) application. **D** Normalized T-type Ca<sup>2+</sup> current responses plotted against cycle number elicited by the protocol shown in A. *Black circles*: current amplitude, measured from peak to baseline current at -50 mV. *Open circles*: decay slope of T-type Ca<sup>2+</sup> currents (see Supplemental Experimental Procedures). Values are significantly smaller starting with the third cycle ( $p < 0.05$ ).

### Electrophysiological properties of SK1<sup>-/-</sup>, SK2<sup>-/-</sup> and littermate control animals

Values for passive input resistance, measured with brief 10 mV hyperpolarizing voltage steps, were  $250 \pm 16 \text{ M}\Omega$  ( $n = 41$ ) in SK1<sup>-/-</sup> animals, and  $207 \pm 16 \text{ M}\Omega$  in SK2<sup>-/-</sup> animals ( $n = 25$ ), not significantly different from a randomly selected group of WT littermate controls ( $225 \pm 16 \text{ M}\Omega$ ,  $n = 33$ ,  $p > 0.05$ ). Moreover, cells showed unaltered amplitudes of resting membrane potential (for SK1<sup>-/-</sup>:  $-79.8 \pm 1.5 \text{ mV}$ ,  $n = 40$ ; for SK2<sup>-/-</sup>:  $-77.6 \pm 1.6 \text{ mV}$ ,  $n = 27$ ; in control:  $-77.9 \pm 1.6 \text{ mV}$ ,  $n = 39$ ;  $p > 0.05$ ), amplitudes of T-type Ca<sup>2+</sup> currents at a test potential of -62 to 67 mV (for SK1<sup>-/-</sup>:  $-481 \pm 48 \text{ pA}$ ,  $n = 33$ ; for SK2<sup>-/-</sup>:  $-429 \pm 34 \text{ pA}$ ,  $n = 20$ ;

for wild-type:  $-478 \pm 53$  pA,  $n = 15$ ,  $p > 0.05$ ), steady-state inactivation curves, and time courses of recovery from inactivation (data not shown).

**Supplemental Figure S3: A computational model of T-type  $\text{Ca}^{2+}$  and SK channel coupling and SERCA**

Previous computational models of nRt cells generated dampened oscillations within a single-compartment, containing Hodgkin-Huxley models of voltage-gated channels and two  $\text{Ca}^{2+}$ -activated conductances, a  $\text{K}^+$  and a cation conductance (Destexhe et al., 1994). Following this model, a single-compartment model incorporating T-type  $\text{Ca}^{2+}$  channels,  $\text{Ca}^{2+}$ -dependent  $\text{K}^+$  channels, and sequestration mechanisms was used. Passive properties were implemented as described by Destexhe et al. (1994), with

$$C_m dV/dt = -g_L(V - E_L) - I_T - I_{SK}$$

where  $V$  is the membrane potential,  $C_m = 1 \mu\text{F}/\text{cm}^2$ ,  $E_L = -78$  mV, and  $g_L = 0.05$  mS/ $\text{cm}^2$ ,  $I_T$  is the T-type  $\text{Ca}^{2+}$  current, and  $I_{SK}$  the  $\text{Ca}^{2+}$ -dependent  $\text{K}^+$  current.

T-type  $\text{Ca}^{2+}$  channels were modelled according to

$$I_T = g_{ca} * m^2 * h * (V - E_{ca})$$

with the activation parameter  $m(V,t)$  described by

$$dm/dt = - [1/\tau_m(V)] * [m - m_\infty(V)]$$

and the inactivation parameter  $h(V,t)$

$$dh/dt = - [1/\tau_h(V)] * [h - h_\infty(V)]$$

The voltage dependence of  $m$ ,  $h$ , and the time constants followed

$$m_\infty(V) = 1 / [1 + \exp [(-V + 52) / 7.4]]$$

$$h_{\infty}(V) = 1 / [1 + \exp [(V + 80) / 5]]$$

$$\tau_m(V) = 0.44 + 0.15 / [\exp((V + 27) / 10) + \exp(-(V + 102) / 15)]$$

$$\tau_h(V) = 22.7 + 0.27 / [\exp((V + 48) / 4) + \exp(-(V + 407) / 50)]$$

The maximum conductance  $g_{ca}$  was 1.75 mS/cm<sup>2</sup>, and  $E_{ca} = 100$  mV the reversal potential.

Similarly,  $I_{SK}$  was described by

$$I_{SK} = g_{SK} * m_{SK} * h_{SK} * (V - E_{ca})$$

with the gating parameter  $m_{SK}$  described by

$$dm_{SK}/dt = - [1/\tau_{mSK}([Ca^{2+}]_i)] * [m_{SK} - m_{SK,\infty}([Ca^{2+}]_i)]$$

The steady-state activation parameter  $m_{SK,\infty}([Ca^{2+}]_i)$  was described by a dependence on the fourth power ( $n = 4$ ) of  $[Ca^{2+}]_i$  and  $\alpha$  was set to  $0.4 * 10^{12} \text{ ms}^{-1}\text{mM}^{-4}$  and  $\beta$  to  $0.025 \text{ ms}^{-1}$ , according to

$$m_{SK,\infty}([Ca^{2+}]_i) = \alpha [Ca^{2+}]_i^n / (\alpha [Ca^{2+}]_i^n + \beta)$$

$$\tau_{mSK}([Ca^{2+}]_i) = 1 / (\alpha [Ca^{2+}]_i^n + \beta)$$

In this manner, half-activation of the  $K^+$  channels occurred at  $\sim 0.5 \mu\text{M}$   $[Ca^{2+}]_i$ . The maximal  $K^+$  conductance was set to 3 mS/cm<sup>2</sup>.

$Ca^{2+}$  sequestration mechanisms were modelled as described in equation (10) of Destexhe et al. (1994).

$$d [Ca^{2+}]_i / dt = - K_T * [Ca^{2+}]_i / [[Ca^{2+}]_i + K_d]$$

Two such mechanisms were implemented, the first with Michaelis-Menten constants of  $K_T = 10^{-4} \text{ mMms}^{-1}$  and  $K_d = 10^{-4} \text{ mM}$  and the second with 5-fold smaller  $K_T$  and  $K_d$ .  $[\text{Ca}^{2+}]_i(t)$  was then modelled according to the sum sequestration and influx, with the latter one defined as

$$d [\text{Ca}^{2+}]_i / dt = - [k / 2Fd] * I_T$$

where  $k = 0.1$ ,  $F$  is the Faraday constant and  $d = 1 \text{ }\mu\text{m}$ .

Initial conditions were a resting membrane potential of  $-90 \text{ mV}$ , a  $[\text{Ca}^{2+}]_i$  of  $100 \text{ nM}$ , and the gating parameters for the T-type  $\text{Ca}^{2+}$  current were set to  $m(t=0) = 0.0$  and  $h(t=0) = 1.0$ .

Slow recovery from inactivation was introduced by requiring that the time evolution of the inactivation parameter  $h(t)$  is governed by  $\tau_h(V)$  when  $h(t) > h_\infty(V)$  but by  $\tau_{\text{slow}} = 2 \text{ s}$  when  $h(t) < h_\infty(V)$ . In this manner, the voltage-dependence of inactivation described by Frazier et al. (2001) was approximated. Blocking SERCA was modelled by removing the second  $\text{Ca}^{2+}$  sequestration mechanism.

In this model, we reproduced on-going oscillatory bursting in the absence of the cationic conductance. Removing  $\text{Ca}^{2+}$  sequestration from this model fully abolished the oscillations, because  $\text{Ca}^{2+}$  was not cleared and the cells became tonically hyperpolarized (data not shown). This is not observed experimentally when blocking SERCA selectively, and indicates that more than one sequestration mechanism controls  $\text{Ca}^{2+}$  removal after a LT burst in a real cell. To take this into account, we implemented two sequestration mechanisms with a 5-fold difference in affinity and kinetics. This, by itself, did not affect the on-going oscillations (left traces). We then implemented a formalism following values reported by Frazier et al. (2001) to phenomenologically take slow recovery from inactivation into account. This led to a marked dampening that involved the generation of submaximal LT bursts and  $\text{Ca}^{2+}$  signals (middle traces). Within this extended model, we studied the role of  $[\text{Ca}^{2+}]_i$  handling. Removal of the low-affinity sequestration only generated a pattern in which oscillations occurred, albeit with a weakened dampening (right traces). This reduction was accompanied by an enhanced number of  $[\text{Ca}^{2+}]_i$  transients, and a small decrease in the amplitude of the first two  $\text{Ca}^{2+}$  signals. This illustrates that the recovery from inactivation strongly shapes the temporal evolution of oscillatory dampening, while the sequestration of  $\text{Ca}^{2+}$  finely modulates the interaction between T-type  $\text{Ca}^{2+}$  and rapidly activated  $\text{K}^+$  channels (see Discussion).

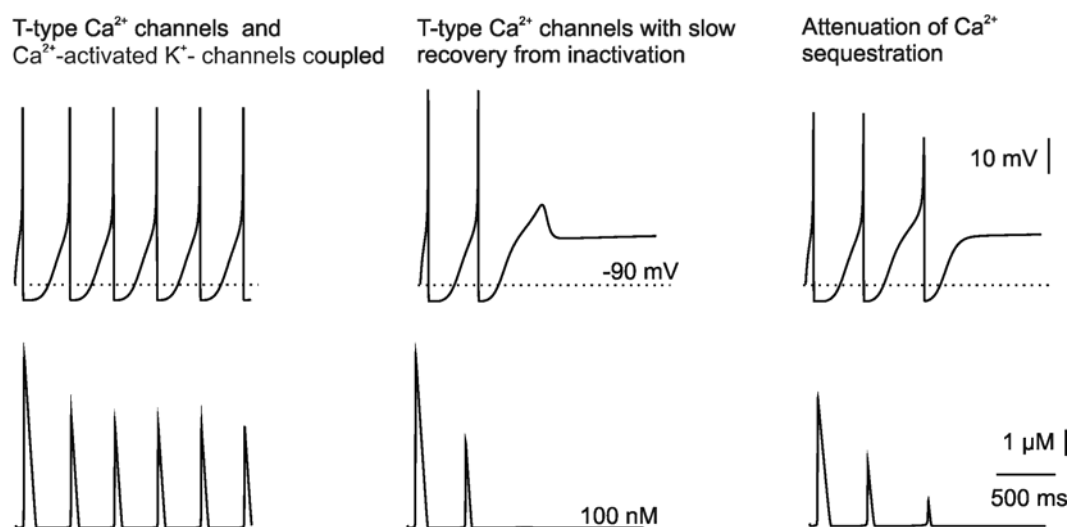


**Figure S3.** A computational model of nRt oscillations, reproducing on-going oscillations when T-type  $\text{Ca}^{2+}$  channels were coupled to a  $\text{Ca}^{2+}$ -activated  $\text{K}^+$  conductance (left). The cell contained two  $\text{Ca}^{2+}$  sequestration mechanisms. Time course of  $[\text{Ca}^{2+}]_i$  is shown below. When slow recovery was introduced (middle), oscillations were dampened. Removal of a slow  $\text{Ca}^{2+}$  sequestration, mimicking SERCA blockade, attenuated the dampening (right).

**Supplemental Figure S4A, 4B and Supplemental Table S1. Sleep-wake behavior and EEG analysis of SK2<sup>-/-</sup> and SK2<sup>+/+</sup> mice**

Large differences in EEG power density were observed between genotypes (Figure 8). To verify whether, besides difference in absolute values, the relative contribution of the various frequencies to the EEG was affected by genotype, relative spectra were calculated by expressing the power density in each frequency bin as a percentage of total EEG power over the entire frequency range (excluding the 45-55 Hz range) for that state (Figure S4A). During NREMS, the relative contribution of delta activity to the EEG was decreased, and of a wide range of fast frequencies, including beta (18 – 25 Hz) and gamma (35- 60 Hz), increased. Differences in the relative REMS spectra were most prominent in theta (5 – 10 Hz) and beta frequency ranges. Gamma activity was not affected (not shown). Differences in the theta range were due to a significant ( $p < 0.05$ ,  $t$ -test, asterisk) 0.3 Hz slowing of theta peak frequency (see inset) during this state in SK2<sup>-/-</sup> mice. Changes in the relative waking EEG were limited to a pronounced decrease at 10 Hz that resulted from a (non-significant) slowing in theta oscillations also in this state (see inset of Figure S4A). Theta peak frequency was determined by selecting the frequency bin with the highest power density within the theta range (5-10Hz) within individual mice (mean  $\pm$  SEM; bi-directional). A contour plot shows

the spectral composition of the EEG at frequencies up to 90 Hz at NREMS to REMS transitions (Figure S4B).

Despite pronounced differences in NREMS fragmentation (Figure 8), overall time-spent-asleep was not significantly affected by genotype (Table S1). Calculated over 24 h, SK2<sup>-/-</sup> mice (n = 4) slept somewhat less (- 30min) compared to SK2<sup>+/+</sup> (n=5), due largely to a 43 min deficit in sleep time during the 12 h dark (D) or active period.

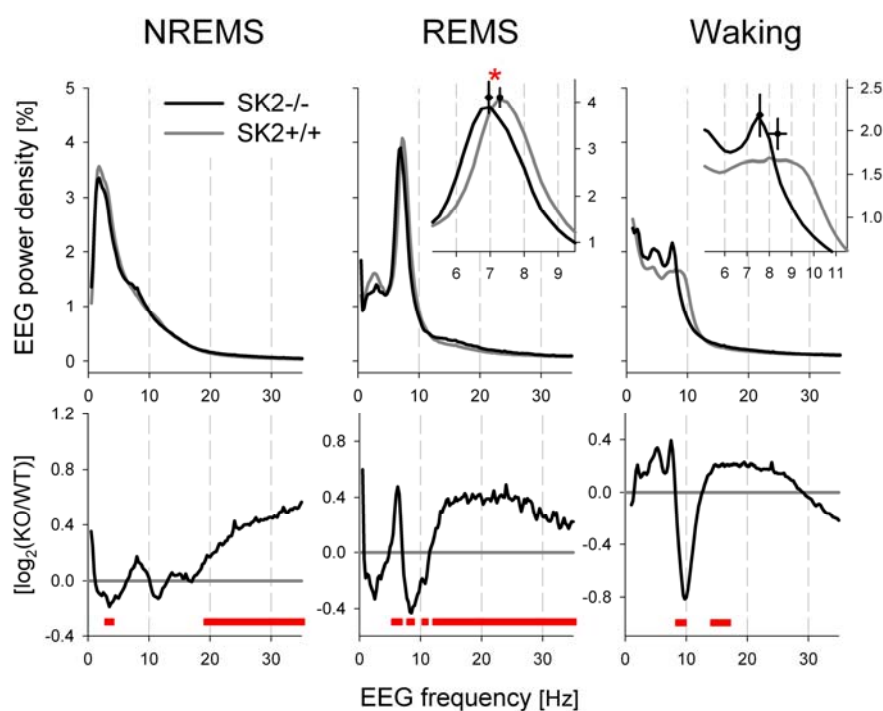


**Figure S4A:** Mean relative (upper panels) EEG spectra for NREMS (left), REMS (middle), and waking (right panels) during baseline. Relative EEG spectra were calculated for each state by expressing power density in each frequency bin as a percentage of total power over all frequency bins within each state. Genotype differences (lower panels) were calculated as Log<sub>2</sub>-transformed SK2<sup>-/-</sup> / SK2<sup>+/+</sup> ratios. Red bars mark frequency bins that significantly differed between genotype (post-hoc, *t*-tests, *P*<0.05).



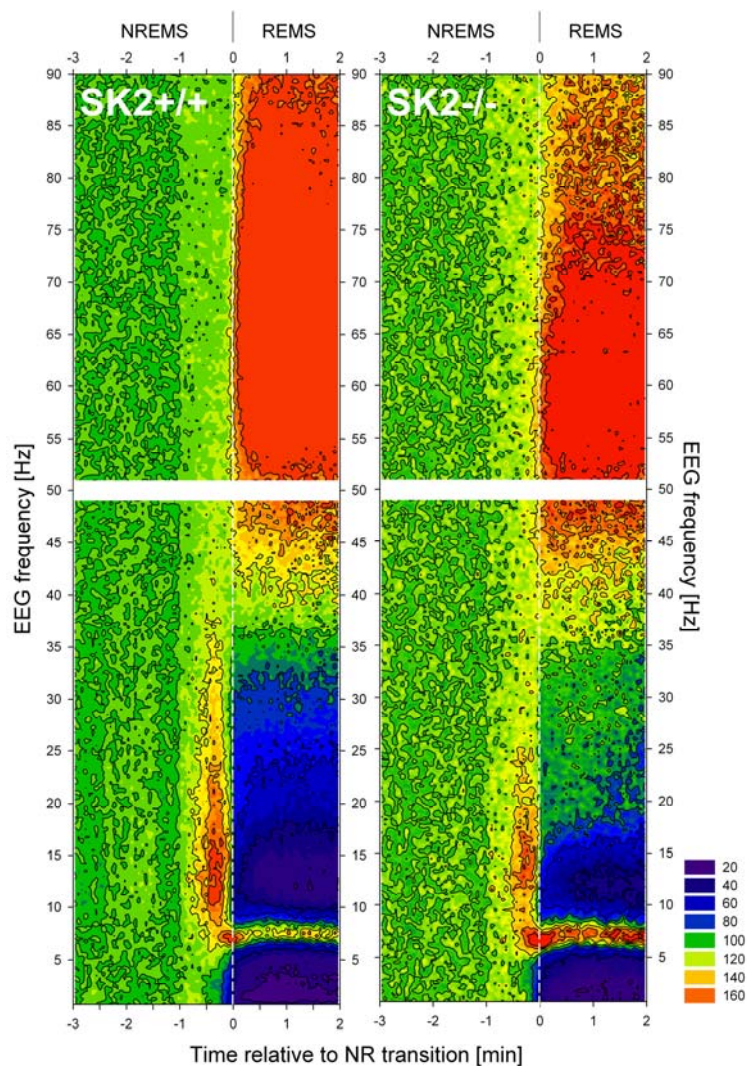


**Figure S4B:** Contour plot of the changes in the EEG spectral composition at the transition from NREMS (-3 to 0min) to REMS (0 to +2min) for SK2<sup>+/+</sup> (left; n=7) and SK2<sup>-/-</sup> (right panel; n=6) mice. ‘Heat map’ was constructed by aligning and averaging spectra from all transitions selected during the 24- or 48 h baseline recordings, first within and then among mice. Power density within 0.25 Hz bins were expressed as a percentage of the mean power density for that bin over 4 s epochs scored as NREMS in the 1<sup>st</sup> 2min (i.e., -3 to -1min) of the transition to visualize relative spectral changes. Contour lines connect levels of similar relative power in 8 color-coded 20% increments. White dashed lines at time = 0 indicate the time between the last 4s epoch scored as NREMS and the 1<sup>st</sup> 4s epoch scored as REMS. EEG changes start during the 1 min prior to REMS onset and entail a marked increase in EEG activity in the spindle frequency range (10 – 15 Hz; see also Figure 8D) shortly followed by an increase in theta activity (5 – 10 Hz). Maximum spindle activity is reached around -25 s, while maximum theta activity is reached at the transition. After the transition, spectral values reach their typical REMS levels with, below 35 Hz, no other activity than theta and above 35 Hz, including the gamma band (35 - 60Hz) activity that exceeds high frequency EEG activity in NREMS up to 3- fold. Genotype differences concern the less prominent surge in spindle activity prior to REMS onset (see Figure 8D) and a smaller relative increase in gamma/high-frequency activity and smaller relative decreases in delta and spindle activity (dark blue areas) during REMS in SK2<sup>-/-</sup> mice.

	Genotype	Waking [h]	NREMS [h]	REMS [min]
12h L-period	SK2 <sup>-/-</sup>	4.97 ± 0.15	6.16 ± 0.20	52.2 ± 6.3
	SK2 <sup>+/+</sup>	5.16 ± 0.13	5.85 ± 0.11	59.3 ± 3.1
12h D-period	SK2 <sup>-/-</sup>	10.22 ± 0.17	1.60 ± 0.15	10.3 ± 1.6
	SK2 <sup>+/+</sup>	9.50 ± 0.26	2.23 ± 0.23	16.0 ± 2.1
L-D difference	SK2 <sup>-/-</sup>	5.20 ± 0.13*	4.47 ± 0.15*	43.8 ± 2.9
	SK2 <sup>+/+</sup>	4.34 ± 0.21	3.61 ± 0.17	43.4 ± 3.0
24 h	SK2 <sup>-/-</sup>	15.19 ± 0.28	7.78 ± 0.28	62.5 ± 7.9
	SK2 <sup>+/+</sup>	14.67 ± 0.31	8.08 ± 0.29	75.3 ± 3.3

**Table S1:** Summary of time spent in waking, NREMS and REMS for SK2<sup>-/-</sup> and SK2<sup>+/+</sup> animals during the light (L) or the dark (D) period or over 24 h. The decrease in NREMS time in the D-period combined with a (non-significant) increase during the light period, led to a significantly increased L-D difference in NREMS time in SK2<sup>-/-</sup> mice (2-way ANOVA interaction between factors ‘Genotype’ and ‘LD-period’ (with repeated measures for LD-period): Waking  $P=0.0064$ ; NREMS  $P=0.0032$ . \*Mark significant genotype differences ( $P < 0.01$ ; post-hoc  $t$ -test). Analyses were based on 2 baseline recordings and represent means ± SEM.

### 3) Supplemental References

- Avanzini, G., de Curtis, M., Panzica, F., and Spreafico, R. (1989). Intrinsic properties of nucleus reticularis thalami neurones of the rat studied *in vitro*. *J Physiol* 416, 111-122.
- Bal, T., and McCormick, D.A. (1993). Mechanisms of oscillatory activity in guinea-pig nucleus reticularis thalami *in vitro*: a mammalian pacemaker. *J Physiol* 468, 669-691.
- Blethyn, K.L., Hughes, S.W., Tóth, T.I., Cope, D.W., and Crunelli, V. (2006). Neuronal basis of the slow (<1 Hz) oscillation in neurons of the nucleus reticularis thalami *in vitro*. *J Neurosci* 26, 2474-2486.
- Destexhe, A., Contreras, D., Sejnowski, T.J., and Steriade, M. (1994). A model of spindle rhythmicity in the isolated thalamic reticular nucleus. *J Neurophysiol* 72, 803-818.
- Domich, L., Oakson, G., and Steriade, M. (1986). Thalamic burst patterns in the naturally sleeping cat: a comparison between cortically projecting and reticularis neurones. *J Physiol* 379, 429-449.
- Franken, P., Dudley, C.A., Estill, S.J., Barakat, M., Thomason, R., O'Hara, B.F., and McKnight, S.L. (2006). NPAS2 as a transcriptional regulator of non-rapid eye movement sleep: genotype and sex interactions. *Proc Natl Acad Sci U S A* 103, 7118-7123.
- Franken, P., Malafosse, A., and Tafti, M. (1998). Genetic variation in EEG activity during sleep in inbred mice. *Am J Physiol* 275, R1127-R1137.
- Franken, P., Malafosse, A., and Tafti, M. (1999). Genetic determinants of sleep regulation in inbred mice. *Sleep* 22, 155-169.
- Huguenard, J.R., and Prince, D.A. (1992). A novel T-type current underlies prolonged  $Ca^{2+}$ -dependent burst firing in GABAergic neurons of rat thalamic reticular nucleus. *J Neurosci* 12, 3804-3817.
- Hyrz, K.L., Bownik, J.M., and Goldberg, M.P. (2000). Ionic selectivity of low-affinity ratiometric calcium indicators: mag-Fura-2, Fura-2FF and BTC. *Cell Calcium* 27, 75-86.
- Joksovic, P.M., Bayliss, D.A., and Todorovic, S.M. (2005). Different kinetic properties of two T-type  $Ca^{2+}$  currents of rat reticular thalamic neurones and their modulation by enflurane. *J Physiol* 566, 125-142.
- Luján, R., Nusser, Z., Roberts, J.D., Shigemoto, R., and Somogyi, P. (1996). Perisynaptic location of metabotropic glutamate receptors mGluR1 and mGluR5 on dendrites and dendritic spines in the rat hippocampus. *Eur J Neurosci* 8, 1488-1500.
- Naraghi, M. (1997). T-jump study of calcium binding kinetics of calcium chelators. *Cell Calcium* 22, 255-268.
- Ogden, D., Khodakhah, K., Carter, T., Thomas, M., and Capiod, T. (1995). Analogue computation of transient changes of intracellular free  $Ca^{2+}$  concentration with the low affinity  $Ca^{2+}$  indicator fura-2 during whole-cell patch-clamp recording. *Pflugers Arch* 429, 587-591.
- Pedarzani, P., Mosbacher, J., Rivard, A., Cingolani, L.A., Oliver, D., Stocker, M., Adelman, J.P., and Fakler, B. (2001). Control of electrical activity in central neurons by modulating the gating of small conductance  $Ca^{2+}$ -activated  $K^{+}$  channels. *J Biol Chem* 276, 9762-9769.
- Steriade, M., Contreras, D., Curró Dossi, R., and Nuñez, A. (1993). The slow (< 1 Hz) oscillation in reticular thalamic and thalamocortical neurons: scenario of sleep rhythm generation in interacting thalamic and neocortical networks. *J Neurosci* 13, 3284-3299.
- Sun, Q.Q., Huguenard, J.R., and Prince, D.A. (2001). Neuropeptide Y receptors differentially modulate G-protein-activated inwardly rectifying  $K^{+}$  channels and high-voltage-activated  $Ca^{2+}$  channels in rat thalamic neurons. *J Physiol* 531, 67-79.

### **5.3 Publication 2**

**Minireview Article**

**T-type Ca<sup>2+</sup> channels in neurons: from burst generators to sources for intracellular Ca<sup>2+</sup> ions**

**Lucius Cueni<sup>1</sup>, Marco Canepari<sup>1</sup>, John P. Adelman<sup>2</sup> and Anita Lüthi<sup>1</sup>**

<sup>1</sup> Division of Pharmacology and Neurobiology, Biozentrum, University of Basel, 4056 Basel, Switzerland

<sup>2</sup> Vollum Institute, OHSU, Portland, Oregon 97239, USA

## Introduction

Voltage-gated  $\text{Ca}^{2+}$  channels are key mediators of rapid  $[\text{Ca}^{2+}]_i$  increases in neurons in response to membrane depolarization. Intracellular  $\text{Ca}^{2+}$  ions entered through these channels adopt a multitude of signalling tasks that are involved in all major neuronal functions. To these belong, on the short-term, immediate effects on  $\text{Ca}^{2+}$ -dependent ion channels and enzymes, on the intermediate-term, regulation of transmitter release and excitability, and on the long-term, the control of gene transcription and the plasticity of synaptic strength. The nervous system expresses a number of  $\text{Ca}^{2+}$  channel subtypes, each with distinct biophysical properties and cellular distributions. The large majority of signalling roles are carried out by the  $\text{Ca}^{2+}$  ions entering through the high-voltage-activated (HVA)  $\text{Ca}^{2+}$  channels, which are generated by the  $\text{Ca}_v1$  and  $\text{Ca}_v2$   $\text{Ca}^{2+}$  channel families (for reviews, see (Berridge, 1998; Catterall, 1998; Dolphin, 2006; Khosravani and Zamponi, 2006)).

In contrast to the well-documented roles of  $\text{Ca}^{2+}$  provided by members of the  $\text{Ca}_v1$  and  $\text{Ca}_v2$  family, the  $\text{Ca}_v3$  channels are much less known in terms of their contribution to  $[\text{Ca}^{2+}]_i$  in neurons and their intracellular signalling functions. These channels, also called T-type  $\text{Ca}^{2+}$  channels, show the most distinctive biophysical characteristics amongst the voltage-gated  $\text{Ca}^{2+}$  channel family. They are activated by subthreshold membrane depolarizations and, by virtue of their rapid and mostly complete inactivation at moderate depolarizations, generate spike-like, transient membrane depolarizations, which earned them the name T-current (Huguenard, 1996; Perez-Reyes, 2003). Channel recruitment typically requires a preceding period of hyperpolarization, during which channels recover from inactivation and become primed to activate once activation threshold is crossed. Therefore,  $\text{Ca}_v3$  channel activation occurs, in most cases, as a rebound to inhibitory input, typically accompanied by high-frequency action potentials bursts.

There are a number of reasons for which our understanding of  $\text{Ca}^{2+}$  signals generated through T-type  $\text{Ca}^{2+}$  channels has just begun. First, T-type  $\text{Ca}^{2+}$  currents are typically co-expressed with HVA channels, albeit at smaller channel densities. Therefore, their contribution to  $[\text{Ca}^{2+}]_i$  is masked by the robust  $\text{Ca}^{2+}$  signals generated by HVA  $\text{Ca}^{2+}$  channels. Second, the lack of potent and selective pharmacological tools to block T-channels has hampered progress in dissecting their function. The most frequently used drugs are low  $\text{Ni}^{2+}$  concentrations (50-100  $\mu\text{M}$ ) and mibefradil (10-100  $\mu\text{M}$ ), but both substances affect other voltage-gated  $\text{Ca}^{2+}$  channels. Third, T-type  $\text{Ca}^{2+}$  channels have a comparatively low single-channel conductance and inactivate rapidly and virtually completely (Huguenard, 1996). This

transient nature of the current inherently limits  $\text{Ca}^{2+}$  influx. Fourth, in many cell types, T-type  $\text{Ca}^{2+}$  channels are expressed in neuronal dendrites (Christie et al., 1995; Destexhe et al., 1998; Kavalali et al., 1997; Magee et al., 1995), and their density increases in thin distal protrusions (Christie et al., 1995; Destexhe et al., 1996). Measurement of electrical and fluorescent signals in these requires sensitive optical techniques to be combined with dendritic recordings. Finally, in hippocampal and amygdalar cells, the R-type  $\text{Ca}^{2+}$  channel is also expressed strongly in dendrites and spines (Humeau et al., 2005) and the similarity of its pharmacological profile (Isomura et al., 2002; Markram and Sakmann, 1994) required that distinctions between T-type and R-type signals were carried out with additional pharmacological tools (see e.g. (Humeau et al., 2005; Tai et al., 2006)).

Currently, there is considerable evidence for potentially significant  $\text{Ca}^{2+}$  signalling roles associated with T-type  $\text{Ca}^{2+}$  currents in neurons, yet the  $[\text{Ca}^{2+}]_i$  signals generated and the messenger mechanisms involved have not been addressed. In several cell types,  $\text{Ca}^{2+}$  entering during burst discharge is important for the temporal patterning of oscillations (Bal and McCormick, 1993; Crunelli et al., 2006; Diana et al., 2007; Lüthi and McCormick, 1998; Swensen and Bean, 2003), although the exact role of T-type  $\text{Ca}^{2+}$  currents is not known.  $\text{Ca}_v3$  channels are also expressed in non-bursting cells and contribute to  $\text{Ca}^{2+}$  elevations generated by action potentials (McCobb and Beam, 1991; Wolfart and Roeper, 2002). Furthermore, several forms of long-term synaptic plasticity depend on T-type  $\text{Ca}^{2+}$  currents (Aizenman et al., 1998; Birtoli and Ulrich, 2004; Czarnecki et al., 2007; Nevian and Sakmann, 2006; Oliet et al., 1997; Pugh and Raman, 2006). Finally, specific T-current-dependent  $\text{Ca}^{2+}$  signalling has been proposed to rely on spatial co-localization with its target ion channels (Wolfart and Roeper, 2002). Third, pathological oscillations, such as those found during epilepsies, have been associated with genetic alterations in  $\text{Ca}_v3$   $\text{Ca}^{2+}$  channel subunits, which lead to altered current voltage dependence (Tsakiridou et al., 1995) and altered  $\text{Ca}^{2+}$  signalling (Kuisle et al., 2006).

This review gives an overview over recent reports documenting that T-type  $\text{Ca}^{2+}$  channels do act as an important  $\text{Ca}^{2+}$  source. It is focussed on T-type  $\text{Ca}^{2+}$  channels in neurons, but refers to non-neuronal cell types in cases where exemplary functions for  $\text{Ca}^{2+}$  entering through T-type  $\text{Ca}^{2+}$  channels were described. Altogether, this article not only illustrates that  $\text{Ca}^{2+}$  entering through T-type  $\text{Ca}^{2+}$  channels may dominate  $\text{Ca}^{2+}$  levels in intracellular compartments. It aims to emphasize particularly that signalling via  $\text{Ca}^{2+}$  entering through T-type  $\text{Ca}^{2+}$  channels is accompanied by elaborate compartmentalization and localization strategies to allow for a unique physiological use of this  $\text{Ca}^{2+}$  source.

### **Ca<sup>2+</sup> entry resulting from unique voltage-gating**

Three of the peculiar voltage-gating characteristics render Ca<sub>v</sub>3 channels a potentially unique Ca<sup>2+</sup> source. First, T-type Ca<sup>2+</sup> currents are activated around resting membrane potentials and hence may produce [Ca<sup>2+</sup>]<sub>i</sub> elevations at subthreshold potentials. Indeed, a Ni<sup>2+</sup>-sensitive low-threshold Ca<sup>2+</sup> signal accompanies subthreshold excitatory input in cortical layer V dendrites (Magee et al., 1995; Markram and Sakmann, 1994), whereas it makes a minor contribution to the Ca<sup>2+</sup> entry resulting from a single action potential (Markram et al., 1995; McCobb and Beam, 1991). Therefore, T-type Ca<sup>2+</sup> channels electrically boost weak depolarizing input (Gillissen and Alzheimer, 1997) and will thus facilitate the coupling of synaptic input to dendritic action potential initiation zones (Larkum et al., 1999b) and the generation of action potential bursts (Larkum et al., 1999a). Furthermore, T-type Ca<sup>2+</sup> channels could provide an intracellular Ca<sup>2+</sup> signal that helps to prime and amplify subsequent Ca<sup>2+</sup>-dependent processes. For example, Ca<sup>2+</sup> imaging of hippocampal dendrites of young rat revealed a greater T-type Ca<sup>2+</sup> channel-dependent signal in distal compared to proximal dendrites (Christie et al., 1995). Such a mechanism could be particularly important in these distal processes, in which the amplitude of backpropagating action potentials, in contrast to proximal dendrites, is too small to elicit significant Ca<sup>2+</sup> influx. The associated depolarization could also help in the generation of plateau potentials in hippocampal pyramidal cells (Cai et al., 2004) and complex spikes in cerebellar Purkinje cells (Cavelier et al., 2002). An amplification of distal input through T-type Ca<sup>2+</sup> channels has also been invoked in the context of boosting the sensitivity of peripheral sensory perception. In olfactory receptor neurons, odor-induced Ca<sup>2+</sup> transients in the cilia-containing knob are produced by cyclic-nucleotide-gated channels, but are boosted by T-type Ca<sup>2+</sup> currents by more than 50%. Without this boosting, only weak signals appear in the somata of these neurons, suggesting that T-type Ca<sup>2+</sup> currents help in the propagation of olfactory signals to the soma (Gautam et al., 2007).

Second, T-type Ca<sup>2+</sup> channels deactivate slowly after repolarization and may thus allow for Ca<sup>2+</sup> entry long after neuronal discharge has been completed. Indeed, proportionally more Ca<sup>2+</sup> ions flow through T-type Ca<sup>2+</sup> currents during a rapid action potential than what would be expected based on their small current amplitude, mostly due to a slow tail current after repolarization (McCobb and Beam, 1991). Furthermore, significant deactivating T-current flows during interburst intervals in Purkinje cells, coincident with the time course of



activation of  $\text{Ca}^{2+}$ -dependent afterhyperpolarizing currents (Swensen and Bean, 2003), suggesting that the gating of these may be steered by  $\text{Ca}^{2+}$  entered through T-type  $\text{Ca}^{2+}$  currents.

Third, although T-type  $\text{Ca}^{2+}$  channels are well-known for their prominent inactivation, all three isoforms of the channel show a small, but significant window current, resulting from a small fraction of channels remaining open and giving rise to a stationary  $\text{Ca}^{2+}$  influx, and a persistent enhancement of free intracellular  $\text{Ca}^{2+}$  levels (Crunelli et al., 2005). Electrophysiologically, such a standing current gives rise to a membrane potential bistability and the capability of switching abruptly between “up” and “down” states (Williams et al., 1997b). An interesting case for the signalling role of this steady  $\text{Ca}^{2+}$  elevation has been associated with the differentiation of skeletal muscle cells. The establishment of skeletal muscle requires the differentiation and eventual fusion of myoblasts into multinucleated myotubes. This is a  $\text{Ca}^{2+}$ -dependent process that eventually leads to the transcription of muscle-specific genes. At the onset of the fusion process, a subpopulation of myoblasts shows an elevated  $[\text{Ca}^{2+}]_i$  level. Buffering this increase prevents fusion (Arnaudeau et al., 2006; Bijlenga et al., 2000). Furthermore, differentiating myotubes start expressing  $\text{Ca}_v3.2$  T-type  $\text{Ca}^{2+}$  channels, and their pharmacological inhibition prevents the development of myotubes with elevated resting  $[\text{Ca}^{2+}]_i$  levels. Therefore, T-type  $\text{Ca}^{2+}$  channels appear responsible for the augmentation of basal  $[\text{Ca}^{2+}]_i$ , consistent with an incomplete inactivation of T-channels in these cells. Therefore, a small fraction of activated channels will remain open and give rise to a steady  $\text{Ca}^{2+}$  influx, and a persistent enhancement of free intracellular  $\text{Ca}^{2+}$  levels. Notably, activation of a window current in myoblasts is enabled through a gradual hyperpolarization of the membrane potential, caused by the expression of an inward rectifier  $\text{K}^+$  current (Konig et al., 2006). In central neurones, window currents are activated during slow oscillatory discharges in thalamic cells that accompany a slow ( $< 1$  Hz) sleep rhythm (Crunelli et al., 2005). The persistent  $\text{Ca}^{2+}$  influx, together with the recruitment of  $\text{Ca}^{2+}$ -dependent cationic currents, permit the persistence in a plateau-like up-state for periods of seconds (Blethyn et al., 2006).

### **T-type channel $\text{Ca}^{2+}$ signalling due to unique localization and co-localization**

Single-channel recordings,  $\text{Ca}^{2+}$  imaging, and modelling studies point to a non-uniform expression of T-type  $\text{Ca}^{2+}$  channels along the somatodendritic axis in diverse neuronal cell types. In hippocampal dendrites, T-type  $\text{Ca}^{2+}$  channels contribute  $\sim 40\%$  of the  $\text{Ca}^{2+}$  signal

generated by repetitive action potentials at dendritic sites  $> 150 \mu\text{m}$  distant from the soma, but only 30% at proximal sites (Christie et al., 1995; Magee and Johnston, 1995). In thalamocortical cells, the density of T-type  $\text{Ca}^{2+}$  channels is highest in the thick stem dendritic segment 20-30  $\mu\text{m}$  from the soma, whereas low densities were found at somatic and more distal dendritic sites (Williams and Stuart, 2000). Conversely, in neurons of the nucleus reticularis thalami, T-type  $\text{Ca}^{2+}$  channels are found in both somata and dendrites (Joksovic et al., 2005), but a computational study suggested a particularly high density in the fine distal dendrites of these cells (Destexhe et al., 1996). In unipolar brush cells of the vestibulocerebellum, large  $\text{Ca}^{2+}$  signals are generated by low-threshold spikes in the distal brush, whereas these are minor in the soma or proximal dendrites (Diana et al., 2007). Burst firing in these cells hence leads to a strong signal in the brush, and tonic action potential firing produces a homogeneous  $\text{Ca}^{2+}$  increase throughout the cell. Therefore, the bimodal activity pattern in these cells is accompanied by a distinctly compartmentalized  $\text{Ca}^{2+}$  signalling system. In nucleus reticularis thalami cells, T-type  $\text{Ca}^{2+}$  channels in dendrites are expressed together with  $\text{Ca}^{2+}$ -dependent  $\text{K}^+$  channels of the SK-type. These cells are well-known for their vigorous oscillatory burst discharges during sleep-related oscillations, which emerge from interplay between low-threshold bursts and afterhyperpolarizations mediated by SK currents. The dendritic co-localization of a high-density of T-type  $\text{Ca}^{2+}$  channels and SK channels enables their rapid and efficient functional coupling and the generation of vigorous oscillations (Cueni et al., 2007).

Dendritic  $\text{Ca}^{2+}$  signals underlie dendritic transmitter release (Egger et al., 2005; Rancz and Häusser, 2006), facilitate the induction of synaptic plasticity (Kampa et al., 2006), are implicated in gene transcription (West et al., 2002) and in activity-dependent growth and maintenance of dendritic arbors (Poo and Zheng, 2006; Redmond and Ghosh, 2005). Dendritic T-type  $\text{Ca}^{2+}$  channels, including those localized to spines, are involved in some forms of long-term synaptic plasticity (Isomura et al., 2002; Nevian and Sakmann, 2006) (see also below). Interestingly, the dendritic confinement of T-type  $\text{Ca}^{2+}$  channels occurs in later developmental stages. In hippocampus, currents are easily recorded in acutely dissociated cells from immature hippocampus, indicating their presence at soma and proximal dendrites, but currents are no longer recorded in adult cells (Thompson and Wong, 1991), presumably due to the restricted expression at more distal dendritic portions. Whether and how this initially strong expression in somata and dendrites is involved in hippocampal development remains to be assessed.

$\text{Ca}^{2+}$  entering through T-type  $\text{Ca}^{2+}$  channels can take over selective signalling roles due to tight coupling with  $\text{Ca}^{2+}$ -dependent ion channel targets, possibly resulting from their physical proximity to these. A repeatedly observed motif is the coupling of T-type  $\text{Ca}^{2+}$  channels to  $\text{Ca}^{2+}$ -dependent SK-type  $\text{K}^+$  channels. Electrophysiological studies revealed that, in dopaminergic midbrain neurons, SK channels are activated almost exclusively by T-type  $\text{Ca}^{2+}$  channels, although these neurons also express HVA channels (Wolfart and Roeper, 2002). This interacting ion channel pair gives rise to a small outward current that provides the small hyperpolarization necessary for a regular, periodic action potential discharge. During neonatal stages of dopaminergic neuron development, the dual coupling of T-type  $\text{Ca}^{2+}$  channels to SK channels and ryanodine receptors (RyR) also gives rise to spontaneous SK channel-dependent miniature outward currents that deregularizes spontaneous action potential discharge (Cui et al., 2004). These are thought to be due to spontaneous opening of single T-type  $\text{Ca}^{2+}$  channels, a small  $\text{Ca}^{2+}$  localized influx and a subsequent boosting by  $\text{Ca}^{2+}$  release via RyR that is then sufficient to activate SK channels. The selective coupling between T-type  $\text{Ca}^{2+}$  and SK2 channels is also prominent in nRt cells (Cueni et al., 2007), which is enabled through the presence of both channels in the thin dendrites of these cells, with a minor contribution of HVA  $\text{Ca}^{2+}$  channels. Interestingly, in these cells, the sarco/endoplasmic  $\text{Ca}^{2+}$  ATPases (SERCA) selectively sequester  $\text{Ca}^{2+}$  when entered through dendritic T-type  $\text{Ca}^{2+}$  channels, whereas it leaves unaffected  $\text{Ca}^{2+}$  entered through high-voltage activated  $\text{Ca}^{2+}$  channels. This suggests that SERCA may be localized in the vicinity of T-type  $\text{Ca}^{2+}$  but not HVA  $\text{Ca}^{2+}$  channels. A preferential localization of SERCA on dendritic ER protrusions could underlie its selectivity for T-type  $\text{Ca}^{2+}$ , whereas SERCA may be lacking or somewhat remote in compartments expressing HVA  $\text{Ca}^{2+}$  channels. So far, however, little is known about the molecular details via which the selective T-type  $\text{Ca}^{2+}$ /SK channel coupling is enabled, the spatial scales on which it occurs and on their positioning relative to intracellular  $\text{Ca}^{2+}$  compartments.

A coupling of T-type  $\text{Ca}^{2+}$  channels to  $\text{Ca}^{2+}$ -activated  $\text{K}^+$  channels has also been suggested for the  $\text{Ca}_v3.2$  isoform expressed in the vascular smooth muscle of coronary arteries. Mice lacking the  $\text{Ca}_v3.2$  isoform show chronically constricted and malformed arteries, and relaxation of arterial vessels by vasodilating agents was markedly impaired (Chen et al., 2003). The deficiency in arterial relaxation was proposed to be due to a failure of  $\text{Ca}^{2+}$ , entering through  $\text{Ca}_v3.2$  channels, to antagonize contraction.  $\text{Ca}_v3.2$  channels co-sediment with  $\text{Ca}^{2+}$ -activated  $\text{K}^+$  channels of the BK type, suggesting that their close co-localization could translate  $\text{Ca}^{2+}$  entry into membrane hyperpolarization and stop contraction.

Thus, at least in coronary arteries, T-type  $\text{Ca}^{2+}$  channels mediate vasodilatation through producing  $[\text{Ca}^{2+}]_i$  increases.

An at least partial coupling of T-type  $\text{Ca}^{2+}$  channels to diverse types of  $\text{Ca}^{2+}$ -dependent  $\text{K}^+$  channels has been reported in a number of bursting neurons, such cholinergic nucleus basalis neurons (Williams et al., 1997a), intralaminar thalamic neurons (Goaillard and Vincent, 2002), Purkinje neurons (Swensen and Bean, 2003) and cartwheel cells of dorsal cochlear nucleus (Kim and Trussell, 2007). In thalamocortical and habenular neurons, T-type  $\text{Ca}^{2+}$  current could also be coupled to  $\text{Ca}^{2+}$ -dependent cationic currents, thereby leading to pronounced afterdepolarizations (Blethyn et al., 2006; Chang and Kim, 2004).

### **Coupling to intracellular $\text{Ca}^{2+}$ release**

An emerging aspect of  $\text{Ca}^{2+}$  signalling via T-type  $\text{Ca}^{2+}$  channels is the activation of  $\text{Ca}^{2+}$ -induced  $\text{Ca}^{2+}$  release (CICR). Aside from their major counterpart, the L-type  $\text{Ca}^{2+}$  channels, T-type  $\text{Ca}^{2+}$  channels act as  $\text{Ca}^{2+}$  sources in cardiac functions and couple to the sarcoplasmic reticulum to induce  $\text{Ca}^{2+}$  release (Sipido et al., 1998). T-type  $\text{Ca}^{2+}$  channel density is highest in pacemaking structures, whereas low levels are found in ventricular cells (Vassort et al., 2006). In pacemaking sinoatrial node and atrial cells, T-type  $\text{Ca}^{2+}$  channels contribute to the late phase of diastolic depolarization (Hagiwara et al., 1988). During this period, numerous rapid (20-30 ms), localized  $\text{Ca}^{2+}$  sparks appear at the sarcolemmal surface of these cells, which precede the rapid rise at the onset of the cardiac action potential (Hüser et al., 2000). These sparks sum up to a pedestal increase in  $[\text{Ca}^{2+}]_i$  at subthreshold potentials and are further boosted by  $\text{Ca}^{2+}$  release from the SR. Sarcolemmal  $\text{Ca}^{2+}$  signals are known to drive  $\text{Na}^+$ - $\text{Ca}^{2+}$  exchange current, hence resulting in further membrane depolarization, further  $\text{Ca}^{2+}$  entry and acceleration of the diastolic depolarization (Hüser et al., 2000). Thus, via the amplification of their intracellular  $\text{Ca}^{2+}$  signals through sarcolemmal  $\text{Ca}^{2+}$  release sites, T-type  $\text{Ca}^{2+}$  channels adopt an important role in cardiac pacemaking. Consistent with this finding, mice lacking the  $\text{Ca}_v3.1$   $\text{Ca}^{2+}$  channel subunit show no T-type  $\text{Ca}^{2+}$  currents in pacemaking cardiac tissue, a slowing of the late phase of diastolic depolarization and bradycardia (Mangoni et al., 2006).

T-type  $\text{Ca}^{2+}$  channel-dependent signalling also contributes to cardiac excitation-contraction coupling, although its density is too low in ventricular myocytes to significantly add to the contraction induced by L-type  $\text{Ca}^{2+}$  channels. However, in Purkinje fibers, a comparison of L-type and T-type  $\text{Ca}^{2+}$  channel-induced contraction was carried out under

controlled voltage-clamp conditions (Zhou and January, 1998). In these cells,  $\text{Ca}^{2+}$  entry through T-type  $\text{Ca}^{2+}$  channels could elicit contractions that were not much smaller than those triggered by L-type  $\text{Ca}^{2+}$  channels and that were also mediated by SR-dependent  $\text{Ca}^{2+}$  release. However, responses had a greater latency and built up more slowly, indicating that T-type  $\text{Ca}^{2+}$  channels coupled less efficiently to the internal release machinery. A possible explanation for this decreased efficacy could rely on a less tight integration of T-type  $\text{Ca}^{2+}$  channels in the local  $\text{Ca}^{2+}$  signalling microdomains described for L-type channels.

In neurons, two studies clearly document that T-type  $\text{Ca}^{2+}$  channels may induce release, namely in dopaminergic neurons of neonatal midbrain (Cui et al., 2004) and in midline thalamic neurons (Richter et al., 2005).

Neonatal dopaminergic neurons show spontaneous action potential discharge at a slow and irregular rate, which is then replaced by a pacemaker-like discharge pattern in adulthood. Cui et al. found that irregularity could be explained by the generation of spontaneous miniature hyperpolarizations, which are generated by SK channel-mediated spontaneous miniature outward currents (SMOC). Two different SMOC, which both are absent in adult dopaminergic neurons, are distinguished according to their amplitude. The induction of large-amplitude SMOC ( $\geq 22$  pA) requires the selective coupling of T-type  $\text{Ca}^{2+}$  channels, ER-bound RYR and SK channels, since different inhibition of each signalling component abolish the generation of SMOC.

In midline thalamic neurons the physiological relevance of T-type  $\text{Ca}^{2+}$  channel-induced CICR is not known. However, the occurrence of T-type  $\text{Ca}^{2+}$  channel-mediated CICR predominantly in midline thalamic neurons, but not within the nRt and specific thalamocortical nuclei indicating a relevance in specific firing properties, since midline thalamic neurons exhibit, in contrast to nRt and thalamocortical neurons, little spontaneous activity.

### **Involvement in synaptic transmission**

Synaptic transmission belongs to the most extensively studied  $\text{Ca}^{2+}$ -dependent processes (Schneggenburger and Neher, 2005).  $\text{Ca}^{2+}$  signals involved in synaptic transmission belong to the largest and most highly localized transients, reaching levels of up to tens of micromolar within  $< 1$  ms on spatial scales of 10-100 nm during fast synaptic transmission.  $\text{Ca}^{2+}$  binds to proteins of the SNARE complex, which contains the putative  $\text{Ca}^{2+}$  sensor synaptotagmin to trigger rapid vesicle exocytosis (Südhof, 2004). Channels of the HVA family, in particular the

N, and P/Q-type channels, play a dominant role in generating these transients (Reid et al., 2003). In contrast, to date, there are few reports on an involvement of T-type  $\text{Ca}^{2+}$  channels in neurotransmission. Slower forms of secretion, such as hormone release from neuroendocrine cells, involve a contribution of T-type  $\text{Ca}^{2+}$  channels (Carbone et al., 2006). In chromaffin cells, this contribution varies according to the conditions to which cells are exposed, being increased by cAMP-producing stimuli and by hypoxia. Secretion controlled by T-type  $\text{Ca}^{2+}$  channels in these cells is initiated at more hyperpolarized potentials, but couples with equal efficacy and velocity to the release apparatus (Giancippoli et al., 2006), thus permitting catecholamine release in response to previously subthreshold stimuli.

More recently, a number of research groups provided strong evidence that T-type  $\text{Ca}^{2+}$  channels are involved in neurotransmitter release in neurons as well, thereby endowing these with a low-threshold component of fast exocytosis. Such a mechanism appears to make physiological sense for graded forms of vesicular release, in which synaptic transmission occurs in response to gradual changes in membrane voltage. A remarkable case is the graded transmission of reciprocally connected inhibitory leech heart neurons, which generate burst discharges in alternating sequence (Ivanov and Calabrese, 2000). T-type  $\text{Ca}^{2+}$ -current-dependent burst discharges lead to robust  $\text{Ca}^{2+}$  increases at the sites of synaptic contact, whereas tonic action potentials produced minor  $[\text{Ca}^{2+}]_i$  elevations. The amplitude of T-type  $\text{Ca}^{2+}$  currents correlates with the presynaptic dynamics and with the graded synaptic transmission, even when measured at the fine sites of synaptic contact, strongly indicating that the currents measured at the soma were indeed the main triggers of release (Ivanov and Calabrese, 2000). A role for T-type  $\text{Ca}^{2+}$  currents in graded transmission has also been identified for retinal bipolar cells. These second-order retinal cells transform input from retinal ganglion cells into a constant depolarization and use ribbon-type synapses to contact amacrine neurons. It has remained unclear by which mechanism the constant depolarization of the bipolar cells leads to a transient component in the synaptic response of amacrine cells. Pan et al. (Pan et al., 2001) used fluorescent  $\text{Ca}^{2+}$  imaging and capacitance measurement techniques to identify a role for T-type  $\text{Ca}^{2+}$  currents in triggering vesicle fusion at the giant terminals of bipolar cells. Although stronger depolarizations evoked an L-type  $\text{Ca}^{2+}$  current component of transmission, the release initiated by T-type  $\text{Ca}^{2+}$  currents could be strong enough to elicit feedback inhibitory currents in these cells. Indeed, recruitment of T-type  $\text{Ca}^{2+}$  currents doubles the amplitude of evoked glutamatergic responses in amacrine cells without strongly altering their time course, suggesting a similar efficacy of T-type and L-type currents in coupling to the release apparatus (Singer and Diamond, 2003). The transient nature of T-

type  $\text{Ca}^{2+}$  currents was proposed to represent a possible mechanism underlying the transformation of a tonic depolarization into a transient output. However, a later study revealed that transient components could also occur at membrane potential ranges at which T-type  $\text{Ca}^{2+}$  current activation is no longer significant, indicating the involvement of other mechanisms in this transformation (Singer and Diamond, 2003).

T-type  $\text{Ca}^{2+}$  currents mediate action-potential-evoked neurotransmitter release granule cells of the olfactory bulb (Egger et al., 2003). These are axonless inhibitory neurons that generate lateral inhibition via dendrodendritic synapses formed with the major output cells of the bulb, the mitral cells. Additionally, granule cells receive the major synaptic feedback from olfactory cortex. Dendrodendritic interactions may occur both in a local mode, in which only single synapses communicate reciprocally, or via eliciting an action potential in granule cells. Activation of such action potentials from the resting membrane voltage of around -70 mV is sufficient to elicit a marked T-type  $\text{Ca}^{2+}$ -current-dependent increase in  $[\text{Ca}^{2+}]_i$  that couples to the release of GABA. Notably, these  $[\text{Ca}^{2+}]_i$  transients are particularly robust in the distal dendritic zones of granule cells, from which most contact sites are formed. Thus, T-type  $\text{Ca}^{2+}$  currents may be involved in mediating global forms of lateral inhibition.

Altogether, accruing evidence shows that T-type  $\text{Ca}^{2+}$  currents do make a significant contribution to neurotransmitter release, albeit these are found in a restricted number of cell types with graded or dendritic forms of synaptic release. It will be of interest to determine, in the future, whether other cell types which combine a dominance of T-type  $\text{Ca}^{2+}$  current-related  $\text{Ca}^{2+}$  entry in dendrites with dendrodendritic specializations, such as nRt neurons, also utilize this  $\text{Ca}^{2+}$  to trigger dendrodendritic neuropeptide release (Sun et al., 2003).

### **Involvement in synaptic plasticity**

To date, several forms of associative synaptic plasticity involving activation of metabotropic glutamate receptors (mGluRs) are thought to require  $\text{Ca}^{2+}$  entry through T-type  $\text{Ca}^{2+}$  currents. In neonatal and young hippocampus, classic extracellular stimulation protocols via repeated stimulation of hippocampal Schaffer collaterals at theta frequencies (5 Hz, 3 min) evoked a long-term depression (LTD) that was mediated by activation of metabotropic glutamate receptors (mGluRs) and blocked by low concentrations of  $\text{Ni}^{2+}$  (Oliet et al., 1997). In mature hippocampus, discharge properties of CA1 pyramidal cells during such low-frequency stimulation were noted to involve burst firing, with typically three action potentials being generated around 150-200 Hz (Thomas et al., 1998). At this age, conditioning induced a

long-term potentiation (LTP) that was fully blocked only by combined application of both NMDAR antagonists and low  $\text{Ni}^{2+}$ . Analysis of the site dependence of LTP along the apical dendrites of hippocampal cells revealed that this  $\text{Ni}^{2+}$  dependence was greatest in the distal dendritic portions, at which T-type  $\text{Ca}^{2+}$  currents are most strongly expressed (Isomura et al., 2002). An involvement of T-type  $\text{Ca}^{2+}$  currents in mGluR-dependent associative plasticity was also found in neocortex when pairing single action potential or burst discharges of cortical pyramidal cells with EPSPs (Birtoli and Ulrich, 2004; Nevian and Sakmann, 2006). The mechanisms of action of  $\text{Ca}^{2+}$  entering through T-type  $\text{Ca}^{2+}$  currents have not yet been fully elaborated. Several pieces of evidence point to a presynaptic expression of LTD depending on both mGluRs and T-type  $\text{Ca}^{2+}$  currents, suggesting the release of a retrograde messenger. In young hippocampus, mGluR-dependent LTD was accompanied by a decrease in the frequency of miniature synaptic events (Oliet et al., 1997). In neocortex, mGluR-LTD leads to recruitment of phospholipase C (PLC) and subsequent release of endocannabinoids (Nevian and Sakmann, 2006). Interestingly, the  $\text{Ca}^{2+}$  signal during LTD induction is not affected by mGluR blockade, indicating that the role of mGluR activation is limited to trigger the PLC cascade, while the  $\text{Ca}^{2+}$  is provided by voltage-gated  $\text{Ca}^{2+}$  channels. T-type  $\text{Ca}^{2+}$  current activation is obligatory when LTD is induced by pairing with single action potentials, but not when bursts of action potentials are generated. Under these latter conditions, low  $\text{Ni}^{2+}$  concentrations needs to be combined with L-type channel antagonists to fully abolish LTD, suggesting that the  $\text{Ca}^{2+}$  signal may be generated by the activation of a combination of voltage-dependent  $\text{Ca}^{2+}$  channels. Altogether,  $\text{Ca}^{2+}$  signalling through T-type  $\text{Ca}^{2+}$  currents may thus contribute at several stages of the induction cascade, most likely by regulating proteins leading to endocannabinoid release. However, the exclusive role of these channels during weak postsynaptic activity may be overruled by high-voltage-activated  $\text{Ca}^{2+}$  channels when action potential bursts are generated.

Rebound burst discharges generated by T-type  $\text{Ca}^{2+}$  channels have been recently implicated in plasticity in the cerebellum, although the contribution of  $\text{Ca}^{2+}$  entering through these channels has not yet been elucidated in detail. Low-frequency stimulation of inhibitory afferents onto neurons of the deep cerebellar nuclei, each evoking a rebound burst discharge, led to a LTP or LTD of IPSCs, depending on the number of action potentials generated during the rebound bursting (Aizenman et al., 1998). When mossy fiber activation was paired with postsynaptic rebound current, a LTP of mossy fiber EPSCs was generated that strongly dependent on the relative timing of synaptic stimulation and rebound current (Pugh and Raman, 2006). Thus, the rebound current had to occur during, or shortly after the synaptic



stimuli, for plasticity to be induced, while no change was observed when it preceded EPSCs. It is currently believed that  $\text{Ca}^{2+}$  entry during T-type  $\text{Ca}^{2+}$  channels may help to boost a plasticity-promoting  $\text{Ca}^{2+}$  signal generated by the synaptic stimuli. Such a mechanism would point to an important role of non-synaptic  $\text{Ca}^{2+}$  signals generated by T-type  $\text{Ca}^{2+}$  channels in some forms of synaptic plasticity.

## Conclusions

The current literature points to a number of specialized cell types which, expressing T-type  $\text{Ca}^{2+}$  channels at high densities, exploit them as a  $\text{Ca}^{2+}$  source for distinct physiological functions. Indeed, in some cases,  $\text{Ca}^{2+}$  entering through T-type  $\text{Ca}^{2+}$  channels acts as the dominant, if not exclusive, source to trigger a unique  $\text{Ca}^{2+}$ -dependent process. To the most prominent of these belongs the regulation of oscillatory bursting along stretches of dendritic membrane, regulation of developmental processes through regulating resting  $\text{Ca}^{2+}$  levels, dendrodendritic synaptic transmission, and synaptic plasticity involving postsynaptic rebound discharge. In these cases, the specialized  $\text{Ca}^{2+}$  signalling functions carried by  $\text{Ca}^{2+}$  entering through T-type  $\text{Ca}^{2+}$  channels is illustrated most impressively. It appears conceivable that, to further understand the molecular and biophysical basis of T-type  $\text{Ca}^{2+}$  channel signalling, a focus on these specialized cell types would be helpful. Understanding these primary roles of  $\text{Ca}^{2+}$  entering through T-type  $\text{Ca}^{2+}$  channels will further stimulate research on dissecting the roles of T-type  $\text{Ca}^{2+}$  channels in the fundamental cellular mechanisms of excitability, transmission, and plasticity.

## References

- Aizenman, C.D., Manis, P.B., and Linden, D.J. (1998). Polarity of long-term synaptic gain change is related to postsynaptic spike firing at a cerebellar inhibitory synapse. *Neuron* *21*, 827-835.
- Arnaudeau, S., Holzer, N., Konig, S., Bader, C.R., and Bernheim, L. (2006). Calcium sources used by post-natal human myoblasts during initial differentiation. *J Cell Physiol* *208*, 435-445.
- Bal, T., and McCormick, D.A. (1993). Mechanisms of oscillatory activity in guinea-pig nucleus reticularis thalami *in vitro*: a mammalian pacemaker. *J Physiol* *468*, 669-691.
- Berridge, M.J. (1998). Neuronal calcium signaling. *Neuron* *21*, 13-26.
- Bijlenga, P., Liu, J.H., Espinos, E., Haenggeli, C.A., Fischer-Lougheed, J., Bader, C.R., and Bernheim, L. (2000). T-type alpha 1H Ca<sup>2+</sup> channels are involved in Ca<sup>2+</sup> signaling during terminal differentiation (fusion) of human myoblasts. *Proc Natl Acad Sci U S A* *97*, 7627-7632.
- Birtoli, B., and Ulrich, D. (2004). Firing mode-dependent synaptic plasticity in rat neocortical pyramidal neurons. *J Neurosci* *24*, 4935-4940.
- Blethyn, K.L., Hughes, S.W., Tóth, T.I., Cope, D.W., and Crunelli, V. (2006). Neuronal basis of the slow (<1 Hz) oscillation in neurons of the nucleus reticularis thalami *in vitro*. *J Neurosci* *26*, 2474-2486.
- Cai, X., Liang, C.W., Muralidharan, S., Kao, J.P., Tang, C.M., and Thompson, S.M. (2004). Unique roles of SK and K<sub>v</sub>4.2 potassium channels in dendritic integration. *Neuron* *44*, 351-364.
- Carbone, E., Gianniccoli, A., Marcantoni, A., Guido, D., and Carabelli, V. (2006). A new role for T-type channels in fast "low-threshold" exocytosis. *Cell Calcium* *40*, 147-154.
- Catterall, W.A. (1998). Structure and function of neuronal Ca<sup>2+</sup> channels and their role in neurotransmitter release. *Cell Calcium* *24*, 307-323.
- Cavelier, P., Pouille, F., Desplantez, T., Beekenkamp, H., and Bossu, J.-L. (2002). Control of the propagation of dendritic low-threshold Ca<sup>2+</sup> spikes in Purkinje cells from rat cerebellar slice cultures. *J Physiol* *540*, 57-72.
- Chang, S.-Y., and Kim, U. (2004). Ionic mechanism of long-lasting discharges of action potentials triggered by membrane hyperpolarization in the medial lateral habenula. *J Neurosci* *24*, 2172-2181.
- Chen, C.C., Lamping, K.G., Nuno, D.W., Barresi, R., Prouty, S.J., Lavoie, J.L., Cribbs, L.L., England, S.K., Sigmund, C.D., Weiss, R.M., *et al.* (2003). Abnormal coronary function in mice deficient in alpha1H T-type Ca<sup>2+</sup> channels. *Science* *302*, 1416-1418.
- Christie, B.R., Eliot, L.S., Ito, K., Miyakawa, H., and Johnston, D. (1995). Different Ca<sup>2+</sup> channels in soma and dendrites of hippocampal pyramidal neurons mediate spike-induced Ca<sup>2+</sup> influx. *J Neurophysiol* *73*, 2553-2557.
- Crunelli, V., Cope, D.W., and Hughes, S.W. (2006). Thalamic T-type Ca<sup>2+</sup> channels and NREM sleep. *Cell Calcium* *40*, 175-190.
- Crunelli, V., Tóth, T.I., Cope, D.W., Blethyn, K., and Hughes, S.W. (2005). The 'window' T-type calcium current in brain dynamics of different behavioural states. *J Physiol* *562*, 121-129.
- Cueni, L., Canepari, M., Luján, R., Emmenegger, Y., Watanabe, M., Bond, C.T., Franken, P., Adelman, J.P., and Lüthi, A. (2007). A competition between SK2 channels and SERCAs for Ca<sup>2+</sup> entry through T-type channels gates sleep-related oscillations in thalamic dendrites.

- Cui, G., Okamoto, T., and Morikawa, H. (2004). Spontaneous opening of T-type  $\text{Ca}^{2+}$  channels contributes to the irregular firing of dopamine neurons in neonatal rats. *J Neurosci* 24, 11079-11087.
- Czarnecki, A., Birtoli, B., and Ulrich, D. (2007). Cellular mechanisms of burst firing-mediated long-term depression in rat neocortical pyramidal cells. *J Physiol* 578, 471-479.
- Destexhe, A., Contreras, D., Steriade, M., Sejnowski, T.J., and Huguenard, J.R. (1996). *In vivo*, *in vitro*, and computational analysis of dendritic calcium currents in thalamic reticular neurons. *J Neurosci* 16, 169-185.
- Destexhe, A., Neubig, M., Ulrich, D., and Huguenard, J. (1998). Dendritic low-threshold calcium currents in thalamic relay cells. *J Neurosci* 18, 3574-3588.
- Diana, M.A., Otsu, Y., Maton, G., Collin, T., Chat, M., and Dieudonne, S. (2007). T-type and L-type  $\text{Ca}^{2+}$  conductances define and encode the bimodal firing pattern of vestibulocerebellar unipolar brush cells. *J Neurosci* 27, 3823-3838.
- Dolphin, A.C. (2006). A short history of voltage-gated calcium channels. *Br J Pharmacol* 147 Suppl 1, S56-62.
- Egger, V., Svoboda, K., and Mainen, Z.F. (2003). Mechanisms of lateral inhibition in the olfactory bulb: efficiency and modulation of spike-evoked calcium influx into granule cells. *J Neurosci* 23, 7551-7558.
- Egger, V., Svoboda, K., and Mainen, Z.F. (2005). Dendrodendritic synaptic signals in olfactory bulb granule cells: local spine boost and global low-threshold spike. *J Neurosci* 25, 3521-3530.
- Gautam, S.H., Otsuguro, K.I., Ito, S., Saito, T., and Habara, Y. (2007). T-type  $\text{Ca}^{2+}$  channels mediate propagation of odor-induced  $\text{Ca}^{2+}$  transients in rat olfactory receptor neurons. *Neuroscience* 144, 702-713.
- Giancippoli, A., Novara, M., de Luca, A., Baldelli, P., Marcantoni, A., Carbone, E., and Carabelli, V. (2006). Low-threshold exocytosis induced by cAMP-recruited  $\text{Ca}_v3.2$  ( $\alpha_{1H}$ ) channels in rat chromaffin cells. *Biophys J* 90, 1830-1841.
- Gillessen, T., and Alzheimer, C. (1997). Amplification of EPSPs by low  $\text{Ni}^{2+}$ - and amiloride-sensitive  $\text{Ca}^{2+}$  channels in apical dendrites of rat CA1 pyramidal neurons. *J Neurophysiol* 77, 1639-1643.
- Goaillard, J.-M., and Vincent, P. (2002). Serotonin suppresses the slow afterhyperpolarization in rat intralaminar and midline neurones by activating 5 HT-7 receptors. *J Physiol* 541, 453-465.
- Hagiwara, N., Irisawa, H., and Kameyama, M. (1988). Contribution of two types of calcium currents to the pacemaker potentials of rabbit sino-atrial node cells. *J Physiol* 395, 233-253.
- Huguenard, J.R. (1996). Low-threshold calcium currents in central nervous system neurons. *Annu Rev Physiol* 58, 329-348.
- Humeau, Y., Herry, C., Kemp, N., Shaban, H., Fourcaudot, E., Bissiere, S., and Lüthi, A. (2005). Dendritic spine heterogeneity determines afferent-specific Hebbian plasticity in the amygdala. *Neuron* 45, 119-131.
- Hüser, J., Blatter, L.A., and Lipsius, S.L. (2000). Intracellular  $\text{Ca}^{2+}$  release contributes to automaticity in cat atrial pacemaker cells. *J Physiol* 524 415-422.
- Isomura, Y., Fujiwara-Tsukamoto, Y., Imanishi, M., Nambu, A., and Takada, M. (2002). Distance-dependent  $\text{Ni}^{2+}$ -sensitivity of synaptic plasticity in apical dendrites of hippocampal CA1 pyramidal cells. *J Neurophysiol* 87, 1169-1174.
- Ivanov, A.I., and Calabrese, R.L. (2000). Intracellular  $\text{Ca}^{2+}$  dynamics during spontaneous and evoked activity of leech heart interneurons: low-threshold Ca currents and graded synaptic transmission. *J Neurosci* 20, 4930-4943.
- Joksovic, P.M., Bayliss, D.A., and Todorovic, S.M. (2005). Different kinetic properties of two T-type  $\text{Ca}^{2+}$  currents of rat reticular thalamic neurones and their modulation by enflurane. *J Physiol* 566, 125-142.

- Kampa, B.M., Letzkus, J.J., and Stuart, G.J. (2006). Requirement of dendritic calcium spikes for induction of spike-timing-dependent synaptic plasticity. *J Physiol* 574, 283-290.
- Kavalali, E.T., Zhuo, M., Bito, H., and Tsien, R.W. (1997). Dendritic  $\text{Ca}^{2+}$  channels characterized by recordings from isolated hippocampal dendritic segments. *Neuron* 18, 651-663.
- Khosravani, H., and Zamponi, G.W. (2006). Voltage-gated calcium channels and idiopathic generalized epilepsies. *Physiol Rev* 86, 941-966.
- Kim, Y., and Trussell, L.O. (2007). Ion channels generating complex spikes in cartwheel cells of the dorsal cochlear nucleus. *J Neurophysiol* 97, 1705-1725.
- Konig, S., Beguet, A., Bader, C.R., and Bernheim, L. (2006). The calcineurin pathway links hyperpolarization (Kir2.1)-induced  $\text{Ca}^{2+}$  signals to human myoblast differentiation and fusion. *Development* 133, 3107-3114.
- Kuisle, M., Wanaverbecq, N., Brewster, A.L., Frère, S.G., Pinault, D., Baram, T.Z., and Lüthi, A. (2006). Functional stabilization of weakened thalamic pacemaker channel regulation in rat absence epilepsy. *J Physiol* 575, 83-100.
- Larkum, M.E., Kaiser, K.M., and Sakmann, B. (1999a). Calcium electrogenesis in distal apical dendrites of layer 5 pyramidal cells at a critical frequency of back-propagating action potentials. *Proc Natl Acad Sci U S A* 96, 14600-14604.
- Larkum, M.E., Zhu, J.J., and Sakmann, B. (1999b). A new cellular mechanism for coupling inputs arriving at different cortical layers. *Nature* 398, 338-341.
- Lüthi, A., and McCormick, D.A. (1998). Periodicity of thalamic synchronized oscillations: the role of  $\text{Ca}^{2+}$ -mediated upregulation of  $I_h$ . *Neuron* 20, 553-563.
- Magee, J.C., Christofi, G., Miyakawa, H., Christie, B., Lasser-Ross, N., and Johnston, D. (1995). Subthreshold synaptic activation of voltage-gated  $\text{Ca}^{2+}$  channels mediates a localized  $\text{Ca}^{2+}$  influx into the dendrites of hippocampal pyramidal neurons. *J Neurophysiol* 74, 1335-1342.
- Magee, J.C., and Johnston, D. (1995). Characterization of single voltage-gated  $\text{Na}^+$  and  $\text{Ca}^{2+}$  channels in apical dendrites of rat CA1 pyramidal neurons. *J Physiol* 487, 67-90.
- Mangoni, M.E., Traboulsie, A., Leoni, A.L., Couette, B., Marger, L., Le Quang, K., Kupfer, E., Cohen-Solal, A., Vilar, J., Shin, H.S., *et al.* (2006). Bradycardia and slowing of the atrioventricular conduction in mice lacking  $\text{Ca}_v3.1/\alpha 1G$  T-type calcium channels. *Circ Res* 98, 1422-1430.
- Markram, H., Helm, P.J., and Sakmann, B. (1995). Dendritic calcium transients evoked by single back-propagating action potentials in rat neocortical pyramidal neurons. *J Physiol* 485 (Pt 1), 1-20.
- Markram, H., and Sakmann, B. (1994). Calcium transients in dendrites of neocortical neurons evoked by single subthreshold excitatory postsynaptic potentials via low-voltage-activated calcium channels. *Proc Natl Acad Sci U S A* 91, 5207-5211.
- McCobb, D.P., and Beam, K.G. (1991). Action potential waveform voltage-clamp commands reveal striking differences in calcium entry via low and high voltage-activated calcium channels. *Neuron* 7, 119-127.
- Nevian, T., and Sakmann, B. (2006). Spine  $\text{Ca}^{2+}$  signaling in spike-timing-dependent plasticity. *J Neurosci* 26, 11001-11013.
- Oliet, S.H.R., Malenka, R.C., and Nicoll, R.A. (1997). Two distinct forms of long-term depression coexist in CA1 hippocampal pyramidal cells. *Neuron* 18, 969-982.
- Pan, Z.H., Hu, H.J., Perring, P., and Andrade, R. (2001). T-type  $\text{Ca}^{2+}$  channels mediate neurotransmitter release in retinal bipolar cells. *Neuron* 32, 89-98.
- Perez-Reyes, E. (2003). Molecular physiology of low-voltage-activated T-type calcium channels. *Physiol Rev* 83, 117-161.
- Poo, M.M., and Zheng, J. (2006). Calcium Signaling and Neuronal Motility. *Annu Rev Cell Dev Biol*.

- Pugh, J.R., and Raman, I.M. (2006). Potentiation of mossy fiber EPSCs in the cerebellar nuclei by NMDA receptor activation followed by postinhibitory rebound current. *Neuron* *51*, 113-123.
- Rancz, E.A., and Häusser, M. (2006). Dendritic calcium spikes are tunable triggers of cannabinoid release and short-term synaptic plasticity in cerebellar Purkinje neurons. *J Neurosci* *26*, 5428-5437.
- Redmond, L., and Ghosh, A. (2005). Regulation of dendritic development by calcium signaling. *Cell Calcium* *37*, 411-416.
- Reid, C.A., Bekkers, J.M., and Clements, J.D. (2003). Presynaptic Ca<sup>2+</sup> channels: a functional patchwork. *Trends Neurosci* *26*, 683-687.
- Richter, T.A., Kolaj, M., and Renaud, L.P. (2005). Low voltage-activated Ca<sup>2+</sup> channels are coupled to Ca<sup>2+</sup>-induced Ca<sup>2+</sup> release in rat thalamic midline neurons. *J Neurosci* *25*, 8267-8271.
- Schneggenburger, R., and Neher, E. (2005). Presynaptic calcium and control of vesicle fusion. *Curr Opin Neurobiol* *15*, 266-274.
- Singer, J.H., and Diamond, J.S. (2003). Sustained Ca<sup>2+</sup> entry elicits transient postsynaptic currents at a retinal ribbon synapse. *J Neurosci* *23*, 10923-10933.
- Sipido, K.R., Carmeliet, E., and Van de Werf, F. (1998). T-type Ca<sup>2+</sup> current as a trigger for Ca<sup>2+</sup> release from the sarcoplasmic reticulum in guinea-pig ventricular myocytes. *J Physiol* *508* ( Pt 2), 439-451.
- Südhof, T.C. (2004). The synaptic vesicle cycle. *Annu Rev Neurosci* *27*, 509-547.
- Sun, Q.Q., Baraban, S.C., Prince, D.A., and Huguenard, J.R. (2003). Target-specific neuropeptide Y-ergic synaptic inhibition and its network consequences within the mammalian thalamus. *J Neurosci* *23*, 9639-9649.
- Swensen, A.M., and Bean, B.P. (2003). Ionic mechanisms of burst firing in dissociated Purkinje neurons. *J Neurosci* *23*, 9650-9663.
- Tai, C., Kuzmiski, J.B., and MacVicar, B.A. (2006). Muscarinic enhancement of R-type calcium currents in hippocampal CA1 pyramidal neurons. *J Neurosci* *26*, 6249-6258.
- Thomas, M.J., Watabe, A.M., Moody, T.D., Makhinson, M., and O'Dell, T.J. (1998). Postsynaptic complex spike bursting enables the induction of LTP by theta frequency synaptic stimulation. *J Neurosci* *18*, 7118-7126.
- Thompson, S.M., and Wong, R.K.S. (1991). Development of calcium current subtypes in isolated rat hippocampal pyramidal cells. *J Physiol* *439*, 671-689.
- Tsakiridou, E., Bertollini, L., de Curtis, M., Avanzini, G., and Pape, H.C. (1995). Selective increase in T-type calcium conductance of reticular thalamic neurons in a rat model of absence epilepsy. *J Neurosci* *15*, 3110-3117.
- Vassort, G., Talavera, K., and Alvarez, J.L. (2006). Role of T-type Ca<sup>2+</sup> channels in the heart. *Cell Calcium* *40*, 205-220.
- West, A.E., Griffith, E.C., and Greenberg, M.E. (2002). Regulation of transcription factors by neuronal activity. *Nat Rev Neurosci* *3*, 921-931.
- Williams, S., Serafin, M., Mühlethaler, M., and Bernheim, L. (1997a). Distinct contributions of high- and low-voltage-activated calcium currents to afterhyperpolarizations in cholinergic nucleus basalis neurons of the guinea pig. *J Neurosci* *17*, 7307-7315.
- Williams, S.R., and Stuart, G.J. (2000). Action potential backpropagation and somatodendritic distribution of ion channels in thalamocortical neurons. *J Neurosci* *20*, 1307-1317.
- Williams, S.R., Toth, T.I., Turner, J.P., Hughes, S.W., and Crunelli, V. (1997b). The 'window' component of the low-threshold Ca<sup>2+</sup> current produces input signal amplification and bistability in cat and rat thalamocortical neurones. *J Physiol* *505*, 689-705.
- Wolfart, J., and Roper, J. (2002). Selective coupling of T-type calcium channels to SK potassium channels prevents intrinsic bursting in dopaminergic midbrain neurons. *J Neurosci* *22*, 3404-3413.

Zhou, Z., and January, C.T. (1998). Both T- and L-type  $\text{Ca}^{2+}$  channels can contribute to excitation-contraction coupling in cardiac Purkinje cells. *Biophys J* 74, 1830-1839.

## 6 General discussion

By combining electrophysiological, imaging, immunohistochemical, computational, genetic, and EEG techniques, we described how T-type  $\text{Ca}^{2+}$  signalling underlies the generation of nRt oscillations. We found that thalamic  $I_T$  give rise to marked elevations of  $[\text{Ca}^{2+}]_i$  beyond its role as burst generator. In addition, we identified a tripartite functional complex composed of  $\text{Ca}_v3$  channels, SK2 channels and SERCA pumps, which underlie the generation and the temporal dynamics of nRt oscillations. Furthermore, we found a remarkable correlation between the consequences of SK2-KO at the cellular and EEG levels, strongly suggesting that the mechanism we identified is physiologically relevant to sleep mechanisms. Altogether, my work represents the first study that quantifies the  $\text{Ca}^{2+}$  signals generated by the  $\text{Ca}_v3$  channel family in the context of physiologically relevant cellular oscillations.

### 6.1 The role of $\text{Ca}_v3$ channels during nRt oscillations

In mice, the lack of the  $\text{Ca}_v3.1$  gene causes severe sleep disturbances (Anderson et al., 2005; Lee et al., 2004), suggesting that assessing sleep-related neuronal activities could be a particularly useful approach to further understand  $\text{Ca}_v3$ -dependent  $\text{Ca}^{2+}$  signalling. Our study was dedicated to the nRt cells, a particularly vigorously bursting cell that is further facilitated by the expression of a  $I_T$  with unique voltage-dependent properties (Huguenard and Prince, 1992). The strategically crucial location of the nRt is documented by lesions applied to the nRt, which abolish sleep-related spindle oscillations within the TC network and produce attentional neglect (for review, see (Pinault, 2004)). At the cellular level, the discharge capacities of nRt cells, in conjunction with their strong innervation of TC cells and their glutamatergic control by the layer VI corticothalamic feedback, render them important pacemakers for network oscillations. Furthermore, dampened oscillatory burst discharge, followed by tonic activity, is critical for the transmission of novel aspects of sensory information (Cotillon and Edeline, 2000; Shosaku and Sumitomo, 1983; Swadlow et al., 2005) and is disrupted in an animal model of schizophrenia (Krause et al., 2003). Conversely, enhancing nRt cell activity, either through genetic loss of reciprocal inhibition (Huntsman et

al., 1999) augmentation of LT  $I_T$  (Tsakiridou et al., 1995), excessive cortical activity (Slaught et al., 2002) or through pharmacological strengthening of reciprocal inhibition (Liu et al., 1992), leads to a hyperexcitable nRt network and the emergence of generalized epileptic seizures (Huguenard, 1998). The appropriate control and limitation of nRt neuron bursting activity thus appears essential for balancing TC networks. In the nRt the two isoforms expressed,  $Ca_v3.2$  and  $Ca_v3.3$  (Talley et al., 1999), show markedly different kinetics compared to  $Ca_v3.1$  which are suggestive of enhanced and prolonged capacities of burst generation.  $Ca_v3.2$  channels exhibit rapid inactivation and recovery from inactivation, whereas  $Ca_v3.3$  channels exhibit slow components of inactivation and recovery from inactivation (Talavera and Nilius, 2006). A recent publication reports a rapidly inactivating somatic and a more slowly decaying dendritic  $I_T$  (Joksovic et al., 2005). We obtained the first quantification of an  $I_T$ -dependent  $Ca^{2+}$  signal in a manner that minimally disturbs its natural time course. Notably, these signals account for the large majority of  $[Ca^{2+}]_i$  in nRt dendrites and appear synchronously in the 100-150  $\mu m$  of imaged dendrite, suggesting a uniform and high expression of  $Ca_v3$  channels along the proximal dendritic membrane. The estimated  $Ca_v3$  channel conductance density in our studies (0.6-1  $mS/cm^2$ ) allows us to compare it to previous estimates achieved in computational studies (Destexhe et al., 1996). In these, the threshold density required for LT bursting was determined to be 0.3  $mS/cm^2$ , assuming a uniform distribution of  $Ca_v3$  channels. This threshold was lowered by one order of magnitude (0.045  $mS/cm^2$ ) in models where the distal dendrites had a high channel density (0.5  $mS/cm^2$ ). Although our imaging does not allow us to estimate the  $[Ca^{2+}]_i$  in the fine distal arborizations, the derived value clearly lies above these values and indicates that proximal dendrites play an active role in dendritic  $Ca^{2+}$  electrogenesis. In essence, this means that nRt dendrites are vigorous oscillators, which, by virtue of their high expression of  $Ca_v3$  channels and SK channels, are able to act as single compartments that make rapid transitions between the oscillatory 'up' and 'down' states. This effect, combined with the high surface-to-volume ratio of nRt dendrites (Pinault, 2004), produces a robust oscillatory unit that handles large  $Ca^{2+}$  charge transfer and accumulation over repeated time periods. When further combined with the electrical connectivity between nRt dendrites, via gap junctions and long-range synaptic interactions (Landisman et al., 2002; Pinault, 2004), it appears plausible that nRt dendrites are specialized to form a plexus of synchronously oscillating dendrites throughout major portions of the nRt.

In our study, we also found that later cycles of the oscillation showed decreased  $[Ca^{2+}]_i$  signals. The mechanisms implicated in the reduction of these signals are related to insufficient

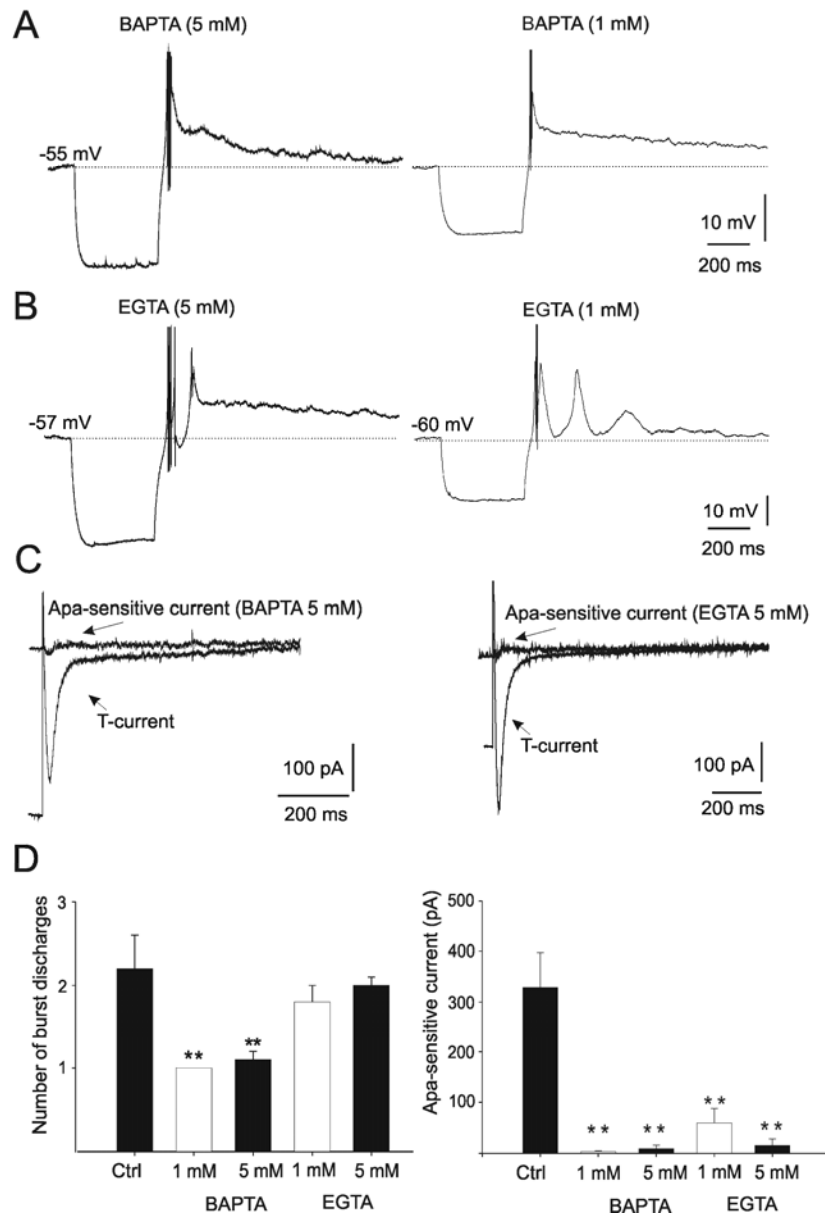


Ca<sub>v</sub>3 channel recruitment, since burst amplitude was proportional to the Ca<sup>2+</sup> signal in all oscillatory cycles. Ca<sup>2+</sup>-induced channel inactivation is well-known for HVA Ca<sup>2+</sup> currents (Budde et al., 2002), but has not been described for native I<sub>T</sub>. Moreover, [Ca<sup>2+</sup>]<sub>i</sub> signals show a minor temporal summation, arguing against incremental Ca<sup>2+</sup>-induced inactivation. However, Ca<sub>v</sub>3 channels go through a cycle of recovery once they have been inactivated, with a time constant of 0.5-1 s at room temperature (Frazier et al., 2001; Huguenard and Prince, 1992). These experimental results are consistent with a slow gating process underlying the decremting Ca<sup>2+</sup> signal. The slow time dependence makes the comparatively small and short hyperpolarizations produced by SK channels insufficient for full Ca<sub>v</sub>3 channel recovery. Computational modelling shows substantial Ca<sub>v</sub>3 channel inactivation during single LT bursts and integrating recovery from inactivation into currently available models robustly reproduces dampening.

## 6.2 SK channel gating during nRt oscillations

SK2 and SK1 are expressed in very high and high levels, respectively in the nRt. In contrast, SK3, which is predominantly expressed in TC cells, is expressed in very low levels in the nRt (Sailer et al., 2004; Stocker and Pedarzani, 2000). Our findings of the dendritically restricted expression pattern of SK2 protein in the nRt fits well in the emergent view that SK2-containing channels are an important attribute of dendritic excitability (Bond et al., 2005). SK channels are exclusively activated by increases in [Ca<sup>2+</sup>]<sub>i</sub> via various Ca<sup>2+</sup> sources (see introduction). Direct binding of Ca<sup>2+</sup> on CaM, which constitutively binds to SK channels, results in the channel opening (Xia et al., 1998). The following outward K<sup>+</sup> current underlies the generation of the AHP, whose decay mirrors the decrease of [Ca<sup>2+</sup>]<sub>i</sub> to baseline levels. In distal dendrites of hippocampal CA1 neurons, HVA Ca<sup>2+</sup> channel-mediated plateau potentials are shortened by SK channel-mediated repolarisation (Cai et al., 2004). Local blocking of SK channels with the selective channel blocker apamin results in the prolongation of the plateau potential. The ability of focally applied glutamate to induce APs increases during apamin-mediated prolongation of the plateau potential. Whereas the dendritic excitability in CA1 neurons changes after a local block of dendritic SK channels, SK channel inhibition has a moderate effect on the excitability of somatic current injections (Bond et al., 2004; Stocker et al., 1999).

In nRt cells, SK channel gating is tightly linked to  $Ca_v3$  channel activation, as demonstrated by our finding that blocking  $I_T$  with mibefradil leads to the disappearance of the apamin-sensitive current. Moreover, this link is supported when considering the temporal scales of current activation and  $Ca^{2+}$  signalling. Heterologously expressed SK2 channels need ~6-8 ms to gate in saturating  $[Ca^{2+}]_i$  (Pedarzani et al., 2001). In CA1 hippocampal cells SK channels, which are co-localized within 50-150 nm of HVA  $Ca^{2+}$  channel open within 15 ms of HVA activation (Marrion and Tavalin, 1998). Taking into account that the generation of the AHP is the result of a change of membrane capacitance due to  $I_T$  deactivation and SK current activation, the slightly longer time delay of on average ~37 ms, is consistent with a very fast rate of  $Ca_v3$ -/SK channel interaction. It is therefore somewhat curious that we found that not only fast (BAPTA), but also slow (EGTA)  $Ca^{2+}$  buffers interfere with SK channel gating in nRt dendrites (Figure D1). Slow and fast  $Ca^{2+}$  buffers differentially attenuate the spatial spread of  $Ca^{2+}$  around its source (Augustine et al., 2003). The presence of BAPTA, (1-5 mM) fully abolished the oscillatory burst discharges of nRt cells within minutes of gaining whole-cell access and replaced neuronal firing with a single burst followed by a slowly decaying plateau potential (Figure D1 A,D), similar to the discharge pattern in Apa-treated or SK2-deficient cells. Dampened oscillations were attenuated, but not abolished, when the pipette contained EGTA (Figure D1 B,D). At 0.1 mM EGTA,  $\Delta[Ca^{2+}]_i$  measured with magfura-2 was undistinguishable from that without EGTA (data not shown). When EGTA was used at 5 mM, neurons typically discharged with 2 bursts interspersed by a rapid but clearly discernible AHP. Thus,  $Ca_v3$ - and SK channel coupling is abolished by fast  $Ca^{2+}$  buffers, while slow  $Ca^{2+}$  chelation leads to attenuation. Spatially averaged  $[Ca^{2+}]_i$  transients thus mediate  $Ca_v3$ -/SK channel coupling, with a minor contribution from localized signals. This finding is consistent with the general notion that SK channels typically remain remote from their  $Ca^{2+}$  sources and are responsible for AHP-mediating currents of intermediate time course in contrast to their rapidly acting BK channel counterparts, which undergo complex formation with  $Ca^{2+}$  channels and are responsible for very fast AHPs (Bean, 2007; Berkefeld et al., 2006).



D Figure 1.  $\text{Ca}^{2+}$  buffers interfered with SK channel gating in nRt dendrites

- (A) Whole-cell recordings of nRt discharge pattern after a brief negative current injection (-100 pA, 400 ms). The fast  $\text{Ca}^{2+}$  buffer BAPTA is applied in the patch pipette. High (5 mM) and low (1 mM) concentrations of BAPTA blocked burst-associated AHPs. Note that the single discharge and the plateau potential are similar to the discharge pattern in apamin and SK2-deficient cells.
- (B) Whole-cell recordings of nRt discharge pattern after a brief negative current injection (-100 pA, 400 ms). The slow  $\text{Ca}^{2+}$  buffer EGTA is applied in the patch pipette. High (5 mM) and low (1 mM) concentrations of EGTA partially blocked burst-associated AHPs.
- (C) Membrane current response elucidated after a hyperpolarizing voltage step (from -50 to -110 mV, 125 ms) and digital isolation of the apamin-sensitive current. High

pipette concentrations from either BAPTA (right) or EGTA (left) abolished SK current while  $I_T$  remained unaltered.

- (D) Pooled data showing the number of LT burst discharges in Ctrl high and low concentrations of BAPTA and EGTA (left). Histogram showing the amplitudes of apamin-sensitive currents recorded under control conditions (Ctrl, n=7) and with BAPTA (n=6) and EGTA (n=10)-containing pipettes (right).

Afterhyperpolarizations generated by SK channels are permissive for repetitive LT burst generation because they help in the recovery of inactivated  $Ca_v3$  channels. In addition, we found that SK channels accelerate LT burst termination because their blockade with apamin or intracellular  $Cs^+$ , or via genetic deletion, reduced  $I_T$  decay slope by more than two-fold and led to pronounced, slowly decaying plateau potentials. The  $I_T$  in nRt cells is mediated by  $Ca_v3$  channels containing  $Ca_v$  3.3 subunits, which form slowly inactivating isoforms (Joksovic et al., 2005; Joksovic et al., 2006) capable of generating plateau potentials (Chevalier et al., 2006). Activation of SK channels shuts down these plateau potentials along the entire dendrite, and thus helps prevent a slow form of  $Ca_v3$  channel inactivation. The SK channel function has been repeatedly described in the context of terminating plateau potentials in neurons (Bond et al., 2005). The coupling between  $I_T$  and SK currents can go as far as to prevent bursting once SK currents activate rapidly enough to antagonize  $I_T$  spike generation (Wolfart and Roper, 2002). SK channel gating thus appears to be tailored to control the functional impact of  $Ca_v3$  channels according to neuronal discharge characteristics.

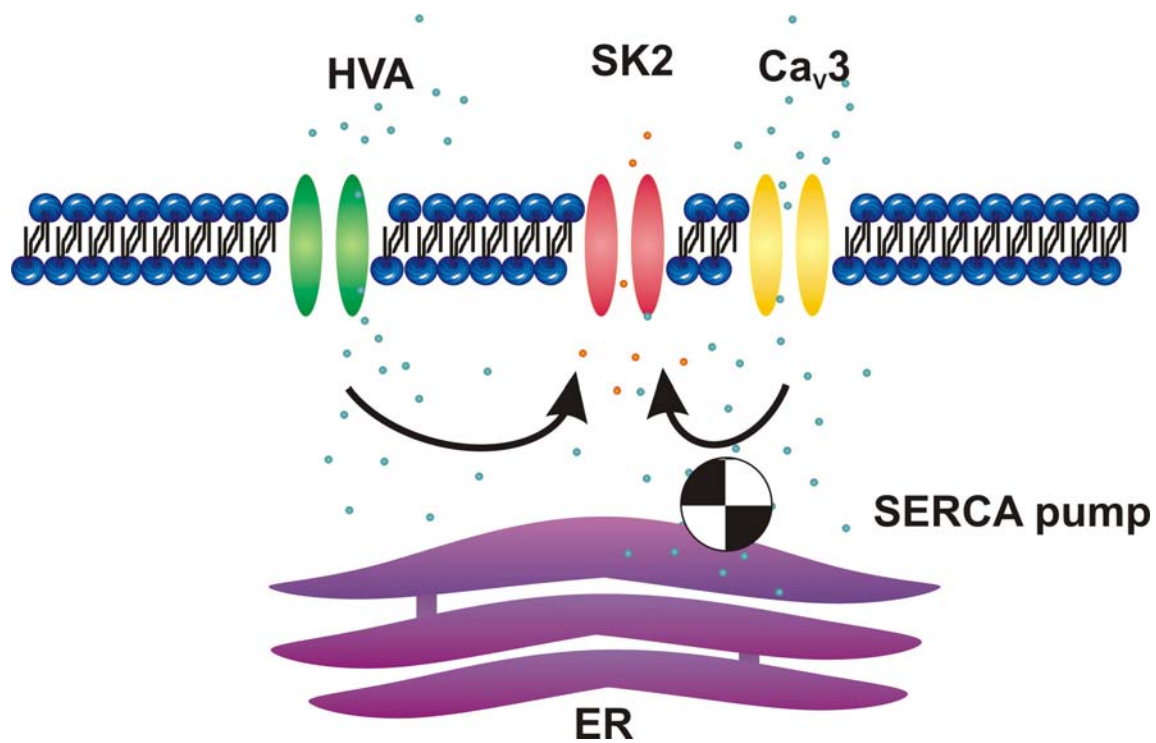
Previous studies have addressed some of the ionic mechanisms underlying the time course of dampened nRt cell bursting. The generation of a burst AHP that decreases in amplitude from one burst to the next, associated with burst fading, is typically reported for somatically (Avanzini et al., 1989) and synaptically (Bal and McCormick, 1993) evoked, as well as spontaneous (Blethyn et al., 2006) intrinsic oscillations. Small conductance  $Ca^{2+}$ -activated  $K^+$  channel currents are widely recognized to be central for the burst AHP, but additional currents have been advocated to explain the dampening of neuronal oscillations. These include persistent  $Na^+$  currents (Avanzini et al., 1989; Mulle et al., 1986),  $Ca^{2+}$ -activated cationic currents that activate due to  $Ca^{2+}$  accumulation (Bal and McCormick, 1993; Blethyn et al., 2006), and  $Na^+$ -activated  $K^+$  currents (Blethyn et al., 2006; Kim and McCormick, 1998). The biophysical and molecular properties of these secondarily activated currents are not known. Our current data now show that many of the events underlying dampened nRt activity may be well explained based on the quantitative aspects of  $Ca_v3$ - and

SK channel coupling. First, imaging of  $[Ca^{2+}]_i$  reveals that  $Ca^{2+}$  transients generated by LT bursts decay completely during each AHP and do not summate, making activation of slow  $Ca^{2+}$ -dependent conductances unlikely. Second, inclusion of high concentrations of the rapid chelator BAPTA prevents SK channel gating but does not prevent the burst AHP, which is thought to be mediated by  $Ca^{2+}$ -dependent cationic conductance. Third, we find that SK channel gating is rapidly attenuated during oscillations, because  $Ca^{2+}$  transients decay quickly, thereby limiting the recovery of inactivated  $Ca_v3$  channels and the generation of the next LT burst. Fourth, strengthening  $Ca^{2+}$  binding to SK channels by 1-EBIO potentiates bursting, and retards the transition into the tonic discharge mode, showing that SK channel gating is the critical factor limiting LT burst generation. Altogether, we suggest that  $Ca_v3$ - and SK channel coupling is the major determinant of the temporal aspects of nRt oscillations. Afterhyperpolarizations generated by SK channels are, on the one hand, rate-limiting for repetitive LT burst generation. On the other hand, they are also important for accelerating  $I_T$  decay by suppressing  $I_T$ -dependent plateau potentials, which could, in fact, be due to slow inactivation of  $I_T$  isoforms expressed in nRt cells (Cavelier et al., 2002; Frazier et al., 2001; Joksovic et al., 2005) or to the “window” components of the current (Blethyn et al., 2006). Activation of SK channels is strong and rapid enough to shut down the plateau potentials, a function which is consistent with their role in terminating plateau potentials in a number of neurons (Beurrier et al., 1999; Cai et al., 2004).

### 6.3 The role of SERCA during nRt oscillations

Sarco-Endoplasmic Reticulum  $Ca^{2+}$  ATPase pumps are important elements in the homeostatic regulation of  $[Ca^{2+}]_i$  many cells, including neurons (Verkhatsky, 2005). Prolonged blockade of SERCA pumps result in neuronal death (Nguyen et al., 2002) and mice lacking SERCA2 die perinatally/postnatally (Prasad et al., 2004). In neurons, SERCA pumps have been thought to primarily shape neuronal excitability by ensuring the appropriate filling of the ER with  $Ca^{2+}$ , which would then become available for CICR (Berridge, 2002). In addition to being the most important intracellular source of  $Ca^{2+}$ , the ER plays a central role as a  $Ca^{2+}$  sink by virtue of its expression of energy-driven ATPases, the SERCAs (Misquitta et al., 1999). During the cardiac heartbeat, SERCA pumps are among the mechanisms terminating the large turnover of  $Ca^{2+}$  and speeding up the recovery from cardiac refractoriness (Szentesi et al., 2004). In marked contrast to the heart, how the uptake of

intracellular  $\text{Ca}^{2+}$  controls the dynamics of neuronal discharge has been poorly addressed, although it is well established that SERCA-mediated sequestration occurs continuously at subthreshold potentials (Garaschuk et al., 1997; Power and Sah, 2005), shapes the waveform of cytosolic  $\text{Ca}^{2+}$  signals (Fierro et al., 1998; Wanaverbecq et al., 2003) and is accelerated by phosphorylation (Usachev et al., 2006). Moreover, SERCA also limit the decay kinetics ( $< 100$  ms) of dendritic (Markram et al., 1995) and spinous (Majewska et al., 2000)  $\text{Ca}^{2+}$  transients, pointing to localized and efficient ER protrusions within neuronal processes (Pozzo-Miller et al., 2000).



D Figure 2. Hypothetical scheme illustrating the proposed co-localization of  $\text{Ca}_v3$  channels, SK2 channels and SERCA pumps

During sleep-related oscillations, such as LT burst oscillations, massive influx of T-type  $\text{Ca}^{2+}$  selectively and rapidly gates SK2 channels in nRt dendrites, indicating the formation of a functional complex between  $\text{Ca}_v3$  and SK2 channels. SERCA pumps selectively sequester T-type  $\text{Ca}^{2+}$  suggesting that they may be co-localized with the  $\text{Ca}_v3$ -SK channel complex but not with HVA  $\text{Ca}^{2+}$  channels. The rapid sequestration of T-type  $\text{Ca}^{2+}$  by SERCA pumps restricts the  $\text{Ca}^{2+}$  available for SK2 activation. SERCA pumps and SK2 channels compete for T-type  $\text{Ca}^{2+}$  in nRt dendrites during LT burst oscillations, thus limiting  $\text{Ca}_v3$  channel recovery, which underlies the dampening of the oscillations.

$\text{Ca}^{2+}$  release from the ER has repeatedly been demonstrated to amplify SK channel gating (Cordoba-Rodriguez et al., 1999; Cui et al., 2004; Davies et al., 1996; Morikawa et al., 2000; Seutin et al., 2000; Yoshizaki et al., 1995). However, CICR does not appear to occur in nRt (Richter et al., 2005). The dampening of nRt oscillations, although robustly controlled by the dynamics of  $\text{Ca}_v3$ - and SK-channel coupling, underlies modulation by SERCA. Neuronal SERCA pumps act on a comparatively rapid ( $< 100$  ms) time scale (Markram et al., 1995) and have a high affinity for  $\text{Ca}^{2+}$  ( $K_{1/2} \sim 0.1\text{-}1 \mu\text{M}$ ). This enables the ER to sequester and accumulate  $\text{Ca}^{2+}$  rapidly, very efficiently and in high concentration ( $100 \mu\text{M}$ ). The properties of these pumps thus enable them to act on the time scales of  $\text{Ca}_v3$ -/SK-channel coupling, and to stand in competition with SK channels for available  $\text{Ca}^{2+}$  (Figure D2). In outer hair cells, the inhibition of SERCA pumps by CPA prevents the deactivation of  $\text{Ca}^{2+}$ -activated  $\text{K}^+$ -conductances, suggesting that  $\text{Ca}^{2+}$  sequestration by SERCA pumps competes for  $\text{Ca}^{2+}$  with SK channels and is necessary to terminate  $\text{Ca}^{2+}$ -activated  $\text{K}^+$ -conductance (Sridhar et al., 1997). The competition is supported by our data on the effects of CPA on apamin-sensitive currents, on interburst AHP and burst number, and by the modelling results. The role of these pumps could thus, on the one hand, involve the limitation of SK channel gating during LT bursts, and the promotion of  $\text{Ca}_v3$  channel inactivation. On the other hand, SERCA pumps may contribute to shorten the exposure of SK channels to  $\text{Ca}^{2+}$  during the AHP, thereby limiting  $\text{Ca}_v3$  channel recovery, consistent with a slow tail component in SK currents during CPA application. Remarkably, SERCA pumps act specifically on  $I_T$ -dependent  $\text{Ca}^{2+}$  entry, suggesting that they may be localized in the vicinity of  $\text{Ca}_v3$ - but not HVA  $\text{Ca}^{2+}$  channels (Figure D2). A preferential localization of SERCA pumps on dendritic ER protrusions could underlie its selectivity for T-type  $\text{Ca}^{2+}$ , whereas SERCA pumps may be lacking or somewhat remote in compartments expressing HVA  $\text{Ca}^{2+}$  channels (Budde et al., 1998).

## 7 Conclusions and outlook

The past decades have witnessed a major interest in the role of LT bursts in the TC system in relation to the control of arousal states (Bezudnaya et al., 2006; Crunelli et al., 2006), and to rhythmogenesis (Contreras, 2006; Llinás et al., 2005). In contrast, their potential intracellular consequences on cellular functions remained poorly understood. Our work addresses the latter issue by revealing that  $\text{Ca}_v3$  channels generate large  $[\text{Ca}^{2+}]_i$  transients that, strategically placed with their signalling targets, are importantly implicated in oscillatory dynamics.

Beyond the biophysical and network implications, we hope that the results presented here also initiate further work on  $\text{Ca}^{2+}$  signalling in relation to TC activities during sleep. In this context, we point to the selective sequestration of  $\text{Ca}^{2+}$  entering through  $\text{I}_T$ , in particular since luminal  $\text{Ca}^{2+}$  levels regulate major ER functions in cell physiology, including gene transcription and protein synthesis. This makes it conceivable that the T-type  $\text{Ca}^{2+}$ , once introduced in the ER, may adopt yet additional signalling functions pertinent to physiological processes controlled by sleep. Furthermore,  $\text{Ca}_v3$  channels are implicated in pathological rhythms, such as those found during generalized epilepsies and neurodegenerative disorders (Contreras, 2006; Shin et al., 2006). Abnormal  $\text{Ca}^{2+}$  load in the ER, and perturbed  $\text{Ca}^{2+}$  homeostasis (Berridge et al., 2003), may very well be one of the core manifestations in the cells afflicted.

This thesis represents an interdisciplinary study, combining sleep-wake behaviour monitoring, EEG measurements, electrophysiological recordings,  $\text{Ca}^{2+}$  imaging, immunoelectron microscopy and computational modelling to elaborate a detailed picture of  $\text{Ca}^{2+}$  signalling through low-voltage activated  $\text{Ca}^{2+}$  channels in nRt neurons and its physiological relevance. The work provides evidences of several novelties in the signalling role of T-type  $\text{Ca}^{2+}$ . First, in nRt neurons  $\text{Ca}_v3$  channels are selectively coupled to SK channels and form an expeditious functional complex. Second, the identification and quantification of T-type- $\text{Ca}^{2+}$  in nRt neurons revealed a massive, quick influx and dominance of T-type- $\text{Ca}^{2+}$  in  $\text{Ca}^{2+}$  signalling in nRt dendrites. Third, the selective coupling of  $\text{Ca}_v3$  channels to SK2 subunit-containing SK channels underlies the AHP, typical for rhythmic intrinsic burst discharges in nRt neurons. Fourth, endoplasmic  $\text{Ca}^{2+}$  sequestration modulates oscillatory discharges in the



nRt via a competitive interaction of SERCA pumps with SK2 channels for T-type  $\text{Ca}^{2+}$  in a functionally significant manner. Fifth, transgenic mice lacking the SK2 channel encoding gene, exhibit a disruption of nRt oscillations and a marked decrease in EEG frequency bands typical for NREMS. Last, the lack of SK2 channels causes destabilized sleep in mice, as they wake more often from sleep.

My work opens novel perspectives on several levels of investigations in relating ion channels,  $[\text{Ca}^{2+}]_i$  dynamics, cellular oscillations to the *in vivo* hallmarks of sleep. Here, I would like to give a brief outline of these perspectives, structured clearly from the molecular to the cellular to the systems level.

## 7.1 Gating of SK2 channels by $\text{Ca}^{2+}$ in nRt

Neurons of the nRt participate in diverse forms of oscillations that are guided by both intrinsic and synaptic mechanisms (McCormick and Bal, 1997). So far, we concentrated on the simplest form of an nRt oscillation, one generated exclusively via intrinsic ion channels. However, during natural oscillations, such as sleep spindle waves, both intrinsic (e.g.  $\text{Ca}_v3$  channels) and synaptic (e.g. NMDAR)  $\text{Ca}^{2+}$  sources will control SK2 channel gating. Indeed, it has been shown recently that SK2 channels are under the control of  $\text{Ca}^{2+}$  entry through NMDARs in the hippocampus (Ngo-Anh et al., 2005). Understanding these will be necessary to fully appreciate the dramatic consequences of SK2-KO on cellular oscillations.

*Question 1:* Which  $\text{Ca}_v3$  channels are involved in regulating SK2 channels?

Two  $\text{Ca}_v3$  channel subtypes could be involved in mediating nRt bursts:  $\text{Ca}_v3.2$  and  $\text{Ca}_v3.3$  (Talley et al., 1999). To date, it is not been addressed, which of these contribute to dendritic  $\text{Ca}^{2+}$  signals. I would like to exploit the differential  $\text{Ni}^{2+}$  sensitivity (Yunker, 2003), the differential redox sensitivity (Todorovic et al., 2001) and the differential neurotransmitter sensitivity (e.g. muscarine (Hildebrand et al., 2007)) of  $\text{Ca}_v3.2$  and  $\text{Ca}_v3.3$  to find out which  $\text{Ca}^{2+}$  channel is responsible for SK2 channel gating. I would also like to use the  $\text{Ca}_v3.2$  KO animals that are now available (Joksovic et al., 2006). We have been speculating in the paper that it could be  $\text{Ca}_v3.3$  that is responsible. Demonstrating this would be the first proof for an important role of  $\text{Ca}_v3.3$  as a  $\text{Ca}^{2+}$  source in the CNS.

*Question 2:* What is the role of HVA channels in gating SK2 channels?

We found that SK2 is mostly expressed in dendrites, yet HVA channels generate almost no  $\text{Ca}^{2+}$  signal in the dendrites. Nevertheless HVA channels and SK2 channels are coupled. How is this possible? One possibility could be that the few SK2 channels expressed on the soma are tightly co-localized with HVA channels. This question could be addressed by testing the effects of slow and fast  $\text{Ca}^{2+}$  buffers on  $\text{Ca}_v3$ -/SK2- and HVA/SK2 channel coupling. Moreover, we will also need to carry out imaging experiments in the soma of nRt cells.

*Question 3:* Do NMDARs gate SK2 channels in the nRt?

Neurons of the nRt are typically triggered to burst by excitatory synaptic input (e.g. during spindle waves). N-methyl-D-aspartate receptors may activate SK2 channels (Ngo-Anh et al., 2005). Moreover, SK2 channels are expressed perisynaptically in nRt (our results). Therefore, I would predict that NMDARs activate SK2 channels. I would like to use NMDAR subtype pharmacology to test which NMDAR contribute (both synaptic and extrasynaptic). This is interesting because nRt seems to express the more “juvenile” NMDAR isoforms NR2C and D (Jones et al., 1998), which are more  $\text{Ca}^{2+}$ -permeable. What is their functional role?

*Question 4:* What is the nature of the competition for T-type  $\text{Ca}^{2+}$ ?

In our paper, we show that SERCA pumps compete with SK2 channel for available  $\text{Ca}^{2+}$ . I would like to better understand this competition. Is it dependent upon cellular metabolic status? Is it dependent upon the “filling” status of the ER, i.e. upon intraluminal  $\text{Ca}^{2+}$  levels? We have done some experiments showing that, if we give repeated depolarizing voltage commands to elicit  $\text{Ca}^{2+}$  entry through HVA channels, we strengthen  $\text{Ca}_v3$ -/SK channel interaction.

## **7.2 Modulation of SK2 channel function in nRt**

We have identified in our paper a tripartite functional complex between  $\text{Ca}_v3$  channels, SK2 channels and SERCA pumps. It is known from the heart that SERCA pumps are

important for removing  $\text{Ca}^{2+}$  entering during the systole and for accelerating cardiac recovery. SERCA pump activity is tightly regulated in the heart (Misquitta et al., 1999), but almost nothing is known about SERCA pump regulation in neurons. Sarco-Endoplasmic Reticulum  $\text{Ca}^{2+}$  ATPase pump regulation could possibly play a role in setting the strength of nRt oscillations.

*Question 1:* Does other neurotransmitter receptor activity modulate the  $\text{Ca}_v3$ -SK channel coupling?

There are a number of candidate neurotransmitter receptors that I would like to test for their effects on  $\text{Ca}_v3$ -SK channel coupling. For example, nRt cells express beta2-adrenergic receptors (Rainbow et al., 1984), known to act via PKA in highly compartmentalized cAMP signalling domains. Do these modulate  $\text{Ca}_v3$ -SK channel coupling?

*Question 2:* Do nRt neurons show plasticity in SK2 channel expression?

This idea is inspired by our observation of strong cytoplasmic labelling for SK2 immunoparticles in nRt dendrites, which could be a mechanism to modulate the strength of nRt pacemaking during different arousal states. I am currently thinking about using corticothalamic afferent stimulation to elicit strong NMDAR activation in nRt cells and then monitor SK2 channel function. It is well established that nRt cells are heavily innervated by cortical afferents (Pinault, 2004), but whether they induce plastic changes in ion channels involved in rhythmogenesis is not known.

### **7.3 Consequences of SK2-lack on nRt function**

In my work, we have focused on intrinsic discharge properties of nRt neurons in the absence of SK2. It appears that the lack of SK2 does not grossly alter ionic cellular properties, but prevents cellular oscillations and puts the neurons into some kind of depolarization-block after a single burst generation. It is to be expected that this lack of oscillations and the depolarization-block will alter the dendritic functions of nRt neurons, the  $\text{Ca}^{2+}$  signals they experience, as well as their interaction in the thalamic network. It would be interesting to carry out a more detailed analysis of nRt characteristics in the SK2 KO.

*Question 1:* What do  $\text{Ca}^{2+}$  signals in nRt dendrites of SK2 KO mice look like?

Conducting the same  $\text{Ca}^{2+}$  imaging experiments as we have done in WT mice, I would predict that the  $\text{Ca}^{2+}$  signals would be greatly prolonged and strengthened in amplitude.

*Question 2:* What do  $\text{Ca}^{2+}$  signals in the oscillatory network of WT and SK2 KO mice look like?

Today methods to image  $\text{Ca}^{2+}$  signals in large neuronal populations exist, e.g. by using acetoxymethyl ester dyes (Takahashi et al., 2007). I would like to image nRt population activity in WT and in SK2 KO nRt and see how it propagates in the network.

*Question 3:* What is the function of SK2 in generalized epilepsies?

Numerous studies document an important role of nRt in generalized epilepsies (abnormally strong burst firing, abnormal expression of  $I_T$ ) (for review see e.g. (Steriade, 2005)). To my knowledge, nobody has tested the function of SK2 in rodent models of absence epilepsy (GAERS, Stargazer, lethargic).

*Question 4:* Are there compensatory effects due to the lack of SK2 channels?

Potential compensatory effects due to the lack of SK2 channels could be investigated in more detail. Are the expression levels of SK1 or SK3, or other hyperpolarizing conductances, like HCN channels, altered?

## **7.4 SK2 channel function in sleep**

SK2 channels strongly influence sleep homeostasis. In our work, we found that the lack of SK2 abolishes the sleep rebound typical after sleep deprivation, whose hallmark is an increase in low-frequency components of slow-wave sleep. To my knowledge, this is the first ion channel implicated in sleep homeostasis and it could, therefore, help to assess the mechanisms underlying sleep homeostasis.

*Question 1:* Does sleep deprivation affect SK2 function in a measurable manner?

The idea would be to carry out our sleep deprivation procedure (Kopp et al., 2006) and combine it then with electrophysiological experiments on SK2 and with measurements of nRt cell oscillations .

*Question 2:* What are the genetic/transcriptional mechanisms of sleep homeostasis?

We mentioned in the paper that it could be interesting to test the involvement of SK2 in well-described mouse models with perturbed sleep homeostasis (e.g. NPAS2 KO) (Dudley et al., 2003). I would be interested in beginning to generate links between the genetic/transcriptional mechanisms involved in sleep homeostasis and their consequences on ion channels implicated in rhythmogenesis, such as SK2.

*Question 3:* Is the decrease in EEG frequency bands typical for NREMS in SK2 KO mice a consequence of the disruption of nRt oscillations *in vitro*?

Although, *in vivo*, burst discharges in nRt are most prominent during NREMS related oscillations, the disruption of nRt oscillations *in vitro* and the decrease in EEG frequency bands typical for NREMS in SK2 KO mice could be a coincidence rather than a consequence. Therefore, in order to link these two observations, conditional nRt SK2 KO mice and/or *in vivo* intracellular recordings of nRt neurons in SK2 KO mice could be conductive.

*Question 4:* What is the effect of SK channel modulators on the generation of sleep related oscillations and NREM EEG?

*In vivo*, intraperitoneal and subcutaneous injections of 1-EBIO, a SK channel modulator that increases the  $\text{Ca}^{2+}$  affinity, results in an increased seizure threshold and reduces seizure incidence in seizure models (Anderson et al., 2006). Moreover, bath application of 1-EBIO during patch clamp recordings of nRt neurons, leads to 222 % increase of  $\text{Ca}_v3$ -mediated SK current. It would therefore be interesting to investigate the effect of an *in vivo* intrathalamic injection of 1-EBIO on the generation of sleep related oscillations and NREM EEG (Walter et al., 2006). To further investigate the role of SK channels in the generation of sleep related

oscillations and its role in sleep physiology, experiments, similar to those performed during my thesis would be interesting to do using mice overexpressing SK2 (Hammond et al., 2006).

## 8 References

- Aiba, A., Kano, M., Chen, C., Stanton, M.E., Fox, G.D., Herrup, K., Zwingman, T.A., and Tonegawa, S. (1994). Deficient cerebellar long-term depression and impaired motor learning in mGluR1 mutant mice. *Cell* 79, 377-388.
- Akiba, S., and Sato, T. (2004). Cellular function of calcium-independent phospholipase A2. *Biol Pharm Bull* 27, 1174-1178.
- Anderson, M.P., Mochizuki, T., Xie, J., Fischler, W., Manger, J.P., Talley, E.M., Scammell, T.E., and Tonegawa, S. (2005). Thalamic Ca<sub>v</sub>3.1 T-type Ca<sup>2+</sup> channel plays a crucial role in stabilizing sleep. *Proc Natl Acad Sci U S A* 102, 1743-1748.
- Anderson, N.J., Slough, S., and Watson, W.P. (2006). In vivo characterisation of the small-conductance KCa (SK) channel activator 1-ethyl-2-benzimidazolinone (1-EBIO) as a potential anticonvulsant. *Eur J Pharmacol* 546, 48-53.
- Augustine, G.J., Santamaria, F., and Tanaka, K. (2003). Local calcium signaling in neurons. *Neuron* 40, 331-346.
- Avanzini, G., de Curtis, M., Panzica, F., and Spreafico, R. (1989). Intrinsic properties of nucleus reticularis thalami neurones of the rat studied *in vitro*. *J Physiol* 416, 111-122.
- Bal, T., and McCormick, D.A. (1993). Mechanisms of oscillatory activity in guinea-pig nucleus reticularis thalami *in vitro*: a mammalian pacemaker. *J Physiol* 468, 669-691.
- Bal, T., and McCormick, D.A. (1996). What stops synchronized thalamocortical oscillations? *Neuron* 17, 297-308.
- Bean, B.P. (2007). The action potential in mammalian central neurons. *Nat Rev Neurosci* 8, 451-465.
- Benington, J.H., Woudenberg, M.C., and Heller, H.C. (1995). Apamin, a selective SK potassium channel blocker, suppresses REM sleep without a compensatory rebound. *Brain Res* 692, 86-92.
- Berkefeld, H., Sailer, C.A., Bildl, W., Rohde, V., Thumfart, J.O., Eble, S., Klugbauer, N., Reisinger, E., Bischofberger, J., Oliver, D., *et al.* (2006). BK<sub>Ca</sub>-Cav channel complexes mediate rapid and localized Ca<sup>2+</sup>-activated K<sup>+</sup> signaling. *Science* 314, 615-620.
- Berridge, M.J. (1997). Elementary and global aspects of calcium signalling. *J Physiol* 499 ( Pt 2), 291-306.
- Berridge, M.J. (2002). The endoplasmic reticulum: a multifunctional signaling organelle. *Cell Calcium* 32, 235-249.
- Berridge, M.J. (2003). Cardiac calcium signalling. *Biochem Soc Trans* 31, 930-933.
- Berridge, M.J., Bootman, M.D., and Roderick, H.L. (2003). Calcium signalling: dynamics, homeostasis and remodelling. *Nat Rev Mol Cell Biol* 4, 517-529.
- Berridge, M.J., Lipp, P., and Bootman, M.D. (2000). The versatility and universality of calcium signalling. *Nat Rev Mol Cell Biol* 1, 11-21.
- Beurrier, C., Congar, P., Bioulac, B., and Hammond, C. (1999). Subthalamic nucleus neurons switch from single-spike activity to burst-firing mode. *J Neurosci* 19, 599-609.
- Bezdudnaya, T., Cano, M., Bereshpolova, Y., Stoelzel, C.R., Alonso, J.M., and Swadlow, H.A. (2006). Thalamic burst mode and inattention in the awake LGNd. *Neuron* 49, 421-432.
- Blaustein, M.P., and Lederer, W.J. (1999). Sodium/calcium exchange: its physiological implications. *Physiol Rev* 79, 763-854.

- Blethyn, K.L., Hughes, S.W., Tóth, T.I., Cope, D.W., and Crunelli, V. (2006). Neuronal basis of the slow (<1 Hz) oscillation in neurons of the nucleus reticularis thalami *in vitro*. *J Neurosci* 26, 2474-2486.
- Bond, C.T., Herson, P.S., Strassmaier, T., Hammond, R., Stackman, R., Maylie, J., and Adelman, J.P. (2004). Small conductance Ca<sup>2+</sup>-activated K<sup>+</sup> channel knock-out mice reveal the identity of calcium-dependent afterhyperpolarization currents. *J Neurosci* 24, 5301-5306.
- Bond, C.T., Maylie, J., and Adelman, J.P. (2005). SK channels in excitability, pacemaking and synaptic integration. *Curr Opin Neurobiol* 15, 305-311.
- Budde, T., Meuth, S., and Pape, H.C. (2002). Calcium-dependent inactivation of neuronal calcium channels. *Nat Rev Neurosci* 3, 873-883.
- Budde, T., Munsch, T., and Pape, H.C. (1998). Distribution of L-type calcium channels in rat thalamic neurones. *Eur J Neurosci* 10, 586-597.
- Buzsáki, G., and Gage, F.H. (1989). The cholinergic nucleus basalis: a key structure in neocortical arousal. *Exs* 57, 159-171.
- Cai, X., Liang, C.W., Muralidharan, S., Kao, J.P., Tang, C.M., and Thompson, S.M. (2004). Unique roles of SK and Kv4.2 potassium channels in dendritic integration. *Neuron* 44, 351-364.
- Carlisle, H.J., and Kennedy, M.B. (2005). Spine architecture and synaptic plasticity. *Trends Neurosci* 28, 182-187.
- Catterall, W.A. (2000). Structure and regulation of voltage-gated Ca<sup>2+</sup> channels. *Annu Rev Cell Dev Biol* 16, 521-555.
- Catterall, W.A., Perez-Reyes, E., Snutch, T.P., and Striessnig, J. (2005). International Union of Pharmacology. XLVIII. Nomenclature and structure-function relationships of voltage-gated calcium channels. *Pharmacol Rev* 57, 411-425.
- Cavelier, P., Pouille, F., Desplantez, T., Beekenkamp, H., and Bossu, J.-L. (2002). Control of the propagation of dendritic low-threshold Ca<sup>2+</sup> spikes in Purkinje cells from rat cerebellar slice cultures. *J Physiol* 540, 57-72.
- Chevalier, M., Lory, P., Mironneau, C., Macrez, N., and Quignard, J.F. (2006). T-type Ca<sub>v</sub>3.3 calcium channels produce spontaneous low-threshold action potentials and intracellular calcium oscillations. *Eur J Neurosci* 23, 2321-2329.
- Clapham, D.E. (2003). TRP channels as cellular sensors. *Nature* 426, 517-524.
- Clayton, D.A., Mesches, M.H., Alvarez, E., Bickford, P.C., and Browning, M.D. (2002). A hippocampal NR2B deficit can mimic age-related changes in long-term potentiation and spatial learning in the Fischer 344 rat. *J Neurosci* 22, 3628-3637.
- Contreras, D. (2006). The role of T-channels in the generation of thalamocortical rhythms. *CNS Neurol Disord Drug Targets* 5, 571-585.
- Cordoba-Rodriguez, R., Moore, K.A., Kao, J.P., and Weinreich, D. (1999). Calcium regulation of a slow post-spike hyperpolarization in vagal afferent neurons. *Proc Natl Acad Sci U S A* 96, 7650-7657.
- Cotillon, N., and Edeline, J.M. (2000). Tone-evoked oscillations in the rat auditory cortex result from interactions between the thalamus and reticular nucleus. *Eur J Neurosci* 12, 3637-3650.
- Craven, K.B., and Zagotta, W.N. (2006). CNG and HCN channels: two peas, one pod. *Annu Rev Physiol* 68, 375-401.
- Crunelli, V., Cope, D.W., and Hughes, S.W. (2006). Thalamic T-type Ca<sup>2+</sup> channels and NREM sleep. *Cell Calcium* 40, 175-190.
- Cui, G., Okamoto, T., and Morikawa, H. (2004). Spontaneous opening of T-type Ca<sup>2+</sup> channels contributes to the irregular firing of dopamine neurons in neonatal rats. *J Neurosci* 24, 11079-11087.
- Cull-Candy, S., Brickley, S., and Farrant, M. (2001). NMDA receptor subunits: diversity, development and disease. *Curr Opin Neurobiol* 11, 327-335.



- Davies, P.J., Ireland, D.R., and McLachlan, E.M. (1996). Sources of  $\text{Ca}^{2+}$  for different  $\text{Ca}^{2+}$ -activated  $\text{K}^+$  conductances in neurones of the rat superior cervical ganglion. *J Physiol* 495 ( Pt 2), 353-366.
- Derkach, V.A., Oh, M.C., Guire, E.S., and Soderling, T.R. (2007). Regulatory mechanisms of AMPA receptors in synaptic plasticity. *Nat Rev Neurosci* 8, 101-113.
- Destexhe, A., Contreras, D., Steriade, M., Sejnowski, T.J., and Huguenard, J.R. (1996). *In vivo*, *in vitro*, and computational analysis of dendritic calcium currents in thalamic reticular neurons. *J Neurosci* 16, 169-185.
- Dingledine, R., Borges, K., Bowie, D., and Traynelis, S.F. (1999). The glutamate receptor ion channels. *Pharmacol Rev* 51, 7-61.
- Doherty, P., and Walsh, F.S. (1991). The contrasting roles of N-CAM and N-cadherin as neurite outgrowth-promoting molecules. *J Cell Sci Suppl* 15, 13-21.
- Dolphin, A.C. (2003). G protein modulation of voltage-gated calcium channels. *Pharmacol Rev* 55, 607-627.
- Duchen, M.R. (2000a). Mitochondria and  $\text{Ca}^{2+}$  in cell physiology and pathophysiology. *Cell Calcium* 28, 339-348.
- Duchen, M.R. (2000b). Mitochondria and calcium: from cell signalling to cell death. *J Physiol* 529 Pt 1, 57-68.
- Dudley, C.A., Erbel-Sieler, C., Estill, S.J., Reick, M., Franken, P., Pitts, S., and McKnight, S.L. (2003). Altered patterns of sleep and behavioral adaptability in NPAS2-deficient mice. *Science* 301, 379-383.
- Emptage, N.J., Reid, C.A., and Fine, A. (2001). Calcium stores in hippocampal synaptic boutons mediate short-term plasticity, store-operated  $\text{Ca}^{2+}$  entry, and spontaneous transmitter release. *Neuron* 29, 197-208.
- Favre, C.J., Schrenzel, J., Jacquet, J., Lew, D.P., and Krause, K.H. (1996). Highly supralinear feedback inhibition of  $\text{Ca}^{2+}$  uptake by the  $\text{Ca}^{2+}$  load of intracellular stores. *J Biol Chem* 271, 14925-14930.
- Fierro, L., DiPolo, R., and Llanò, I. (1998). Intracellular calcium clearance in Purkinje cell somata from rat cerebellar slices. *J Physiol* 510 ( Pt 2), 499-512.
- Fill, M., and Copello, J.A. (2002). Ryanodine receptor calcium release channels. *Physiol Rev* 82, 893-922.
- Finkbeiner, S., and Greenberg, M.E. (1998).  $\text{Ca}^{2+}$  channel-regulated neuronal gene expression. *J Neurobiol* 37, 171-189.
- Foskett, J.K., White, C., Cheung, K.H., and Mak, D.O. (2007). Inositol trisphosphate receptor  $\text{Ca}^{2+}$  release channels. *Physiol Rev* 87, 593-658.
- Frazier, C.J., Serrano, J.R., George, E.G., Yu, X., Viswanathan, A., Perez-Reyes, E., and Jones, S.W. (2001). Gating kinetics of the  $\alpha 1\text{I}$  T-type calcium channel. *J Gen Physiol* 118, 457-470.
- Frère, S.G., Kuisle, M., and Lüthi, A. (2004). Regulation of recombinant and native hyperpolarization-activated cation channels. *Mol Neurobiol* 30, 279-305.
- Freund, T.F., and Buzsáki, G. (1996). Interneurons of the hippocampus. *Hippocampus* 6, 347-470.
- Fucile, S. (2004).  $\text{Ca}^{2+}$  permeability of nicotinic acetylcholine receptors. *Cell Calcium* 35, 1-8.
- Gandolfo, G., Schweitz, H., Lazdunski, M., and Gottesmann, C. (1996). Sleep cycle disturbances induced by apamin, a selective blocker of  $\text{Ca}^{2+}$ -activated  $\text{K}^+$  channels. *Brain Res* 736, 344-347.
- Garaschuk, O., Yaari, Y., and Konnerth, A. (1997). Release and sequestration of calcium by ryanodine-sensitive stores in rat hippocampal neurones. *J Physiol* 502 ( Pt 1), 13-30.
- Garcia, M.L., and Strehler, E.E. (1999). Plasma membrane calcium ATPases as critical regulators of calcium homeostasis during neuronal cell function. *Front Biosci* 4, D869-882.

- Goldberg, J.A., and Wilson, C.J. (2005). Control of spontaneous firing patterns by the selective coupling of calcium currents to calcium-activated potassium currents in striatal cholinergic interneurons. *J Neurosci* 25, 10230-10238.
- Guerini, D., Coletto, L., and Carafoli, E. (2005). Exporting calcium from cells. *Cell Calcium* 38, 281-289.
- Gunter, T.E., Buntinas, L., Sparagna, G., Eliseev, R., and Gunter, K. (2000). Mitochondrial calcium transport: mechanisms and functions. *Cell Calcium* 28, 285-296.
- Hammond, R.S., Bond, C.T., Strassmaier, T., Ngo-Anh, T.J., Adelman, J.P., Maylie, J., and Stackman, R.W. (2006). Small-conductance  $Ca^{2+}$ -activated  $K^{+}$  channel type 2 (SK2) modulates hippocampal learning, memory, and synaptic plasticity. *J Neurosci* 26, 1844-1853.
- Hefft, S., and Jonas, P. (2005). Asynchronous GABA release generates long-lasting inhibition at a hippocampal interneuron-principal neuron synapse. *Nat Neurosci* 8, 1319-1328.
- Heizmann, C.W., and Hunziker, W. (1991). Intracellular calcium-binding proteins: more sites than insights. *Trends Biochem Sci* 16, 98-103.
- Hildebrand, M.E., David, L.S., Hamid, J., Mulatz, K., Garcia, E., Zamponi, G.W., and Snutch, T.P. (2007). Selective inhibition of Cav3.3 T-type calcium channels by Galphaq/11-coupled muscarinic acetylcholine receptors. *J Biol Chem* 282, 21043-21055.
- Hille, B. (1992). Ioni channels of excitable membranes, 2nd edn (Sunderland, Massachusetts: Sinauer Associates Inc).
- Hirsch, J.C., Fourment, A., and Marc, M.E. (1983). Sleep-related variations of membrane potential in the lateral geniculate body relay neurons of the cat. *Brain Res* 259, 308-312.
- Hong, K., Nishiyama, M., Henley, J., Tessier-Lavigne, M., and Poo, M. (2000). Calcium signalling in the guidance of nerve growth by netrin-1. *Nature* 403, 93-98.
- Huguenard, J.R. (1998). Anatomical and physiological considerations in thalamic rhythm generation. *J Sleep Res* 7 *Suppl 1*, 24-29.
- Huguenard, J.R., and Prince, D.A. (1992). A novel T-type current underlies prolonged  $Ca^{2+}$ -dependent burst firing in GABAergic neurons of rat thalamic reticular nucleus. *J Neurosci* 12, 3804-3817.
- Huntsman, M.M., Porcello, D.M., Homanics, G.E., DeLoey, T.M., and Huguenard, J.R. (1999). Reciprocal inhibitory connections and network synchrony in the mammalian thalamus. *Science* 283, 541-543.
- Ichise, T., Kano, M., Hashimoto, K., Yanagihara, D., Nakao, K., Shigemoto, R., Katsuki, M., and Aiba, A. (2000). mGluR1 in cerebellar Purkinje cells essential for long-term depression, synapse elimination, and motor coordination. *Science* 288, 1832-1835.
- Inoue, T., Kato, K., Kohda, K., and Mikoshiba, K. (1998). Type 1 inositol 1,4,5-trisphosphate receptor is required for induction of long-term depression in cerebellar Purkinje neurons. *J Neurosci* 18, 5366-5373.
- Jahnsen, H., and Llinás, R. (1984). Electrophysiological properties of guinea-pig thalamic neurones: an in vitro study. *J Physiol* 349, 205-226.
- Jaiswal, J.K. (2001). Calcium - how and why? *J Biosci* 26, 357-363.
- Jensen, T.P., Filoteo, A.G., Knopfel, T., and Empson, R.M. (2007). Presynaptic plasma membrane  $Ca^{2+}$  ATPase isoform 2a regulates excitatory synaptic transmission in rat hippocampal CA3. *J Physiol* 579, 85-99.
- Jin, Y., Kim, S.J., Kim, J., Worley, P.F., and Linden, D.J. (2007). Long-term depression of mGluR1 signaling. *Neuron* 55, 277-287.
- Joksovic, P.M., Bayliss, D.A., and Todorovic, S.M. (2005). Different kinetic properties of two T-type  $Ca^{2+}$  currents of rat reticular thalamic neurones and their modulation by enflurane. *J Physiol* 566, 125-142.
- Joksovic, P.M., Nelson, M.T., Jevtovic-Todorovic, V., Patel, M.K., Perez-Reyes, E., Campbell, K.P., Chen, C.C., and Todorovic, S.M. (2006).  $Ca_v3.2$  is the major molecular

- substrate for redox regulation of T-type  $\text{Ca}^{2+}$  channels in the rat and mouse thalamus. *J Physiol* 574, 415-430.
- Jones, E.G., Tighilet, B., Tran, B.V., and Huntsman, M.M. (1998). Nucleus- and cell-specific expression of NMDA and non-NMDA receptor subunits in monkey thalamus. *J Comp Neurol* 397, 371-393.
- Kaupp, U.B., and Seifert, R. (2002). Cyclic nucleotide-gated ion channels. *Physiol Rev* 82, 769-824.
- Khodakhah, K., and Armstrong, C.M. (1997). Induction of long-term depression and rebound potentiation by inositol trisphosphate in cerebellar Purkinje neurons. *Proc Natl Acad Sci U S A* 94, 14009-14014.
- Kim, D., Song, I., Keum, S., Lee, T., Jeong, M.J., Kim, S.S., McEnery, M.W., and Shin, H.S. (2001). Lack of the burst firing of thalamocortical relay neurons and resistance to absence seizures in mice lacking  $\alpha 1\text{G}$  T-type  $\text{Ca}^{2+}$  channels. *Neuron* 31, 35-45.
- Kim, U., and McCormick, D.A. (1998). Functional and ionic properties of a slow afterhyperpolarization in ferret perigeniculate neurons in vitro. *J Neurophysiol* 80, 1222-1235.
- Kopp, C., Longordo, F., and Lüthi, A. (2007). Experience-dependent changes in NMDA receptor composition at mature central synapses. *Neuropharm.*
- Kopp, C., Longordo, F., Nicholson, J.R., and Lüthi, A. (2006). Insufficient sleep reversibly alters bidirectional synaptic plasticity and NMDA receptor function. *J Neurosci* 26, 12456-12465.
- Krause, M., Hoffmann, W.E., and Hajos, M. (2003). Auditory sensory gating in hippocampus and reticular thalamic neurons in anesthetized rats. *Biol Psychiatry* 53, 244-253.
- Landisman, C.E., Long, M.A., Beierlein, M., Deans, M.R., Paul, D.L., and Connors, B.W. (2002). Electrical synapses in the thalamic reticular nucleus. *J Neurosci* 22, 1002-1009.
- Larkum, M.E., Watanabe, S., Nakamura, T., Lasser-Ross, N., and Ross, W.N. (2003). Synaptically activated  $\text{Ca}^{2+}$  waves in layer 2/3 and layer 5 rat neocortical pyramidal neurons. *J Physiol* 549, 471-488.
- Lee, J., Kim, D., and Shin, H.S. (2004). Lack of delta waves and sleep disturbances during non-rapid eye movement sleep in mice lacking  $\alpha 1\text{G}$ -subunit of T-type calcium channels. *Proc Natl Acad Sci U S A* 101, 18195-18199.
- Li, Y., Jia, Y.C., Cui, K., Li, N., Zheng, Z.Y., Wang, Y.Z., and Yuan, X.B. (2005). Essential role of TRPC channels in the guidance of nerve growth cones by brain-derived neurotrophic factor. *Nature* 434, 894-898.
- Lipscombe, D., Helton, T.D., and Xu, W. (2004). L-type calcium channels: the low down. *J Neurophysiol* 92, 2633-2641.
- Liu, S.J., and Zukin, R.S. (2007).  $\text{Ca}^{2+}$ -permeable AMPA receptors in synaptic plasticity and neuronal death. *Trends Neurosci* 30, 126-134.
- Liu, Z., Vergnes, M., Depaulis, A., and Marescaux, C. (1992). Involvement of intrathalamic  $\text{GABA}_B$  neurotransmission in the control of absence seizures in the rat. *Neuroscience* 48, 87-93.
- Llinás, R., and Jahnsen, H. (1982). Electrophysiology of mammalian thalamic neurones in vitro. *Nature* 297, 406-408.
- Llinás, R., Urbano, F.J., Leznik, E., Ramirez, R.R., and van Marle, H.J. (2005). Rhythmic and dysrhythmic thalamocortical dynamics: GABA systems and the edge effect. *Trends Neurosci* 28, 325-333.
- Lüthi, A., and McCormick, D.A. (1998). Periodicity of thalamic synchronized oscillations: the role of  $\text{Ca}^{2+}$ -mediated upregulation of  $I_h$ . *Neuron* 20, 553-563.
- Magnusson, K.R., Nelson, S.E., and Young, A.B. (2002). Age-related changes in the protein expression of subunits of the NMDA receptor. *Brain Res Mol Brain Res* 99, 40-45.

- Majewska, A., Brown, E., Ross, J., and Yuste, R. (2000). Mechanisms of calcium decay kinetics in hippocampal spines: role of spine calcium pumps and calcium diffusion through the spine neck in biochemical compartmentalization. *J Neurosci* 20, 1722-1734.
- Malenka, R.C., and Bear, M.F. (2004). LTP and LTD: an embarrassment of riches. *Neuron* 44, 5-21.
- Markram, H., Helm, P.J., and Sakmann, B. (1995). Dendritic calcium transients evoked by single back-propagating action potentials in rat neocortical pyramidal neurons. *J Physiol* 485 (Pt 1), 1-20.
- Marrion, N.V., and Tavalin, S.J. (1998). Selective activation of Ca<sup>2+</sup>-activated K<sup>+</sup> channels by co-localized Ca<sup>2+</sup> channels in hippocampal neurons. *Nature* 395, 900-905.
- Matulef, K., and Zagotta, W.N. (2003). Cyclic nucleotide-gated ion channels. *Annu Rev Cell Dev Biol* 19, 23-44.
- McCarley, R.W., Benoit, O., and Barrionuevo, G. (1983). Lateral geniculate nucleus unitary discharge in sleep and waking: state- and rate-specific aspects. *J Neurophysiol* 50, 798-818.
- McCormick, D.A., and Bal, T. (1997). Sleep and arousal: thalamocortical mechanisms. *Annu Rev Neurosci* 20, 185-215.
- Misquitta, C.M., Mack, D.P., and Grover, A.K. (1999). Sarco/endoplasmic reticulum Ca<sup>2+</sup> (SERCA)-pumps: link to heart beats and calcium waves. *Cell Calcium* 25, 277-290.
- Morikawa, H., Imani, F., Khodakhah, K., and Williams, J.T. (2000). Inositol 1,4,5-triphosphate-evoked responses in midbrain dopamine neurons. *J Neurosci* 20, RC103.
- Mulle, C., Madariaga, A., and Deschênes, M. (1986). Morphology and electrophysiological properties of reticularis thalami neurons in cat: *in vivo* study of a thalamic pacemaker. *J Neurosci* 6, 2134-2145.
- Ngo-Anh, T.J., Bloodgood, B.L., Lin, M., Sabatini, B.L., Maylie, J., and Adelman, J.P. (2005). SK channels and NMDA receptors form a Ca<sup>2+</sup>-mediated feedback loop in dendritic spines. *Nat Neurosci* 8, 642-649.
- Nguyen, H.N., Wang, C., and Perry, D.C. (2002). Depletion of intracellular calcium stores is toxic to SH-SY5Y neuronal cells. *Brain Res* 924, 159-166.
- Pape, H.C., and McCormick, D.A. (1990). Ionic mechanisms of modulatory brain stem influences in the thalamus. *J Basic Clin Physiol Pharmacol* 1, 107-117.
- Pape, H.C., Munsch, T., and Budde, T. (2004). Novel vistas of calcium-mediated signalling in the thalamus. *Pflugers Arch* 448, 131-138.
- Paterson, D., and Nordberg, A. (2000). Neuronal nicotinic receptors in the human brain. *Prog Neurobiol* 61, 75-111.
- Pedarzani, P., Mosbacher, J., Rivard, A., Cingolani, L.A., Oliver, D., Stocker, M., Adelman, J.P., and Fakler, B. (2001). Control of electrical activity in central neurons by modulating the gating of small conductance Ca<sup>2+</sup>-activated K<sup>+</sup> channels. *J Biol Chem* 276, 9762-9769.
- Perez-Otano, I., and Ehlers, M.D. (2005). Homeostatic plasticity and NMDA receptor trafficking. *Trends Neurosci* 28, 229-238.
- Perez-Reyes, E. (2003). Molecular physiology of low-voltage-activated T-type calcium channels. *Physiol Rev* 83, 117-161.
- Petersen, O.H., Michalak, M., and Verkhratsky, A. (2005). Calcium signalling: past, present and future. *Cell Calcium* 38, 161-169.
- Pinault, D. (2004). The thalamic reticular nucleus: structure, function and concept. *Brain Res Brain Res Rev* 46, 1-31.
- Poncer, J.C., McKinney, R.A., Gahwiler, B.H., and Thompson, S.M. (1997). Either N- or P-type calcium channels mediate GABA release at distinct hippocampal inhibitory synapses. *Neuron* 18, 463-472.
- Power, J.M., and Sah, P. (2005). Intracellular calcium store filling by an L-type calcium current in the basolateral amygdala at subthreshold membrane potentials. *J Physiol* 562, 439-453.

- Pozzan, T., Rizzuto, R., Volpe, P., and Meldolesi, J. (1994). Molecular and cellular physiology of intracellular calcium stores. *Physiol Rev* 74, 595-636.
- Pozzo-Miller, L.D., Connor, J.A., and Andrews, S.B. (2000). Microheterogeneity of calcium signalling in dendrites. *J Physiol* 525 Pt 1, 53-61.
- Prasad, V., Okunade, G.W., Miller, M.L., and Shull, G.E. (2004). Phenotypes of SERCA and PMCA knockout mice. *Biochem Biophys Res Commun* 322, 1192-1203.
- Rainbow, T.C., Parsons, B., and Wolfe, B.B. (1984). Quantitative autoradiography of beta 1- and beta 2-adrenergic receptors in rat brain. *Proc Natl Acad Sci U S A* 81, 1585-1589.
- Ramsey, I.S., Delling, M., and Clapham, D.E. (2006). An introduction to TRP channels. *Annu Rev Physiol* 68, 619-647.
- Richter, T.A., Kolaj, M., and Renaud, L.P. (2005). Low voltage-activated  $\text{Ca}^{2+}$  channels are coupled to  $\text{Ca}^{2+}$ -induced  $\text{Ca}^{2+}$  release in rat thalamic midline neurons. *J Neurosci* 25, 8267-8271.
- Rizzuto, R. (2001). Intracellular  $\text{Ca}(2+)$  pools in neuronal signalling. *Curr Opin Neurobiol* 11, 306-311.
- Rogers, M., and Dani, J.A. (1995). Comparison of quantitative calcium flux through NMDA, ATP, and ACh receptor channels. *Biophys J* 68, 501-506.
- Sailer, C.A., Kaufmann, W.A., Marksteiner, J., and Knaus, H.G. (2004). Comparative immunohistochemical distribution of three small-conductance  $\text{Ca}^{2+}$ -activated potassium channel subunits, SK1, SK2, and SK3 in mouse brain. *Mol Cell Neurosci* 26, 458-469.
- Schneggenburger, R., and Neher, E. (2000). Intracellular calcium dependence of transmitter release rates at a fast central synapse. *Nature* 406, 889-893.
- Sepulveda, M.R., Hidalgo-Sanchez, M., and Mata, A.M. (2004). Localization of endoplasmic reticulum and plasma membrane  $\text{Ca}^{2+}$ -ATPases in subcellular fractions and sections of pig cerebellum. *Eur J Neurosci* 19, 542-551.
- Seutin, V., Mkahli, F., Massotte, L., and Dresse, A. (2000). Calcium release from internal stores is required for the generation of spontaneous hyperpolarizations in dopaminergic neurons of neonatal rats. *J Neurophysiol* 83, 192-197.
- Shin, H.S., Lee, J., and Song, I. (2006). Genetic studies on the role of T-type  $\text{Ca}^{2+}$  channels in sleep and absence epilepsy. *CNS Neurol Disord Drug Targets* 5, 629-638.
- Shosaku, A., and Sumitomo, I. (1983). Auditory neurons in the rat thalamic reticular nucleus. *Exp Brain Res* 49, 432-442.
- Slaght, S.J., Leresche, N., Deniau, J.M., Crunelli, V., and Charpier, S. (2002). Activity of thalamic reticular neurons during spontaneous genetically determined spike and wave discharges. *J Neurosci* 22, 2323-2334.
- Solovyova, N., Veselovsky, N., Toescu, E.C., and Verkhratsky, A. (2002).  $\text{Ca}(2+)$  dynamics in the lumen of the endoplasmic reticulum in sensory neurons: direct visualization of  $\text{Ca}(2+)$ -induced  $\text{Ca}(2+)$  release triggered by physiological  $\text{Ca}(2+)$  entry. *Embo J* 21, 622-630.
- Squire, L., Bloom, F., McConnell, S., Roberts, J., Spitzer, N., Zigmond, M. (2002). *Fundamental Neuroscience*, 2nd edn (Academic Press).
- Sridhar, T.S., Brown, M.C., and Sewell, W.F. (1997). Unique postsynaptic signaling at the hair cell efferent synapse permits calcium to evoke changes on two time scales. *J Neurosci* 17, 428-437.
- Steriade, M. (2003). The corticothalamic system in sleep. *Front Biosci* 8, d878-899.
- Steriade, M. (2005). Sleep, epilepsy and thalamic reticular inhibitory neurons. *Trends Neurosci* 28, 317-324.
- Stocker, M., Krause, M., and Pedarzani, P. (1999). An apamin-sensitive  $\text{Ca}^{2+}$ -activated  $\text{K}^{+}$  current in hippocampal pyramidal neurons. *Proc Natl Acad Sci U S A* 96, 4662-4667.

- Stocker, M., and Pedarzani, P. (2000). Differential distribution of three Ca<sup>2+</sup>-activated K(+) channel subunits, SK1, SK2, and SK3, in the adult rat central nervous system. *Mol Cell Neurosci* 15, 476-493.
- Strehler, E.E., and Zacharias, D.A. (2001). Role of alternative splicing in generating isoform diversity among plasma membrane calcium pumps. *Physiol Rev* 81, 21-50.
- Swadlow, H.A., Bezdudnaya, T., and Gusev, A.G. (2005). Spike timing and synaptic dynamics at the awake thalamocortical synapse. *Prog Brain Res* 149, 91-105.
- Szentesi, P., Pignier, C., Egger, M., Kranias, E.G., and Niggli, E. (2004). Sarcoplasmic reticulum Ca<sup>2+</sup> refilling controls recovery from Ca<sup>2+</sup>-induced Ca<sup>2+</sup> release refractoriness in heart muscle. *Circ Res* 95, 807-813.
- Takahashi, N., Sasaki, T., Usami, A., Matsuki, N., and Ikegaya, Y. (2007). Watching neuronal circuit dynamics through functional multineuron calcium imaging (fMCI). *Neurosci Res* 58, 219-225.
- Talavera, K., and Nilius, B. (2006). Biophysics and structure-function relationship of T-type Ca<sup>2+</sup> channels. *Cell Calcium* 40, 97-114.
- Talley, E.M., Cribbs, L.L., Lee, J.H., Daud, A., Perez-Reyes, E., and Bayliss, D.A. (1999). Differential distribution of three members of a gene family encoding low voltage-activated (T-type) calcium channels. *J Neurosci* 19, 1895-1911.
- Tang, Y.P., Shimizu, E., Dube, G.R., Rampon, C., Kerchner, G.A., Zhuo, M., Liu, G., and Tsien, J.Z. (1999). Genetic enhancement of learning and memory in mice. *Nature* 401, 63-69.
- Thayer, S.A., Usachev, Y.M., and Pottorf, W.J. (2002). Modulating Ca<sup>2+</sup> clearance from neurons. *Front Biosci* 7, d1255-1279.
- Todorovic, S.M., Jevtovic-Todorovic, V., Meyenburg, A., Mennerick, S., Perez-Reyes, E., Romano, C., Olney, J.W., and Zorumski, C.F. (2001). Redox modulation of T-type calcium channels in rat peripheral nociceptors. *Neuron* 31, 75-85.
- Tsakiridou, E., Bertollini, L., de Curtis, M., Avanzini, G., and Pape, H.C. (1995). Selective increase in T-type calcium conductance of reticular thalamic neurons in a rat model of absence epilepsy. *J Neurosci* 15, 3110-3117.
- Usachev, Y.M., Marsh, A.J., Johanns, T.M., Lemke, M.M., and Thayer, S.A. (2006). Activation of protein kinase C in sensory neurons accelerates Ca<sup>2+</sup> uptake into the endoplasmic reticulum. *J Neurosci* 26, 311-318.
- Verkhatsky, A. (2005). Physiology and pathophysiology of the calcium store in the endoplasmic reticulum of neurons. *Physiol Rev* 85, 201-279.
- Visser, F., and Lytton, J. (2007). K<sup>+</sup>-dependent Na<sup>+</sup>/Ca<sup>2+</sup> exchangers: key contributors to Ca<sup>2+</sup> signaling. *Physiology (Bethesda)* 22, 185-192.
- Walter, J.T., Alvina, K., Womack, M.D., Chevez, C., and Khodakhah, K. (2006). Decreases in the precision of Purkinje cell pacemaking cause cerebellar dysfunction and ataxia. *Nat Neurosci* 9, 389-397.
- Wanaverbecq, N., Marsh, S.J., Al-Qatari, M., and Brown, D.A. (2003). The plasma membrane calcium-ATPase as a major mechanism for intracellular calcium regulation in neurones from the rat superior cervical ganglion. *J Physiol* 550, 83-101.
- Wolfart, J., and Roeper, J. (2002). Selective coupling of T-type calcium channels to SK potassium channels prevents intrinsic bursting in dopaminergic midbrain neurons. *J Neurosci* 22, 3404-3413.
- Wuytack, F., Raeymaekers, L., and Missiaen, L. (2002). Molecular physiology of the SERCA and SPCA pumps. *Cell Calcium* 32, 279-305.
- Xia, X.M., Fakler, B., Rivard, A., Wayman, G., Johnson-Pais, T., Keen, J.E., Ishii, T., Hirschberg, B., Bond, C.T., Lutsenko, S., *et al.* (1998). Mechanism of calcium gating in small-conductance calcium-activated potassium channels. *Nature* 395, 503-507.

- Yoshizaki, K., Hoshino, T., Sato, M., Koyano, H., Nohmi, M., Hua, S.Y., and Kuba, K. (1995).  $\text{Ca}^{2+}$ -induced  $\text{Ca}^{2+}$  release and its activation in response to a single action potential in rabbit otic ganglion cells. *J Physiol* 486 ( Pt 1), 177-187.
- Yu, X., Duan, K.L., Shang, C.F., Yu, H.G., and Zhou, Z. (2004). Calcium influx through hyperpolarization-activated cation channels (I(h) channels) contributes to activity-evoked neuronal secretion. *Proc Natl Acad Sci U S A* 101, 1051-1056.
- Yunker, A.M. (2003). Modulation and pharmacology of low voltage-activated ("T-Type") calcium channels. *J Bioenerg Biomembr* 35, 577-598.
- Zhong, N., Beaumont, V., and Zucker, R.S. (2004). Calcium influx through HCN channels does not contribute to cAMP-enhanced transmission. *J Neurophysiol* 92, 644-647.
- Zufall, F., Shepherd, G.M., and Barnstable, C.J. (1997). Cyclic nucleotide gated channels as regulators of CNS development and plasticity. *Curr Opin Neurobiol* 7, 404-412.

## 9 List of abbreviations

[Ca <sup>2+</sup> ]	Ca <sup>2+</sup> concentration
[Ca <sup>2+</sup> ] <sub>i</sub>	Intracellular Ca <sup>2+</sup> concentration
[Ca <sup>2+</sup> ] <sub>L</sub>	Intraluminal Ca <sup>2+</sup> concentration
1-EBIO	1-ethyl-2-benzimidazolinone
ABC	Avidin-biotin peroxidase complex
AHP	Afterhyperpolarization
AMPA	α-Amino-3-hydroxy-5-methyl-4-isoxazol-propion acid receptor
AMP	Adenosine 5'-monophosphate
AP	Action potential
Apa	Apamin
ATP	Adenosine 5'-triphosphate
BAPTA	1,2-Bis(2-aminophenoxy)ethane- <i>N,N,N',N'</i> -tetraacetic acid
BDNF	Brain-derived neurotrophic factor
BK	Large conductance Ca <sup>2+</sup> -activated K <sup>+</sup> channel
CA	Cornu ammonis
CaM	Calmodulin
cAMP	Adenosine 3',5'-cyclic monophosphate
CaO	Calc-alkaline
CASK	Ca <sup>2+</sup> /CaM-dependent protein serine kinase
cGMP	Guanosine 3',5'-cyclic monophosphate
CICR	Ca <sup>2+</sup> -induced Ca <sup>2+</sup> release
CNG	Cyclic nucleotide-gated
CNS	Central nervous system
CPA	Cyclopiazonic acid
Ctrl	Control
DAB	3,3-diaminobenzidine-tetrahydrochloride
DAG	Diacylglycerol
EEG	Electroencephalogram
EGTA	Ethylene glycol Bis(2-aminoethyl ether)- <i>N,N,N',N'</i> -tetraacetic acid
EMG	Electromyogram



EPSC	Excitatory postsynaptic current
EPSP	Excitatory postsynaptic potential
ER	Endoplasmic reticulum
GABA	$\gamma$ -amino butyric acid
GABAR	$\gamma$ -amino butyric acid receptor
GAERS	Genetic absence epilepsy rat from Strasbourg
HCN	Hyperpolarization activated cationic non-selective
HVA	High-voltage-activated
IP <sub>3</sub>	Inositol (1,4,5) trisphosphate
IP <sub>3</sub> R	Inositol (1,4,5) trisphosphate receptor
IPSC	Inhibitory postsynaptic current
IPSP	Inhibitory postsynaptic potential
I <sub>T</sub>	T-type Ca <sup>2+</sup> current
KO	Knock-out
LT	Low-threshold
LTD	Long-term depression
LTP	Long-term potentiation
LVA	Low-voltage-activated
mCU	Mitochondrial Ca <sup>2+</sup> uniporter
mEPSP	Miniature excitatory postsynaptic potential
mGluR	Metabotropic glutamate receptor
Mibe	Mibefradil
Mint-1	Munc18-interacting Protein1
mIPSC	Miniature inhibitory postsynaptic current
nAChR	Nicotinic acetylcholine receptor
NCKX	K <sup>+</sup> -dependent Na <sup>+</sup> /Ca <sup>2+</sup> exchanger
NCX	Na <sup>+</sup> /Ca <sup>2+</sup> exchanger
NGS	Normal goat serum
NMDA	N-methyl-D-aspartate
NMDAR	N-methyl-D-aspartate receptor
NPAS2	Neuronal PAS domain protein 2
NREM	Non-rapid eye movement
NREMS	Non-rapid eye movement sleep
nRt	Nucleus reticularis thalami

NSF	N-ethylmaleimide-sensitive fusion protein
PB	Phosphate buffer
PC	Purkinje cell
PIP <sub>2</sub>	Phosphatidylinositol (4,5) bisphosphate
PKA	Protein kinase A
PKC	Protein kinase C
PKG	Protein kinase G
PLC	Phospholipase C
PMCA	Plasma membrane Ca <sup>2+</sup> ATPase
REM	Rapid eye movement
REMS	Rapid eye movement sleep
RNA	Ribonucleic acid
RYR	Ryanodine receptor
SERCA	Sarco-Endoplasmic Reticulum Ca <sup>2+</sup> ATPase
SK	Small conductance Ca <sup>2+</sup> -activated K <sup>+</sup> channel
SMOC	Spontaneous miniature outward current
SNAP-25	Synaptosomal protein of 25 kDa
SNARE	Soluble NSF attachment protein receptor
SPCA	Secretory-pathway Ca <sup>2+</sup> ATPase
TBS	Tris buffered saline
TC	Thalamocortical
TRP	Transient receptor potential
TTX	Tetrodotoxin
VGCC	Voltage-gated Ca <sup>2+</sup> channel
WT	Wild-type
α-BTX	α-bungarotoxin
ω-CTX MVIIC	ω-conotoxin MVIIC

# 10 Curriculum vitae

## 1. Personal Information

**Name:** Lucius Cueni

**Nationality:** Swiss

**Date and place of birth:** June 16, 1969; Basel

**Address:** Lettenweg 117

4123 Allschwil

Phone P: (+41)-61-481-32-67

Phone O: (+41)-61-267-22-12

E-Mail: Lucius.Cueni@unibas.ch

## 2. Education

2004-2007 PhD in Neurobiology. Biozentrum, University of Basel.

1997-2003 Undergraduate student in Biology, University of Basel.

Diploma in Neurobiology by Prof. M.A Rüegg.

Pharmaceutical science, Pharmacology and Toxicology by Prof. J.Drewe as optional subject.

1992-1997 Gymnasium (High School) Minerva in Basel (Switzerland).

Eidg. Matura Type E (economics and business administration)

1990-1991 Swiss military service

1987-1990 Apprenticeship as a cook. Restaurant Hollee Schloss, Binningen (Switzerland).

### 3. Scientific Experience

2004-2007 **PhD THESIS** at the Biozentrum Basel; Department of Pharmacology and Neurobiology. Supervised by Prof. A. Lüthi.

*“Low-voltage-activated  $Ca^{2+}$  channels: from burst generators to  $Ca^{2+}$  sources in thalamic oscillatory activity”.*

Invited talk at the Annual Meeting of the Swiss Society for Neuroscience.

Talk at the division seminar.

Journal presentations at division seminars for new publications in neuroscience.

Invited talk at the Annual Meeting of the Swiss Physiological Society in the context of the Asher Hess prize.

2002-2003 **DIPLOMA THESIS** at the Biozentrum Basel; Department of Pharmacology and Neurobiology. Supervised by Prof. M.A. Rüegg.

*“Identification and characterisation of genes regulated by the formation of postsynaptic structures in vivo”.*

Talk at the biannual meeting of Agrin-interested research groups in Sils (Switzerland).

2001-2002 **INTERNSHIP** at the MRC, King’s College in London. Three month scientific project by Prof. J. Cohen.

*“Expression pattern of CEPU-1 and F-11 at the dorsalroot entry zone in chick”.*

Project report

Supported by the Werenfels Stiftung Basel and the Jubiläumsstiftung of the Basellandschaftliche Kantonalbank.

## **4. Teaching**

2004, 2005 'Blockkurs in Neurobiologie'- Instructor on electrophysiological demonstrations and experiments, and on computational exercises in neurophysiology.

1998-2004 Secondary school Basel and Basel-Land: Teaching Biology, Mathematics, Geography, Chemistry, Physics, French and German.

## **5. Further training**

University courses in

Communication and cooperation

Leadership

Team development

Project management

## **Bibliography**

### **ABSTRACTS**

Cueni L, Lüthi A (2004) Synergistic regulation of pacemaker currents in reticular thalamic neurons by high and low voltage activated calcium channels. *Ann. Biozentrum symp.*

Cueni L, Lüthi A (2005) Synergistic regulation of pacemaker currents in reticular thalamic neurons by high and low voltage activated calcium channels. *USGEB-SSN\_SSBP Meeting. Abstr. 178*

Cueni L, Lüthi A (2005) Effective and specific control of dampened oscillatory discharges in nucleus reticularis thalami neurons by endoplasmic calcium sequestration. *Ann. Biozentrum symp.*

Cueni L, Lüthi A (2005) Effective and specific control of dampened oscillatory discharges in nucleus reticularis thalami neurons by endoplasmic calcium sequestration. *Society for Neuroscience Meeting. Abstr. 376.17*

Cueni L, Lüthi A (2006) Endoplasmic calcium sequestration controls the dynamics of neuronal oscillations in nucleus reticularis thalami. *SSN Meeting. Abstr. E14*

Cueni L, Bond CD, Adelman JP, Lüthi A (2006) Role of the small-conductance calcium-activated potassium channel SK2 in the dampening of thalamic oscillations. *Society for Neuroscience Meeting*

### **PUBLICATIONS**

Lucius Cueni, Marco Canepari, Rafael Luján, Yann Emmenegger, Masahiko Watanabe, Chris T. Bond, Paul Franken, John P. Adelman and Anita Lüthi (2007) A competition between SK2 channels and SERCAs for Ca<sup>2+</sup> entry through T-type channels gates sleep-related oscillations in thalamic dendrites. *Neuron* (revision submitted according to editorially accepted plan).

Lucius Cueni, Marco Canepari, John P. Adelman and Anita Lüthi (2007) T-type Ca<sup>2+</sup> channels in neurons: from burst generators to sources for intracellular Ca<sup>2+</sup> ions. (In preparation)

Cueni L, Lüthi A (2007) The SK2 channel determines slow-wave sleep oscillations through selective gating by T-type Ca<sup>2+</sup> channels in nucleus reticularis thalami dendrites. Press book article. *Society for Neuroscience Meeting.*